Lídia Alexandra Santos Cavaca

Licenciatura em Bioquímica na Faculdade de Ciências e Tecnologia
da Universidade Nova de Lisboa

New Synthetic Routes for the Valorization of Easily Accessible Bio-renewable Resources

Dissertação para obtenção do Grau de Mestre em
Química Bioorgânica

Orientador: Carlos Alberto Mateus Afonso, Professor Catedrático, Faculdade de Farmácia da Universidade de Lisboa
Co-orientador: Catarina Alexandra Baptista Rodrigues, Investigadora, Faculdade de Farmácia da Universidade de Lisboa

Júri:

Presidente: Prof. Doutora Paula Cristina de Sério Branco, FCT-UNL
Arguente: Prof. Doutora Luísa Maria da Silva Pinto Ferreira, FCT-UNL
Vogal: Prof. Doutor Carlos Alberto Mateus Afonso, FF-UL

FACULDADE DE CIÊNCIAS E TECNOLOGIA
UNIVERSIDADE NOVA DE LISBOA

Setembro de 2017

LOMBADA

New Synthetic Routes for the Valorization of Easily Accessible Bio-renewable Resources
Lídia Cavaca

2017

Lídia Alexandra Santos Cavaca

Licenciatura em Bioquímica na Faculdade de Ciências e Tecnologia
da Universidade Nova de Lisboa

New Synthetic Routes for the Valorization of Easily Accessible Bio-renewable Resources

Dissertação para obtenção do Grau de Mestre em
Química Bioorgânica

Orientador: Carlos Alberto Mateus Afonso, Professor Catedrático, Faculdade de Farmácia da Universidade de Lisboa
Co-orientador: Catarina Alexandra Baptista Rodrigues, Investigadora, Faculdade de Farmácia da Universidade de Lisboa

Júri:

Presidente: Prof. Doutora Paula Cristina de Sério Branco, FCT-UNL
Arguente: Prof. Doutora Luísa Maria da Silva Pinto Ferreira, FCT-UNL
Vogal(ais): Prof. Doutor Carlos Alberto Mateus Afonso, FF-UL

FACULDADE DE CIÊNCIAS E TECNOLOGIA
UNIVERSIDADE NOVA DE LISBOA
Setembro de 2017

Indicação sobre os direitos de cópia

Agradecimentos

Aqui deixo o meu agradecimento a todos os que contribuíram para a realização desta tese e para a minha aprendizagem e evolução como cientista e química.

Ao Professor Carlos Afonso, por me ter recebido e acolhido tão bem no seu laboratório, pelo apoio durante este ano e por toda a orientação científica.

À Professora Paula Branco, por me ter aceite no Mestrado em Química Bioorgânica e assim, através das aulas, permitir alargar os meus conhecimentos e me incentivar a seguir química orgânica.

À Doutora Catarina Rodrigues, por toda a paciência e disponibilidade, e por todo o conhecimento em química orgânica que me transmitiu. Obrigada pela confiança e por todos os bons momentos passados dentro e fora do laboratório.

Ao Doutor Svilen Simeonov, pela orientação e pelos constantes trabalhos de casa e perguntas, que me ajudaram muito a aprender mais sobre química orgânica e, ao Rafael Gomes, pela ajuda na fase final do trabalho.

Ao Dr. Carlos Monteiro, Dr. Hélio Faustino, Fábio Santos e Roberto Russo por toda a ajuda no laboratório, e a todos os meus colegas de laboratório, pela amizade, profissionalismo, constante disponibilidade e partilha de conhecimentos, que me fizeram crescer muito durante este ano e também a ser mais responsável.

Ao Dr. Jaime Coelho, pela ajuda com os cálculos computacionais.

À minha família pelo apoio incondicional, por todos os conselhos e pela confiança que depositam em mim e nas minhas decisões.

Aos meus amigos, pelo apoio e por estarem ao meu lado em todos os momentos.

Um agradecimento final à Faculdade de Ciências e Tecnologia da Universidade Nova de Lisboa e ao iMED.ULisboa por cederem as infraestruturas necessárias à realização desta tese de mestrado e à Fundação para a Ciência e a Tecnologia (FCT) (ref. UID/DTP/04138/2013), COMPETE Programme (SAICTPAC/0019/2015) e European Research Area Network; ERANet LAC (ref. ELAC2014/BEE-0341) pelo apoio financeiro.

Resumo

A oliveira (*Olea europaea*) é fonte natural de uma variedade de compostos fenólicos, incluindo os secoiridóides. A oleuropeína é o secoiridóide que existe em maior quantidade nas oliveiras e noutras plantas da família *Oleaceae*. É encontrada nas azeitonas e pequenos ramos, mas são as folhas que possuem um teor mais elevado deste composto. As folhas de oliveira são produtos secundários provenientes da indústria de produção de azeite, e não têm aplicações significativas, sendo por isso consideradas uma fonte acessível e bio renovável de oleuropeína.

A estrutura molecular da oleuropeína é constituída por três unidades: hidroxitirosol, glucose e monoterpeno. A glucose confere-lhe solubilidade em água, enquanto o hidroxitirosol é responsável pela maioria das suas propriedades biológicas. A unidade monoterpénica é, no entanto, mais interessante do ponto de vista químico, possuindo dois centros assimétricos e sete posições reativas disponíveis para transformações químicas.

Este trabalho consistiu na extração e isolamento de oleuropeína de folhas de oliveira, e no estudo de uma série de transformações semissintéticas ao seu esqueleto, visando a obtenção de novos derivados pela remoção das unidades de glucose e hidroxitirosol, e transformações do *core* da unidade monoterpénica, focando-se num estudo mais completo e aprofundado da reação de metanólise da oleuropeína em condições acídicas. Este baseou-se num *screening* de ácidos próticos e resinas acídicas e um estudo do efeito da temperatura, com análise quantitativa por HPLC-UV, permitindo estudar o mecanismo da reação. Métodos de fluxo contínuo também foram explorados, com resultados positivos.

Numa única reação, a metanólise permitiu várias transformações à estrutura da oleuropeína, com obtenção de um composto com atividade antiviral reportada e utilizado como precursor na síntese de um anti-hipertensivo, para além de compostos com potencial para serem utilizados na síntese de derivados com novas propriedades farmacêuticas ou com outros interesses adicionais.

Palavras chave: Oleuropeína, folhas de oliveira, biomassa, metanólise, catálise.

Abstract

The olive tree (*Olea europaea*) is a natural source of a diversity of phenolic compounds, including secoiridoids. Oleuropein is the major secoiridoid found in olive tree and other plants from the *Oleaceae* family. It is found in olive fruit and small branches, although exists in higher amounts in olive leaves. Olive leaves are by-products from olive oil industries, and have no practical applications, being considered an easily accessible bio-renewable resource of oleuropein.

The molecular structure of oleuropein is divided in three subunits: hydroxytyrosol, glucose and monoterpene moieties. The glucose unit confers solubility in water, while hydroxytyrosol is responsible for most of its biological properties. However, the monoterpene moiety is more interesting in chemical reactivity point of view, having two asymmetric centers and seven potential reactive positions, available for synthetic modifications.

This work consisted on the extraction and isolation of oleuropein from olive leaves and the study of semi-synthetic transformations in order to obtain new derivatives, by removal of the glucose and hydroxytyrosol moieties, and modifications at monoterpene core, focusing on a complete study of the methanolysis reaction of oleuropein in acidic conditions. It was based on a screening of protic acids and acidic resins and a study of the temperature effect, with quantitative analysis by HPLC-UV, complemented by a mechanistic study of the reaction. A continuous flow approach was also performed, with positive results.

In one pot, the methanolysis reaction allowed several transformations on the molecular structure of oleuropein, with formation of a compound with reported antiviral activity and used as precursor on an anti-hypertensive drug synthesis, as well as compounds with potential to be used in the synthesis of derivatives with novel pharmaceutical properties and other additional interest.

Keywords: Oleuropein, olive leaves, biomass, methanolysis, catalysis.

Subject Index

1. Introduction 1

1.1. Olive tree as a natural source of bioactive compounds 1

1.2. Phenolic compounds in olive leaves 3

1.3. Biosynthesis of oleuropein 5

1.4. Biodegradation of oleuropein 7

1.5. Quantification of polyphenols in olive leaves 9

1.5.1 Influence of biotic and abiotic factors 9

1.5.2 Influence of treatment conditions 9

1.5.3 Extraction of polyphenols and analytical methods 11

1.6. Synthetic transformations of oleuropein 19

1.7. Biological activity of oleuropein and its derivatives 25

2. Objectives 29

3. Results and Discussion 31

3.1. Extraction and isolation of oleuropein from olive leaves 31

3.2. Semi-synthetic transformations of oleuropein 35

3.2.1. Krapcho decarbomethoxylation of oleuropein **1** 35

3.2.2. Hydrolysis of the glucose moiety by β-glucosidase 36

3.2.3. Reduction of hydroxytyrosol and methyl esters 38

3.2.4. Hydrolysis of hydroxytyrosol ester 39

3.2.5. Methanolysis of oleuropein **1** in acidic conditions 40

Continuous flow approach of the methanolysis of oleuropein **1** 51

Acid methanolysis of the olive leaves extract 53

4. Conclusions 55

5. Materials and methods 57

5.1. General Remarks 57

5.2. Extraction and isolation of oleuropein **1** 59

5.3. Semi synthetic transformations of oleuropein **1** 61

Oleacein (**2**)……61

Compound (**3**)……62

Jaspolyside (**4**)……62

Compound (**5**)……63

Compound (**6**)……64

Compound (**7**)……65

Screening of acids and temperature effect studies in methanolysis reaction……66

Continuous flow experiments under heterogeneous conditions……66

Methanolysis reaction of crude mixture……66

6. References 67

7. Appendices 75

7.1. Appendix I – NMR spectra and LC-MS-ESI of oleuropein **1** 75

7.2. Appendix II – NMR spectra and ESI-MS of jaspolyside **4** 79

7.3. Appendix III– NMR spectra and ESI-MS of compounds **5** 83

7.4. Appendix IV – NMR spectra and ESI-MS of compounds **6** 87

7.5. Appendix V – NMR spectra and ESI-MS of compounds **7** 91

7.6. Appendix VI – Screening of acids and acidic resins experiment 95

7.7. Appendix VII – Continuous flow experiments 101

7.8. Appendix VIII – Computational Calculations 103

Figure Index

Figure 1.1. Examples of polyphenols in olive leaves. Glc - Glucose; Rut - Rutinose. Adapted from Talhaoui *et al*., *Food Research International*, 77 (**2015**).[7] 3
Figure 1.2. Molecular structure of oleuropein. Representation of hydroxytyrosol, monoterpene and glucose moieties. 4
Figure 1.3. Representation of the hydrogen bond network between hydroxytyrosol and glucose moieties of oleuropein. Hydrogen bonds are represented by dashed lines. Adapted from Gikas *et al.*, *J. Molecular Structure: THEOCHEM*, 821 (**2007**).[32] 4
Figure 1.4. General representation of iridoids (**A**) and secoiridoids (**B**) molecular structures..... 5
Figure 1.5. Monoterpene unit chemical features. Reactive positions represented by arrows; stereocenters represented by (*)..... 19
Figure 1.6. Molecular structures of peracetylated forms of oleuropein, hydroxytyrosol and aglycones. 22
Figure 3.1. ^{1}H NMR spectrum of oleuropein **1**, in CD_3OD..... 33
Figure 3.2. ^{1}H NMR spectrum of oleacein **2**, in $CDCl_3$. 36
Figure 3.3. ^{1}H NMR spectrum of compounds **3**, in $CDCl_3$. 37
Figure 3.4. ^{1}H NMR spectrum of jaspolyside **4**, in D_2O. 39
Figure 3.5. Structures of the compounds **5-7** resulted from the methanolysis of oleuropein **1**..... 41
Figure 3.6. ^{1}H NMR spectrum of compounds **6**, in $CDCl_3$. 42
Figure 3.7. ^{1}H NMR spectrum of compounds **5**, in $CDCl_3$. 43
Figure 3.8. Methanolysis reaction profile using *p*TsOH.H_2O, at 70 ºC. 45
Figure 3.9. Structures and relative free energies (Kcal/mol) of truncated diastereoisomers **5a** and **5b** computed at a B3LYP/6-31G(d) level of theory. 46
Figure 3.10. Methanolysis reaction profile for compound **5a**, at different temperatures, using *p*TsOH.H_2O; Graphic ampliation until 30 minutes. 47
Figure 3.11. Methanolysis reaction profile for compound **5b**, at different temperatures, using *p*TsOH.H_2O. 47
Figure 3.12. Methanolysis reaction profile for compounds **6**, at different temperatures, using *p*TsOH.H_2O. 48
Figure 3.13. ^{1}H NMR spectrum of compounds **7**, in $CDCl_3$. 49
Figure 3.14. Correlations at distance of the major diastereoisomer of **7**..... 50
Figure 3.15. NOESY spectrum of compound **7**, in $CDCl_3$..... 50
Figure 3.16. Methanolysis reaction profile of crude mixture using *p*TsOH.H_2O, at 70 ºC..... 53
Figure 4.1. Molecular structures of compounds **5a**, **6** and the major diastereoisomer of **7**. 55
Figure 7.1. ^{13}C NMR spectrum of oleuropein **1**, in CD_3OD..... 75
Figure 7.2. HSQC spectrum of oleuropein **1**, in CD_3OD. 75

Figure 7.3. HMBC spectrum of oleuropein **1**, in CD_3OD. 76
Figure 7.4. COSY spectrum of oleuropein **1**, in CD_3OD. 76
Figure 7.5. LC-ESI-MS of oleuropein **1**, in positive mode. 77
Figure 7.6. LC-ESI-MS spectrum of oleuropein **1**, in negative mode. 77
Figure 7.7. ^{13}C NMR spectrum of jaspolyside **4**, in D_2O. 79
Figure 7.8. HSQC spectrum of jaspolyside **4**, in D_2O. 79
Figure 7.9. HMBC spectrum of jaspolyside **4**, in D_2O. 80
Figure 7.10. ESI-MS spectrum of jaspolyside **4**, in positive mode. 80
Figure 7.11. ESI-MS spectrum of jaspolyside **4**, in negative mode. 81
Figure 7.12. ^{13}C NMR spectrum of compounds **5**, in $CDCl_3$. 83
Figure 7.13. HSQC spectrum of compounds **5**, in $CDCl_3$. 83
Figure 7.14. HMBC spectrum of compounds **5**, in $CDCl_3$. 84
Figure 7.15. COSY spectrum of compounds **5**, in $CDCl_3$. 84
Figure 7.16. ESI-MS spectrum of compounds **5**, in positive mode. 85
Figure 7.17. ^{13}C NMR spectrum of compounds **5**, in $CDCl_3$. 87
Figure 7.18. HSQC spectrum of compounds **6**, in $CDCl_3$. 87
Figure 7.19. HMBC spectrum of compounds **6**, in $CDCl_3$. 88
Figure 7.20. COSY spectrum of compounds **6**, in $CDCl_3$. 88
Figure 7.21. ESI-MS spectrum of compounds **6**, in positive mode. 89
Figure 7.22. ^{13}C NMR spectrum of compounds **7**, in $CDCl_3$. 91
Figure 7.23. HSQC spectrum of compounds **7**, in $CDCl_3$. 91
Figure 7.24. HMBC spectrum of compounds **7**, in $CDCl_3$. 92
Figure 7.25.COSY spectrum of compounds **7**, in $CDCl_3$. 92
Figure 7.26. ESI-MS spectrum of compounds **7**, in positive mode. 93
Figure 7.27. Calibration curves of oleuropein **1**, compounds **5** and **6**, at 230 nm. 95
Figure 7.28. Chromatograms of oleuropein **1**, compounds **5** and **6**. 96
Figure7.29. Examples of methanolysis reaction profiles for different acids and acidic resins, at 70 ºC. 97
Figure 7.30. Chromatograms of the methanolysis reaction of oleuropein **1**, using *p*TsOH.H_2O; 2 represents compound **5** and **3** represents compound **6**. 98
Figure 7.31. Chromatograms of the methanolysis reaction with crude, using *p*TsOH.H_2O, at 70 ºC; 2 represents compound **5** and 3 represents compound **6**. 99
Figure 7.32. Reactor for continuous flow experiments. 101
Figure 7.33. Continuous flow system. 101
Figure 7.34. Chromatograms from continuous flow experiences, of 1 min, 5 min and 10 min of residence time. 102
Figure 7.35. ^{1}H NMR spectra of **5a** crude sample from flow (up) and previous isolated **5** (down). .. 102

Scheme Index

Scheme 1.1. Proposed biosynthetic pathway for the formation of oleuropein. Adapted from Obied *et al*.,*Natural Product Reports*, 25 (**2008**).[33] 5

Scheme 1.2. Molecular structures of elenolic acid glucose (A) and demethyloleuropein (B), formed by esterase action, and aglycone forms (C and D) and oleuropein aglycone (E) by *β*-glucosidase action. 7

Scheme 1.3. Proposed transformations of oleuropein aglycone by solvents as methanol, chloroform and acidic solutions. Solvents are identified by dashed boxes. Adapted from Paiva-Martins *et al*., *J. Agric. Food Chem.*, 56 (**2008**). [84] 20

Scheme 1.4. Acid hydrolysis of oleuropein with sulfuric acid to produce elenolic acid. 21

Scheme 1.5. Molecular structures of the aglycone forms of oleuropein after treatment with *β*-glucosidase or hydrolysis by lanthanides. 21

Scheme 1.6. Hydrolysis of hydroxytyrosol ester and acetylation of glucose. Adapted from Hanessian *et al*. *Organic Letters*, *8*, **2006**, 4047-9 . [88] 22

Scheme 1.7. Synthesis of pyridine alkaloids from oleuropein; Adapted from Ranarivelo *et al., Nat. Prod. Lett.*, **2001**, *15*(2), 131-7. 23

Scheme 1.8. Reduction of oleuropein to oleuropeinol; hydrolysis of oleuropeinol to compounds a and b; acetylation and reduction of the mixture of compounds a and b. 23

Scheme 1.9. Acid rearrangement of oleuropeinol in methanol. 24

Scheme 1.10. Krapcho decarbomethoxylation of oleuropein to produce oleacein. 24

Scheme 3.1. Two routes for Krapcho decarbomethoxylation of oleuropein **1**. 35

Scheme 3.2. Proposed transformations of oleuropein **1** by *β*-glucosidase. 37

Scheme 3.3. Reduction of oleuropein **1** with $NaBH_4$ to produce oleuropeinol. 38

Scheme 3.4. Basic hydrolysis of hydroxytyrosol ester of oleuropein **1** to produce jaspolyside **4**. 40

Scheme 3.5. Acid methanolysis of hydroxyornoside. 41

Scheme 3.6. Methanolysis reaction under optimum conditions, to obtain compound **7**. 48

Scheme 3.7. Proposed mechanism for the methanolysis of oleuropein **1** in acidic conditions. 51

Table Index

Table 1.1. Published values of oleuropein concentration according to extraction method. 14
Table 1.2. Health benefits of olive leaf extracts, oleuropein and its derivatives. 25
Table 3.1. Extraction and purification conditions of oleuropein from dried olive leaves. 31
Table 3.2. Conversion and best yields obtained with different acid promoters; time is shown in parenthesis. 44
Table 3.3. Results for compound **5a** from continuous flow experiments. 52
Table 7.1. Data for calibration curves of oleuropein **1**, compounds **5** and **6**. 95
Table 7.2. Main results obtained from the screening of acids experiments, after 6 hours. 98
Table 7.3. Results from temperature effect experiments, after 2 hours. 99
Table 7.4.Yields from methanolysis reaction of crude mixture. 99
Table 7.5. Weights for flow calculation. 101
Table 7.6. Data for flow calculation in resin robustness evaluation. 102

Abbreviations

ACN – Acetonitrile

CAL-B – *Candida antarctica* lipase B

COSY – Correlation Spectroscopy

ESI – Electron Spray Ionization

EtOAc – Ethyl Acetate

FD – Freeze Drying

HAD – Hot Air Drying

HCl – hydrochloric acid

HMBC – Heteronuclear Multiple Bond Correlation Spectroscopy

HPLC – High Performance Liquid Chromatography

HSQC – Heteronuclear Single Quantum Coherence Spectroscopy

LC – Liquid Chromatography

MAE – Microwave Assisted Extraction

MS – Mass Spectrometry

NMR – Nuclear Magnetic Resonance

NOESY – Nuclear Overhauser Effect Spectroscopy

PPO – Polyphenol oxidase

***p*TsOH.H_2O –** para-toluene sulfonic acid monohydrated

TFA – Trifluoracetic Acid

TLC – Thin Layer Chromatography

TMS – Tetramethylsilane

UV – Ultraviolet

1. Introduction

Natural products include a large and diverse group of substances obtained from natural sources, as marine organisms, bacteria, fungi and plants.

Nature offers a great variety of chemical scaffolds with several stereocenters and functionalities that by synthetic chemistry are difficult or impossible to obtain. Therefore, unlike human synthesized molecules, natural products are able to interact with a broad range of biological macromolecules, showing their relevance for pharmaceutical research.[1] Because of this, the isolation, structural elucidation and formulation of key active compounds from natural sources has gained increasing importance, which was only possible due to the scientific progress of the last century.

Primarily, synthetic chemists were just focused on improving natural compounds drug-like features. However, natural products can serve as powerful starting materials to generate drug substances with novel therapeutic utility, through synthetic modifications.[2]

1.1. Olive tree as a natural source of bioactive compounds

Plants are one of the most important sources of natural bioactive products since they have developed an effective defense system against predators, involving the production of a large number of different chemical compounds.[3]

Phytochemicals are high-added value natural substances used as ingredients in foods, dietary supplements, cosmetics and pharmaceuticals. The consumers preference for products containing natural additives, generally perceived as safer and healthier, has increased the demand for phytochemical ingredients.[4]

Olea europaea, commonly known as olive tree, is native to Mediterranean countries and has provided huge economic and dietetic benefits since ancient years. Olive trees are cultivated for production of olive oil and table olives, which are two of the most representative ingredients of the traditional Mediterranean diet.[5-7]

Epidemiological studies revealed that lower incidence of coronary heart diseases and some forms of cancer in Mediterranean countries, such as Greece, Italy and Spain, are generally associated to their diet, and is especially due to the high consumption of olive oil. It is also known that the majority of health benefits credited to olive oil are due to the presence of a variety of phenolic compounds.[8] Although they are found in olive oil, polyphenols are also present in other parts of the tree, including leaves and small branches. In fact, leaves are richer in polyphenols than olive oil itself.[9]

Industries generate a large quantity of by-products as waste, which contain high-added value chemical compounds. A high number of by-products and residues are collected from olive tree production and olive processing industry, but most of them have no practical applications.

Olive leaves are a by-product from the olive tree cultivation and can be found in large amounts in olive oil industries. Furthermore, they also accumulate in large volumes on farms during the pruning of

the trees. Usually, leaves are directly thrown away, burned, or grinded and scattered on the field, potentially causing environmental damage, but also with increasing cost for producers due to their removal, storage and elimination. Given this, and the fact that olive leaves are very rich in phenolic substances, they might be considered as a cheap and easily available natural source of these bioactive compounds, with advantages at many levels.[4, 7, 10-15]

Olive leaf extract gained popularity in the global nutraceutical market due to a range of claimed health attributes; they are traditionally used in the treatment of a wide spectrum of diseases. Therefore, olive leaves can be an interesting raw material for research on food and pharmaceutical sciences, and its valorization must be encouraged.[14, 16]

So far, published reviews, focus on olive leaves valorization due to high content in phenolic compounds and their biological properties, especially oleuropein, on the extraction and analytical separation methods of oleuropein and other phenolic compounds[14, 17-24], and also on the influence of different environmental and treatment factors in phenolic compounds content.[7] From 1994 to 2010, physical and spectral data, and information about biological and pharmacological properties of natural secoiridoids, including oleuropein, have been collected and reported in four article reviews. [25-28] However, even in more recent reviews, there is a lack of information about the use of oleuropein as starting material for synthetic transformations.

1.2. Phenolic compounds in olive leaves

Polyphenols are the largest group of phytochemicals. Olive biophenols include a major group of secondary plant metabolites, distinguished by their water solubility and high molecular weights. They are of considerable physiological and morphological importance in plants, displaying high structural variety and performing several key activities. Actually, their excellent properties are a consequence of their function in the tree, namely, in the reactivity against pathogens attack and response to insect injury.[5, 14, 15]

Olive leaves contain a large variety of phenolic derivatives, consisting of simple phenols (phenylethanoids, hydroxybenzoic acids, hydroxycinnamic acids), flavonoids (flavones, flavanones, flavonols, 9-flavanols) and secoiridoids, as shown in Figure 1.1.[17]

Flavonoids and secoiridoids are the major active components in olive leaves. Secoiridoid byphenols are monomers of *seco*-conjugate structure, between phenolic, terpenic and glucoside moieties. They are also characterized by an exocyclic 8,9-olefinic functionality at the terpene ring, and are present only in plants belonging to the *Oleaceae* family (Figure 1.1).[13, 17, 18]

Oleuropein is the major secoiridoid compound in olive leaves. Leaves are richer in oleuropein than other parts of the tree. Oleuropein was detected in olives for the first time in 1908 by Bourquelot and Vintilesco, but its chemical structure was assigned by Panizzi *et al.* in 1960. It is a heterosidic ester of *β*-glucosylated elenolic acid and 3,4-dihydroxy-phenylethanol (hydroxytyrosol), being responsible for the bitter taste in olive oil.

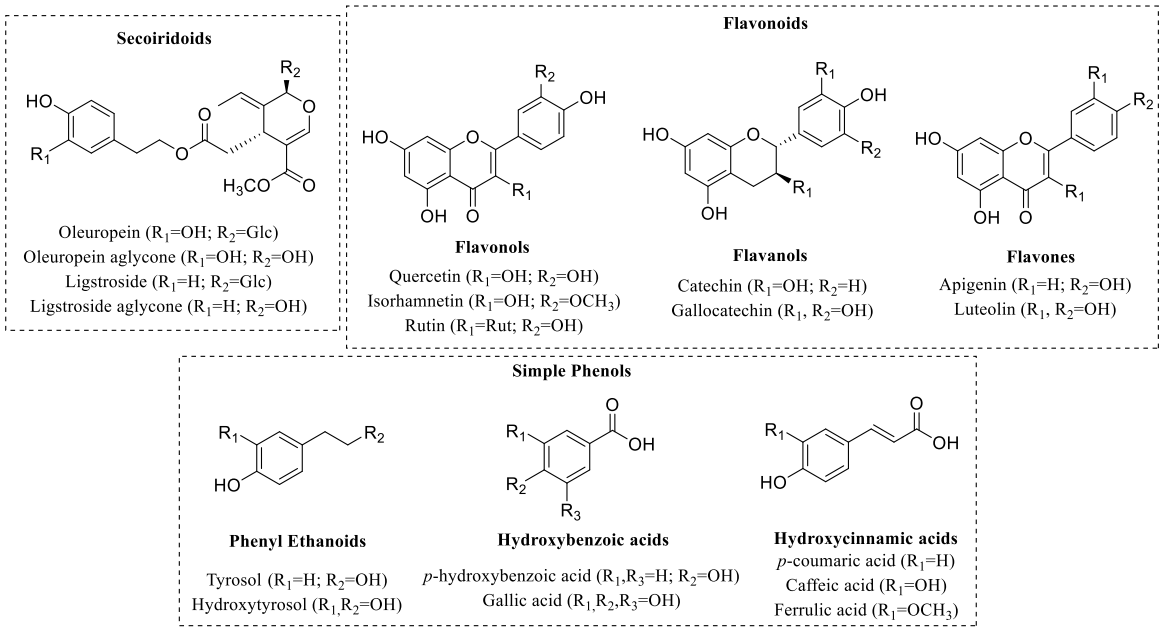

Figure 1.1. Examples of polyphenols in olive leaves. Glc - Glucose; Rut - Rutinose. Adapted from Talhaoui *et al.*, *Food Research International*, 77 (2015).[7]

It has a stereocenter at C-5 with *(S)* configuration and an exocyclic 8,9-double bond with *E* configuration, which are characteristic of secoiridoids. The molecular structure of oleuropein can be divided into three subunits: hydroxytyrosol, monoterpene and glucose moieties (Figure 1.2.).[18, 19, 29-31]

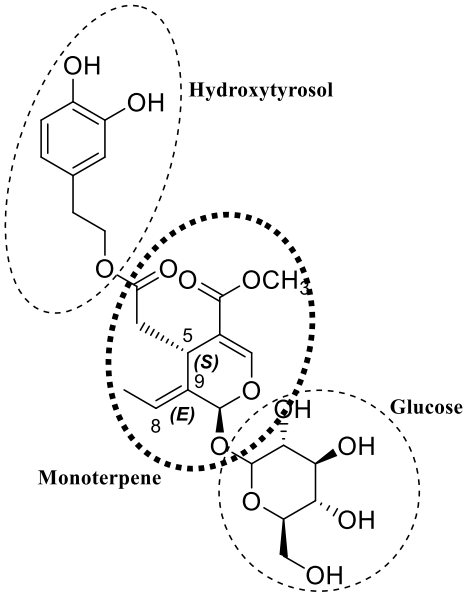

Figure 1.2. Molecular structure of oleuropein. Representation of hydroxytyrosol, monoterpene and glucose moieties.

Gikas *et al.* found the lower energy conformation of oleuropein through semi-empirical and *ab initio* calculations, which was confirmed by molecular dynamics simulations. Their results indicated that oleuropein's minimum energy conformation has a closed geometry where the glucose moiety is in close proximity with hydroxytyrosol, and the structure of the molecule is stabilized by the formation of hydrogen bonds between the phenolic hydrogens and the hydroxyl groups of the sugar moiety. (Figure 1.3.). [32]

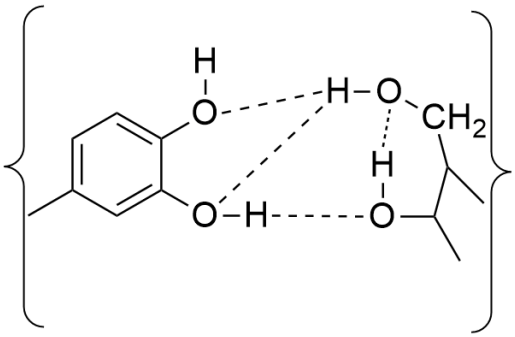

Figure 1.3. Representation of the hydrogen bond network between hydroxytyrosol and glucose moieties of oleuropein. Hydrogen bonds are represented by dashed lines. Adapted from Gikas *et al., J. Molecular Structure: THEOCHEM*, 821 (2007).[32]

1.3. Biosynthesis of oleuropein

Iridoids (**A**) are monoterpenes characterized by a bicyclic fused ring system comprising a six-membered heterocyclic ring and a cyclopentane ring. Secoiridoids (**B**) are derived from iridoids by opening of the cyclopentane ring at the 7,8 bond (Figure 1.4.).[33]

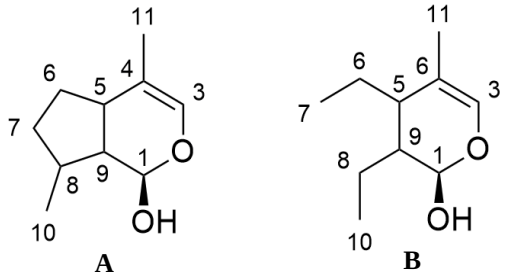

Figure 1.4. General representation of iridoids (A) and secoiridoids (B) molecular structures.

Secoiridoids characterized by an exocyclic 8,9-olefinic functionality, which includes oleuropein, are termed oleosidic secoiridoids or oleosides, and are unique to oleaceous plants.

Secoiridoid conjugates that contain an esterified phenolic moiety, such as oleuropein, result from a branching in the mevalonic acid pathway in which oleoside moiety (monoterpene) synthesis and phenylpropanoid metabolism (phenolic part) merge.[33]

Mevalonic acid comes from the initial condensation of three acetyl-SCoA molecules, originating the ester *β*-hydroxy-*β*-methylglutaryl-CoA (HMG-CoA), which produces mevalonic acid, through an hydrolysis and enzymatic reduction.[34]

The proposed biosynthetic pathway for the formation of oleuropein in *Oleaceae* is shown in Scheme 1.1., via 7-*epi*-loganic acid, with ligstroside as direct precursor.[33]

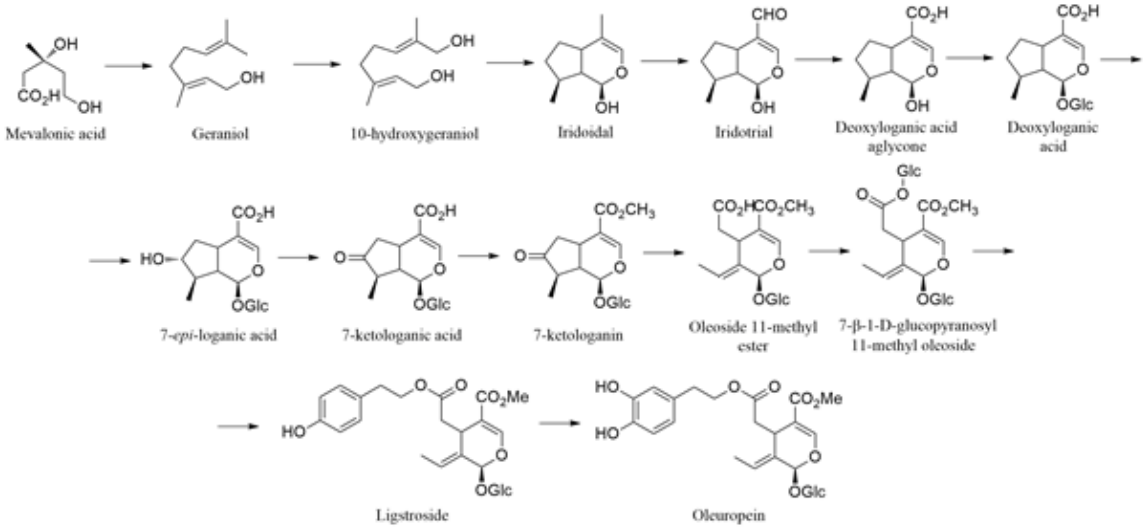

Scheme 1.1. Proposed biosynthetic pathway for the formation of oleuropein. Adapted from Obied *et al.*,*Natural Product Reports,* 25 (2008).[33]

1.4. Biodegradation of oleuropein

Oleuropein levels are affected by several factors, including harvesting season. It has been shown that oleuropein levels decrease during the growth period of fruit, with the lowest content of the year being measured in July, when the olive fruit is fully developed. However, in July, the total phenolic content increases, which suggests that oleuropein suffers degradation and other substances are formed.[35]

In olive fruit, elenolic acid glucoside (jaspolyside) and demethyloleuropein accumulate during ripening of olives, while the oleuropein levels decrease. Oleuropein degradation to these glucosylated derivatives involves cleavage by specific endogenous esterases. Activation of endogenous *β*-glucosidase during crushing or malaxation might produce the aglycone forms (C, D and E) by cleavage of glucose (Scheme 1.2).[36-38]

Ryan *et al.* have reported that different tissues of the olive tree have different phenolic composition, and as such, the metabolism of each plant tissue is characteristic.[39]

However, according to Briante *et al.*, the degradation of oleuropein is similar in olive leaves, since many molecules isolated from leaves are thought to have originated from oleuropein, with endogenous enzymes playing an important role.[29]

Recently, De Leonardis *et al.* found that the enzyme polyphenol oxidase (PPO) is also involved in oleuropein degradation in olive leaves. Fresh leaves and dried leaves showed different enzymatic activity on oleuropein. In the extracts from fresh leaves both the *β*-glucosidase and PPO enzymes were found active. On the other hand, the decrease of oleuropein concentration in dried leaves was mainly attributable to the PPO activity, leading exclusively to the formation of oxidation products.[40]

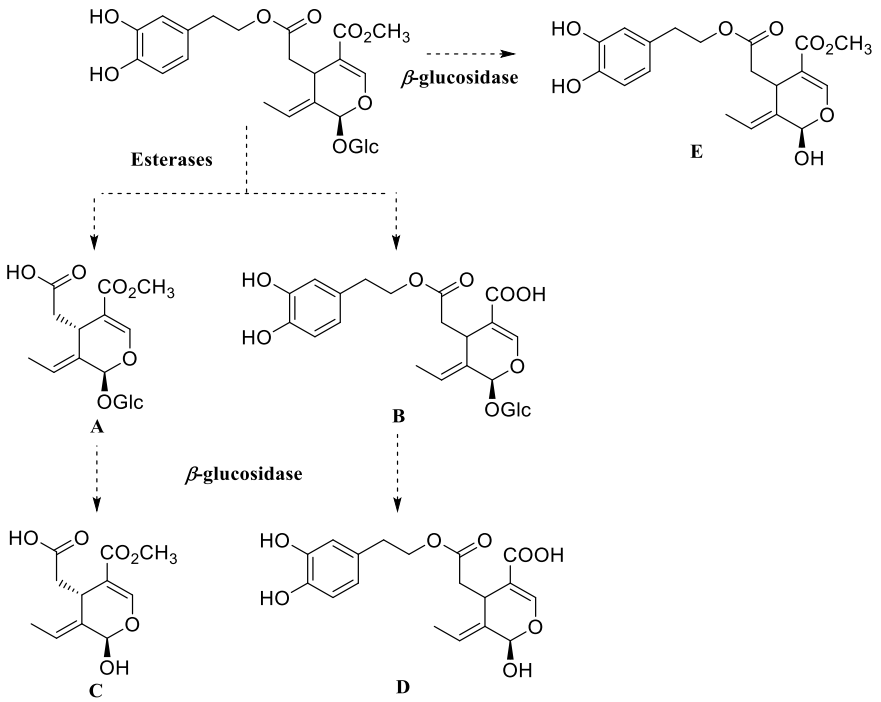

Scheme 1.2. Molecular structures of elenolic acid glucose (A) and demethyloleuropein (B), formed by esterase action, and aglycone forms (C and D) and oleuropein aglycone (E) by *β*-glucosidase action.

1.5. Quantification of polyphenols in olive leaves

1.5.1 Influence of biotic and abiotic factors

In olive leaves, oleuropein and total phenolic levels are affected by abiotic (non-living chemical and physical parts of the environment that affect the tree, such as soil, water, air, temperature, moisture, etc.) and biotic (other plants, fungi and bacteria, animals and human influences) factors.[7] Thus, oleuropein and other phenolic content depend, essentially, of cultivar, harvesting season, maturity of leaves, geographical origin and moisture content.[15]

These differences have been widely reported in the literature, and different extraction and analytical methods have been employed for the determination of polyphenols content.[7, 8, 30, 39, 41-57]

Ortega-García *et al.* reported that oleuropein concentration in leaves was higher after exposure to cold stress, which has been related to oleuropein antioxidant capacity, offering protection against oxidative damage induced by freezing.[44] Petridis *et al.* studied the effect of water deficit on olive leaf phenolic composition, concluding that water stress induces the accumulation of phenolic compounds, especially oleuropein, suggesting their role as antioxidants.[49] Oleuropein is also involved in the olive tree protection against salinity stress in leaves, serving as a glucose-reservoir for osmoregulation and high energy-consuming processes required for plant adaptation to salinity, increasing oleuropein content.[58]

Total phenolic levels in leaves decline as the altitude decreases, which can be related to changes in the climatic conditions. For instance, leaves from trees cultivated in windy and humid air have lower levels of phenolic compounds.[59]

An important biotic factor affecting the phenolic content is the age of the leaves. Oleuropein amount is higher in younger leaves than in mature ones, which suggests a gradual oleuropein degradation with the ageing of the leaves.[39, 52]

1.5.2 Influence of treatment conditions

The conditions in which olive leaves are treated influence their phenolic content. Currently, there are no widely accepted guidelines for the drying of olive leaves and data from literature are insufficient or contradictory. However, in order to stabilize the leaves and to avoid quality losses and undesirable degradation during storage, the dehydration of olive leaves has to be carried out immediately after harvesting.

Traditional methods of drying, as shade or sun drying, are still practiced, but this operation is not well controlled, influencing the final quality of the product. Thus, for industrial purposes, hot air drying is the most used method, allowing an accurate control of the process variables.[20]

Several studies have focused on the investigation and modelling of the drying behaviour of olive leaves. For example, Boudhrioua *et al.* studied the effect of blanching and infrared drying on the colour, total phenol content and moisture removal rate of four olive varieties, using an infrared dryer at 40 ˚C,

50 ˚C, 60 ˚C and 70 ˚C. Infrared drying seemed promising, inducing a considerable moisture removal from the fresh leaves (>85%), short drying time (15 min at 70 ˚C), and increased polyphenol content for leaves dried at this temperature.[60]

Erbay *et al.* used hot air for drying olive leaves. Optimum operating conditions by process intensification were found to be at 53.43 ˚C, air velocity of 0.64 m/s, and process time of 288.32 min. At these conditions, moisture loss was of 69.55%, with minimum total phenolic content and antioxidant activity losses.[61]

Ahmad-Qasem *et al.* studied the freezing-drying of olive leaves. Hot- and freeze- air drying showed a significant effect on the concentration of polyphenols. Hot air drying at 120 ˚C provided a higher phenolic content than freeze-drying, especially in oleuropein, which can be explained by the influence of cold in olive leaves, previously explained in section 1.5.1. The sharp decrease in oleuropein levels observed after brief thawing is probably due to the mixing of oleuropein with endogenous enzymes that are compartmentalized in fresh leaf cells.[62]

Using a laboratory convective solar dryer, Bahloul *et al.* investigated the effect of solar drying conditions on the drying time and on some quality parameters of olive leaves, such as colour, total phenol content and radical scavenging activity. They tested different temperatures (40 ˚C, 50 ˚C and 60 ˚C) and air velocities (1,6 and 3,3 m^3/min) to show that the total phenolics content is influenced by drying air conditions and that it decreases as the drying time increases.[63]

Aouidid *et al.* used a microwave oven, drying leaves twice for two minutes at maximum power of 800 W and lyophilisation were employed prior to oleuropein determination in olive leaves.[64]

The application of an ultrasound energy system was also investigated for drying olive leaves. Kamran *et al.* studied the recovery of phenolic compounds from fresh, air-dried, freeze-dried and oven-dried (60 ˚C and 105 ˚C) olive leaves. Extracts of oven-dried leaves at 105 ˚C showed the highest phenol recoveries. Olive leaves oven-dried at 105 ˚C for three hours increased oleuropein recovery as compared with fresh olive leaves.[16] Cárcel *et al.* studied the influence of the ultrasound power application during drying of olive leaves, at 40 ˚C. Ultrasound influenced the external resistance of the leaves, reducing it and increasing the drying rate.[65]

Erbay *et al.* determined and tested the most appropriate thin-layer drying model with air temperatures of 50 ˚C, 60 ˚C and 70 ˚C, and air velocities of 0.5, 1.0 and 1.5 m/s, to understand the drying behaviour of olive leaves. It was concluded that leaves could be dried successfully by this drying method, and the drying rate depends on velocity and temperature of the air. However, temperature has more influence, and drying rate increase as temperature increases.[66]

Malik and Bradford reported air drying at ambient temperature (25 ˚C) as the most suitable method for processing olive leaves viability and good recoveries of biophenols, fully preserving oleuropein levels, while drying at 60 ˚C results in losses of different polyphenols.[14]

Blanching processes are another factor studied. Olive leaves dried using steam blanching showed increased total phenolic content compared to the fresh ones. However, losses of oleuropein were higher using hot water blanching in leaves than using steam blanching.[6]

1.5.3 Extraction of polyphenols and analytical methods

The most important parameters that affect the recovery of phenols are the method employed and the extraction temperature, solvent and time. The methods and results reported in the literature are related to samples obtained from different species, different sources or different regions and, thus there is a large heterogeneity of results regarding phenol recovery. Besides, sample handling, processing, clean-up and storage conditions, extract stability, analytical technique sensitivity and the purity of standards used for preparation of calibration curves are commonly factors that can account for the wide variation of values in literature. Furthermore, it is difficult to develop a single method for optimal extraction of all phenolic compounds contained in olive leaves or other natural sources, because their polarities vary significantly.

Extraction is one of the most important steps in sample pre-treatment for polyphenols analysis. The most common has been solid-liquid extraction, such as Soxhlet extraction, by maceration of the olive leaves in a solvent, such as methanol, ethanol, acetone, ethyl acetate, and diethyl ether, as well as aqueous alcohol mixtures. However, these methods require large amounts of toxic solvents and long extraction times, with high costs, time waste and environmental pollution. Besides, being time consuming and having poor efficiency, some degree of heating is required, which can easily lead to thermo-sensitive ingredients losing their biological activities or degrading into other substances.[67]

In order to minimize these disadvantages, the extraction techniques have been continuously improved. In this way, techniques like microwave extraction, supercritical fluid extraction, superheated liquid extraction, liquid-liquid extraction, pressurized liquid extraction, derivatized polar extraction, fractionation by solid-phase extraction, dynamic ultrasound assisted extraction and microwave assisted extraction have been studied.[14]

High pressure extraction is a novel technique that utilizes high pressure conditions to extract active ingredients from plants. It increases the mass transfer rate by changing the concentration gradient and diffusivity, causing damage to the plant cell membrane and increasing its permeability. This increases the extracting power, albeit at the expense of process safety.[67] On the other hand, Xie *et al.* applied reduced-pressure boiling extraction to extract oleuropein from olive leaves, and obtained higher yields of oleuropein.[68]

Japón-Luján *et al.* performed the ultrasound-assisted extraction of oleuropein and related biophenols from olive leaves, concluding that this method is faster and more efficient than traditional methods, because cavitation favours penetration and transport through the interface between aqueous or organic liquid phase subjected to ultrasound energy and a solid matrix. The authors also demonstrated that the increase in the temperature caused by ultrasonic irradiation did not degrade oleuropein.[5] Luque and

Luque designed and constructed an ultrasound-assisted Soxhlet extractor combined with supercritical CO_2 extraction with improved rates and yields.[69] Supercritical fluid extraction has received increasing interest, because supercritical fluids provide high solubility, improved mass-transfer rates and the process can be optimized by changing the temperature or pressure. Carbon dioxide (CO_2) is the most used solvent because it is safe, non-toxic, non-flammable, high selective and has moderate critical conditions (31.3 °C and 72.9 atm). However, this technique is limited to compounds of low or medium polarity.[20]

The microwave-assisted extraction technique has the advantages of low consumption of organic solvents and low costs, providing shorter extraction times compared to conventional procedures. In addition, it provides higher extraction efficiency and selectivity, which makes it a desirable method for the extraction of phenolic compounds from olive leaves.[14] Dang *et al.* investigated the optimal operating conditions for enhancing the yield of oleuropein extracted from olive leaves by testing supercritical CO_2 fluid extraction, microwave-assisted extraction and Soxhlet extraction techniques. They have shown that the microwave-assisted technique can provide reduced extraction times.[70] In this case, heating occurs in a targeted and selective manner with practical no heat being lost, since it is a closed system. The moisture when heated up inside the plant cells, evaporates and generates tremendous pressure on the cells wall, culminating with cell wall rupture, which facilitates leaching out of the phytoconstituents. Thus, this unique heating mechanism can significantly reduce the extraction time.[71] This extraction technique has also gain much attention because of minimum degradation of target components.[7]

Recently, biopolymers and polymeric absorbents have been used to separate and purify target compounds from natural plant sources, with low cost and harmless to operator's health. The polymer silk fibroin, used since the 1940s due to its hydrophobic and bonding characteristics, was used by Altiok *et al.* and Bayçin *et al.*, to increase the purity of oleuropein from olive leaves.[72, 73] Besides biopolymers, macroporous resins are important as polymeric absorbent, usually applied in separation and purification of bioactive compounds from natural sources.[13]

Comparing all the different extraction techniques, microwave-assisted extraction and conventional extraction showed to be the best choice for extracting more polar compounds, such as oleuropein and its derivatives.[20]

Green approaches have also been tried with a continuous adsorption/nanofiltration hybrid process and use of imprinted polymer with *in situ* recovery of solvent for the isolation of oleuropein.[74]

A correct choice of solvent is fundamental for obtaining an optimal extraction process. Solvent choice for microwave-assisted extraction is dictated by the solubility of the target analyte, interaction between solvent and plant matrix and by the microwave absorbing properties of the solvent. Thus, solvent need to have good selectivity towards the analyte of interest excluding unwanted matrix components, compatibility with further chromatographic analytical steps and appropriated dielectric properties. Volume of the solvent is also a critical factor. It must be sufficient to ensure that the plant

matrix is always entirely immersed and the heating efficiency of the solvent under microwave should be considered, depending on solvent evaporation.[71]

A polar solvent is necessary to be able to extract oleuropein. Laboratory-scale methods use extractants such as methanol-water mixtures or hexane for the extraction of oleuropein and derivatives from olive leaves. But the increased human use of these compounds makes mandatory the development of methods based on nontoxic extractants, like water.[5]

Recently, Apostolakis *et al.* studied the efficiency of heated water/glycerol mixtures in extracting polyphenols from dried olive leaves. Glycerol is a bio-solvent, with no toxicity and it is a natural constituent of foods. Authors concluded that the use of a heated aqueous glycerol solution was more efficient as compared with a hydro alcoholic solution in extracting olive leaf polyphenols, providing the same differentiated selectivity.[4]

Regarding to the analytical methods, the colorimetric Folin-Ciocalteau assay is the most used and rapid quantitative technique for the determination of total polar phenolics in olive leaves. High performance liquid chromatography (HPLC), usually in reversed-phase mode and coupled with several detectors (UV-Vis, MS, NMR, DAD, etc.), is used for the determination of individual compounds.[20] Nuclear magnetic resonance spectroscopy (NMR) is used in the analysis of complex mixtures without previous separation of the individual components. Gas chromatography (GC) has lower detection limits and better separation, but needs sample pre-treatments, using derivatization reagents. Nevertheless, high/ultra-performance liquid chromatography (HPLC/UPLC) coupled to diode-array detection (DAD) and/or coupled to mass spectrometry (MS) is the most used to quantify and characterize phenolic compounds.[7]

Columns most used in the HPLC analytical technique are a reversed-phase C18 with 5 μm particle size. Gradient elution mode is commonly utilized, because the complexity of the phenolic profile makes it not able to be well-separated by the isocratic elution mode. UV-Vis detection system continued to be one of the most used detection systems for phenolic compounds, generally using as wavelength 280 nm. However, it should be considered that no universal absorbance maximum exists for olive leaf phenolics.[20]

The development of existing methods of separation and introduction of new techniques of high resolution are needed to give rise to the discovery of new effective compounds from phyto-pharmaceutical sources and improve its separation.[71]

There is a considerable variation on the published values for oleuropein's recovery from olive leaves, in the range 0.1-26% (w/w), depending on some factors as discussed before at chapters 1.5.1. and 1.5.2.[16]

Table 1.1 shows a compilation of values of oleuropein content regarding leaves conditions, extraction method and olive tree variety.

Table 1.1. Published values of oleuropein concentration according to extraction method.

Variety	Leaves Conditions	Extraction Method	Oleuropein Quantification	Oleuropein Concentration (mg/g)[1]	Observations	References
Leccino, Moraiolo and Frantoio	Fresh leaves	**Solid-liquid extraction** CH_3OH, 1 week, rt Then, $(CH_3)_2CO/H_2O$ (1:1) Extraction with *n*-pentane, CH_3Cl and ethyl acetate	**Purification** Column chromatography with silica gel CH_3Cl/CH_3OH (9:1) then CH_3Cl/CH_3OH (4:1)	2,95	Oleuropein isolated from ethyl acetate extract	(Gariboldi *et al.*, 1985) [75]
Moraiolo *N3 (Don Carlo)* *N2* *Coratina* *Nociara* *Frantoio* *I-77* *Leccino*	Dried leaves (freeze-dried with liquid N_2)	**Solid-liquid extraction** Different volume ratios of H_2O/Ethanol	**Analytical** HPLC	14,4 8,39 7,06 6,10 3,70 3,19 3,03 1,05	Best extraction solvent mixture: H_2O/Ethanol (1:1) *Moraiolo* variety possesses the highest oleuropein content	(Briante *et al.*, 2002) [29]
Unknown	Dried leaves	**Microwave-assisted extraction (MAE)** 100-200 W, 5-15 min Ethanol 80%-100%	**Analytical** HPLC-DAD (280, 330, 340, 350 nm) Lichrospher 100 RP_{18} column (250×4 mm, 5 µm); Kromasil 5 C18 (15×4,6 mm, 5 µm) 6% acetic acid, 2 mM sodium acetate in H_2O, and ACN Flow: 0,8 mL/min Gradient	23,2	MAE – faster extraction method Optimal extractant – Ethanol/H_2O (8:2)	(Japón-Luján *et al.*, 2006) [76]

[1] Mass of oleuropein in mg per gram of olive leaves dry weight.

Unknown	Dried leaves (40 ˚C, 8 h)	**Superheated liquid extraction (SHLE)** Variables: temperature, static and dynamic extraction time, extractant flow-rate and extractant composition	**Analytical** HPLC-DAD (280, 330, 340 and 350 nm) Lichrospher 100 RP_{18} (250×4 mm, 5 µm) Kromasil 5 C_{18} column (15×4,6 mm, 5 µm) 6% acetic acid, 2 mM sodium acetate in H_2O, and ACN Gradient Flow: 0,8 mL/min	23,0	Pressure: 6 bar Solvent – EtOH: H_2O (7:3), 140 ˚C, 6 min Dynamic mode, extractant: 7 min at 1 mL/min Extraction time: 13 min	(Japón-Luján *et al.*, 2006) [77]
Unknown	Dried leaves	**Ultrasound-assisted extraction** 20KHz, 450 W Variables: irradiation time, extraction flow-rate, Ethanol%, probe position, temperature, radiation amplitude and duty cycle	**Analytical** HPLC-DAD (280, 330, 340 and 350 nm) Lichrospher 100 RP_{18} (250×4 mm, 5 µm) Kromasil 5 C_{18} column (15×4,6 mm, 5 µm) 6% acetic acid, 2 mM sodium acetate in H_2O, and ACN Gradient Flow: 0,8 mL/min	22,6	Optimal conditions: irradiation time – 25 min; extraction flow-rate – 5 mL/min; 59 % EtOH; Probe position – 4 cm; temperature – 40 ˚C; Faster and more efficient than traditional methods.	(Japón-Luján *et al.*, 2006) [5]
Unknown (December 2004)	Dried leaves (37 ˚C, 3 days)	**Solid-liquid extraction** Ethanol, CH_3OH, acetone and their aqueous forms (10%/90%, v/v)	**Analytical** HPLC-UV (280 nm) C_{18} Lichrospher 100 analytical column (250×4 mm, 5 µm), 30 ˚C Flow: 1 mL/min Acetic acid/H_2O (2,5:97,5) and ACN Gradient, 60 min	74,5	70% EtOH: best extractant solvent Silk fibroin as promising adsorbent for oleuropein purification.	(Baiçın *et al.*, 2007) [73]

Chemlali	Dried leaves	**Solid-liquid extraction** CH_3OH/H_2O (4:1) 24 hours	**Analytical** HPLC Shim-pack VP-ODS (250×4,6 mm), 40 ˚C 0,1% phosphoric acid in H_2O, and 70% ACN in H_2O Flow: 0,5 mL/min Gradient, 40 min	43,2	-	(Jemai *et al.*, 2008) [78]
	Dried leaves	**Solid-liquid extraction** CH_3OH/H_2O (4:1) 24 hours	**Analytical** HPLC Shim-pack VP-ODS (250×4,6 mm), 40 ˚C 0,1% phosphoric acid in H_2O, and 70% acetonitrile in H_2O Flow: 0,5 mL/min Gradient, 40 min	24,4	-	(Jemai *et al.*, 2009) [79]
Coralina	Dried leaves	**Microwave-assisted extraction** H_2O, 800 W, 10 min	**Purification** LC Supelco Versa Flash CH_2Cl_2/MeOH (8:2)	8,8 – 21,7	Optimal extraction time: 10 min giving high oleuropein yield ($21,7\times10^{-3}$ mg/g)	(Procopio *et al.*, 2009) [80]
Koroneiki	Air dried leaves	**Supercritical fluid extraction (SFE)** 30 MPa Extraction: 50 ˚C Separation: 55 ˚C Solvent-to-feed ratio: 120 or 290 Co-solvent: 5% or 20 %	**Analytical** HPLC-DAD (248 nm) SupelcoAnalytical Discovery HS C_{18} (250×4,6 mm; 5 µm) 25 ˚C H_2O+1% acetic acid, and CH_3OH Gradient Flow: 1 mL/min	51	Best solvent-to-feed ratio: 290 Co-solvent: 20% EtOH Extraction: 50 ˚C Separation: 55 ˚C Pressure: 30 MPa	(Xynos *et al.*, 2012) [81]

Unknown (November 2010)	Fresh leaves Steam and hot water blanching; air-dried at 60 ˚C	**Solid-liquid extraction** Ethanol/H_2O (7:3)	**Analytical** HPLC-DAD (280 nm) Pinnacle II RP C_{18} (150×4,6 mm, 3 µm), 40 ˚C Kromasil 100-5 C_{18} (3,0/4,6 mm) 0,02 M sodium acetate pH 3,2 + acetic acid, and ACN Flow: 1 mL/min	*Hot water blanched* 4,63-5,06 *Non-blanched* 0,21-2,14	Oleuropein content was higher when steam or hot water blanching were used	(Stamatopoulous *et al.*, 2012) [6]
Chemlali, Chetoui, Meski, Sayali and Zarrazi	Dried leaves (MW-assisted, 800 W, 2 × 2 min)	**Solid-liquid extraction** CH_3OH/H_2O (4:1) 24 hours	**Analytical** Mid-infrared spectroscopy (4000 cm^{-1} and 700 cm^{-1})	109,2 to 171,7	Mid-infrared spectroscopy as rapid tool to predict oleuropein content;	(Aouidi *et al.*, 2012) [64]
Serrana	Fresh leaves Hot air (HAD) or freeze (FD) drying	**Solid-liquid extraction** Ethanol/H_2O (4:1) 24 hours	**Analytical** HPLC-DAD/MS-MS (240, 280 and 330 nm) Lichrospher 100 RP_{18} (250×4 mm, 5 µm) 2,5% acetic acid in H_2O, and acetonitrile Linear gradient Flow: 1 mL/min ESI – negative mode Desolvation temperature: 365 ˚C Vaporizer temperature: 400 ˚C Dry gas: N_2 12 L/min Nebulizer: 4,83 bar	*Fresh HAD 70 ˚C* 69 *Fresh HAD 120 ˚C* 108,6 *FD conventional* 3 *FD N_2* 16,44 *HAD 70 ˚C+FD N_2* 30,1 *HAD 120 ˚C+FD N_2* 48	Hot air drying of leaves gives high oleuropein recovery	(Ahmad-Qasem *et al.*, 2013) [62]

Koroneiki	Air dried leaves	**Pressurized liquid extraction (PLE)** Variables: temperature, static time, extraction cycles and Ethanol % Pressure: 1500 psi	**Analytical** HPLC-DAD (248 nm) Supelco Analytical Discovery HS C_{18} (250×4,6 mm; 5 µm) 25 ˚C H_2O+1% acetic acid, and CH_3OH Gradient Flow: 1 mL/min	261,0	Extraction yield affected by temperature, static time and extraction cycles Optimal conditions for oleuropein extraction: 190 ˚C, EtOH: H_2O (56:44)	(Xynos et al., 2014) [82]

1.6. Synthetic transformations of oleuropein

As reported in chapter 1.2, the molecular structure of oleuropein can be divided into three subunits: hydroxytyrosol, monoterpene and glucose moieties (Figure 1.2.). The glucose moiety is responsible for the water solubility of oleuropein, but to fully take advantage of all oleuropein chemical features it is essential to remove this problematic moiety to produce more handlable molecules.

Secoiridoids easily react with solvents and are transformed into other compounds during extraction processes. This is caused by the easy opening of the secoiridoid ring after hydrolysis of the glucose moiety. Possible transformation pathways of oleuropein aglycone in olive leaves when methanol, chloroform and acidic solvents are used, are shown in Scheme 1.3. [83, 84]

The monoterpene moiety is interesting from chemical reactivity point of view, since it has seven potential reactive positions (→) available for synthetic chemical modifications. In addition, it has two stereocenters (*), a feature that by synthetic chemistry is difficult to obtain (Figure 1.5.).

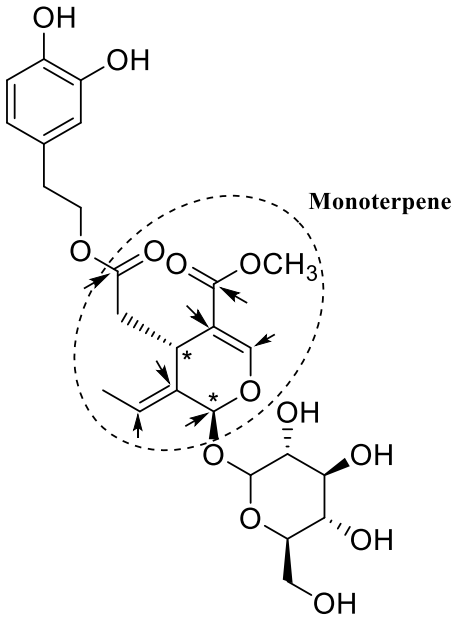

Figure 1.5. Monoterpene unit chemical features. Reactive positions represented by arrows; stereocenters represented by (*).

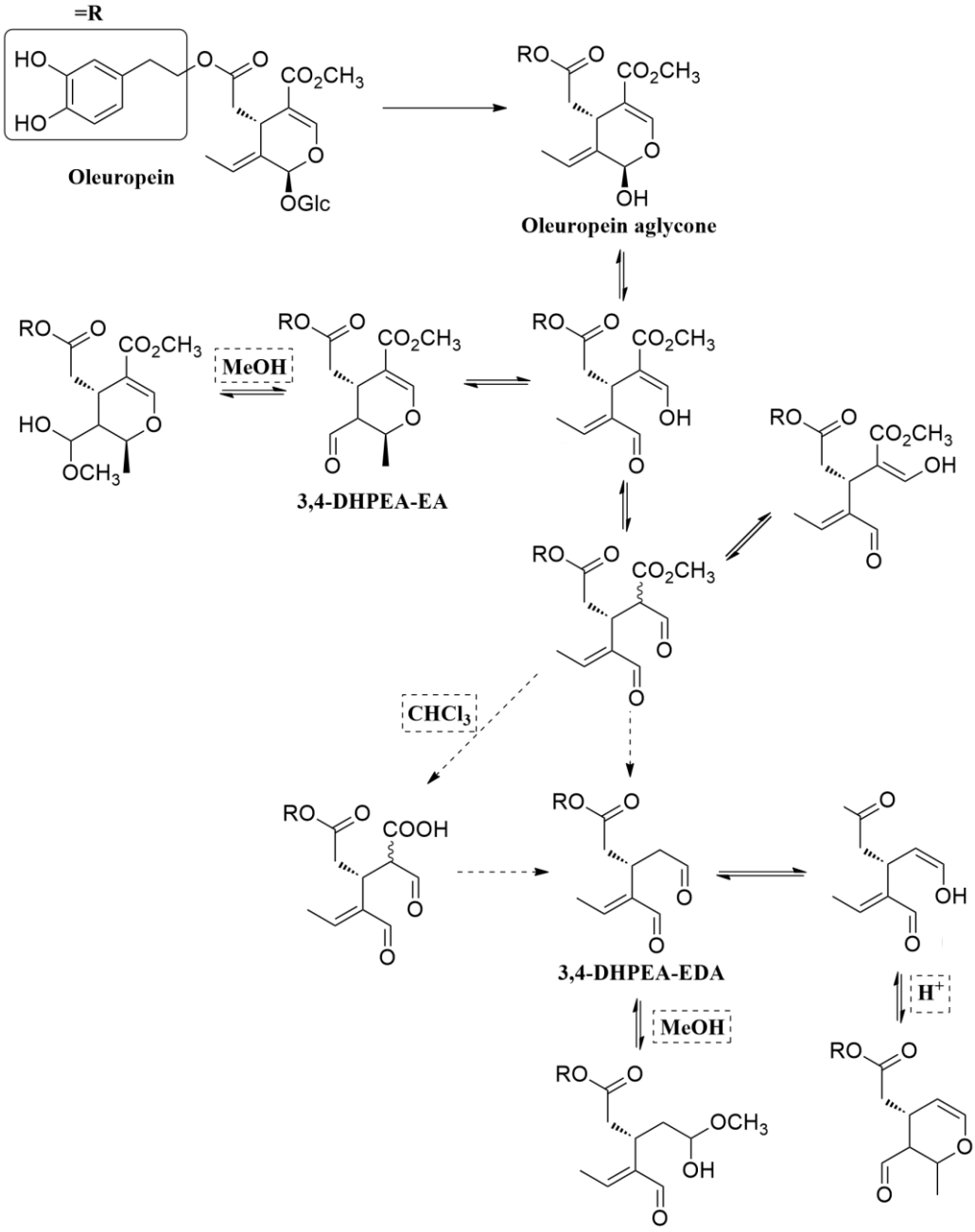

Scheme 1.3. Proposed transformations of oleuropein aglycone by solvents as methanol, chloroform and acidic solutions. Solvents are identified by dashed boxes. Adapted from Paiva-Martins *et al., J. Agric. Food Chem.*, 56 (2008). [84]

Several procedures for the cleavage of the glucose moiety were reported in the literature, using enzymes or by chemical hydrolysis.

Gariboldi *et al.* proposed an acid hydrolysis of oleuropein using sulfuric acid (H_2SO_4) in dioxane to produce elenolic acid in 7 % yield (Scheme 1.4). (75)

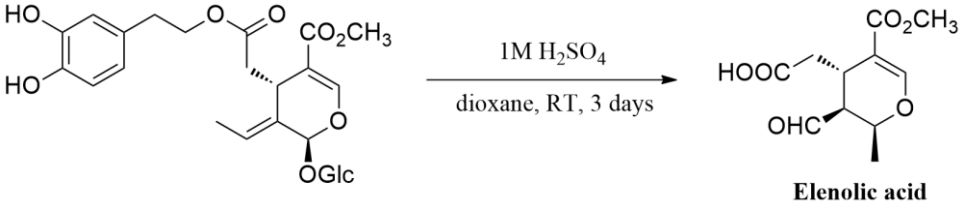

Scheme 1.4. Acid hydrolysis of oleuropein with sulfuric acid to produce elenolic acid.

Guiso *et al.* made the hydrolysis of oleuropein using commercial endogenous *β*-glucosidase from almonds, concluding that oleuropein aglycone by the enzymatic hydrolysis is actually a mixture of compounds with different structures. The relative amounts of these compounds in the mixture depend on the employed enzyme and the hydrolysis protocol. [(85)] Kikuchi *et al.* also studied the enzymatic hydrolysis of oleuropein using this enzyme. [(86)] Briante *et al.* used hyperthermophilic *β*-glucosidase for the hydrolysis of commercially available oleuropein. [(87)]

Procopio *et al.* reported the use of lanthanides, namely erbium (Er), to hydrolyse the glucose moiety.

The molecular structures assigned revealed the presence of two elenolic acid forms, hemiacetal and dialdehyde, as well as a product which results from the rearrangement of the oleuropein aglycone, possibly through a 1,4 - addition of the enolic form of the aldehyde closer to methyl ester to the double bond (Scheme 1.5).

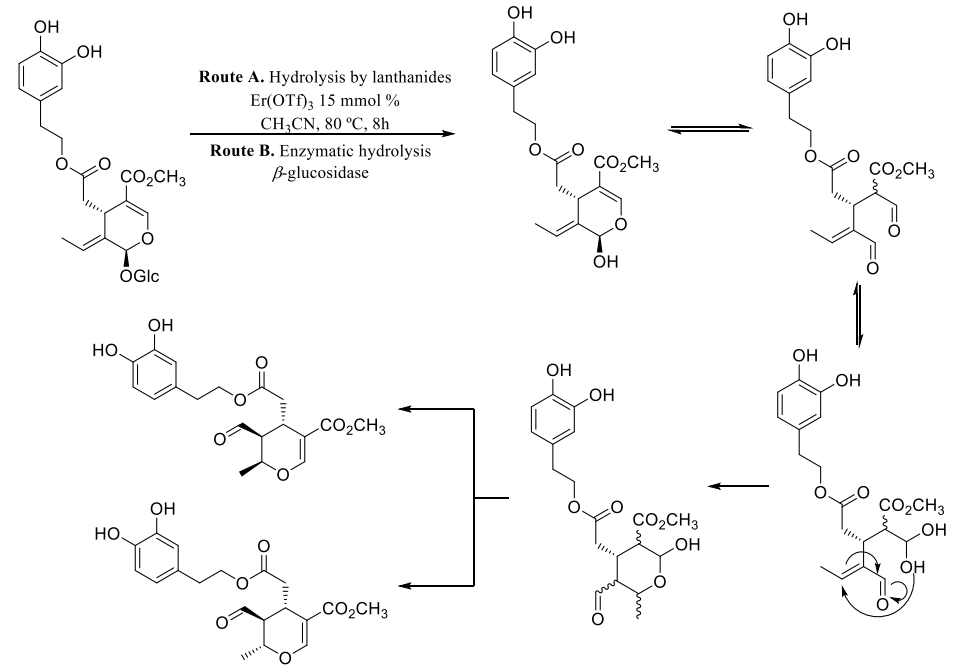

Scheme 1.5. Molecular structures of the aglycone forms of oleuropein after treatment with *β*-glucosidase or hydrolysis by lanthanides.

The authors also synthesized the peracetylated forms of oleuropein, hydroxytyrosol and aglycone compounds in 65 % yield using $Er(OTf)_3$ as catalyst for the peracetylation (Scheme 1.6.). [80]

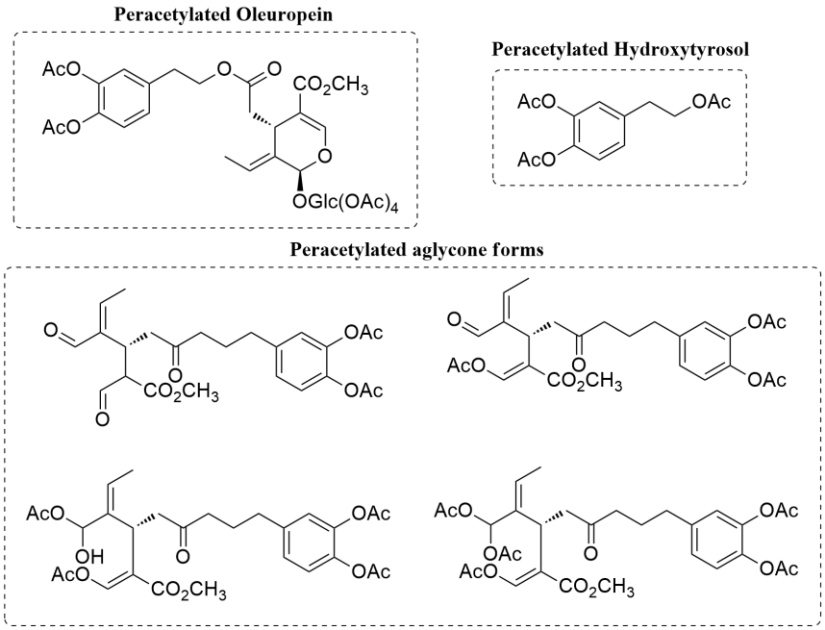

Figure 1.6. Molecular structures of peracetylated forms of oleuropein, hydroxytyrosol and aglycones.

Hanessian *et al*. reported the hydrolysis of hydroxytyrosol ester of oleuropein to the respective carboxylic acid, using sodium hydroxide, followed by acetylation to afford the oleoside monomethyl ester peracetate (Scheme 1.6) [88]

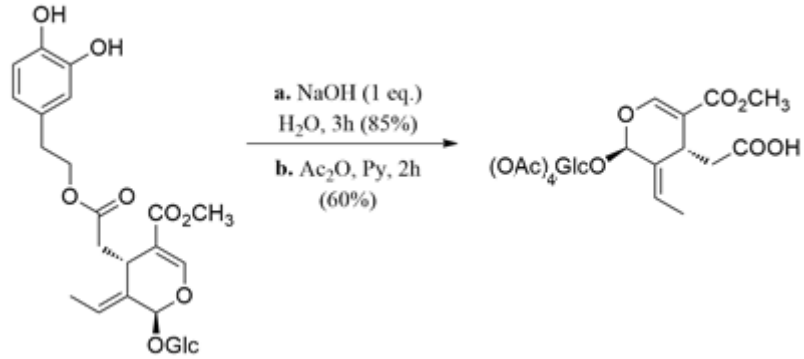

Scheme 1.6. Hydrolysis of hydroxytyrosol ester and acetylation of glucose. Adapted from Hanessian *et al.* Organic Letters, *8*, 2006, 4047-9 . [88]

Other transformations of oleuropein were also reported, to produce different scaffolds.

Ranarivelo *et al*. reported the treatment of oleuropein with *β*-glucosidase in the presence of ammonium chloride to produce monomeric pyridine alkaloids (5 % yield). The use of ammonium acetate permitted conversion of oleuropein into jasminine in 20 % yield (Scheme 1.7). [89]

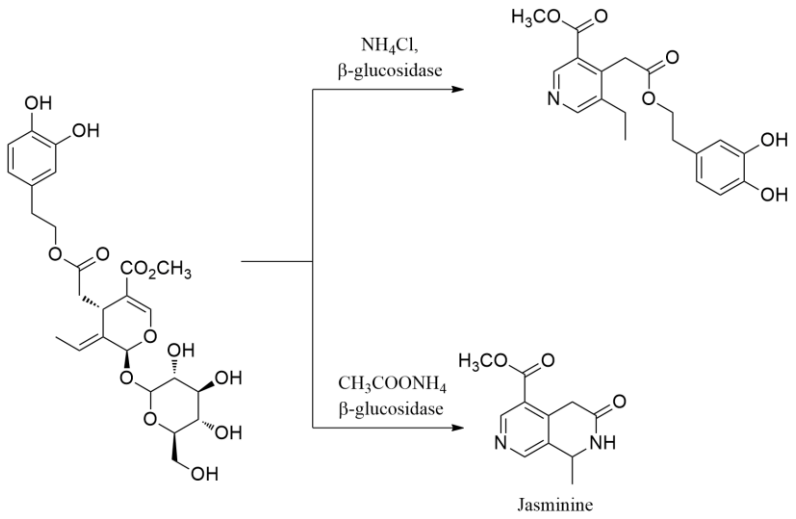

Scheme 1.7. Synthesis of pyridine alkaloids from oleuropein; Adapted from Ranarivelo *et al.*, *Nat. Prod Lett.*, 2001, 15(2), 131-7.[89]

Bianco *et al.* examined the acid rearrangement of secoiridoids. The reduction of oleuropein with sodium borohydride ($NaBH_4$) in water produced oleuropeinol, with reduction of both hydroxytyrosol and methyl esters moieties to the respective alcohols. The further acidic rearrangement of oleuropeinol using aqueous HCl removed the glucose moiety. By thin layer chromatography (TLC) only one compound was observed, but proton spectra in nuclear magnetic resonance (^{1}H NMR) showed an equilibrium between the open dialdehyde form *b* (20 %) and the closed acetal form *a* (80 %). A longer rearrangement of oleuropeinol does not give a major compound, leading to degradation instead. The equilibrium mixture of *a* and *b* was acetylated, giving only one main product *c* (98 %), found to be the monoacetyl derivative of the open form *b*. This means that the equilibrium shifts towards the open form, that is further acetylated. The mixture of *a* and *b* was also reduced with sodium borohydride, in methanol, producing only compound *d* (98 %) (Scheme 1.8). [90]

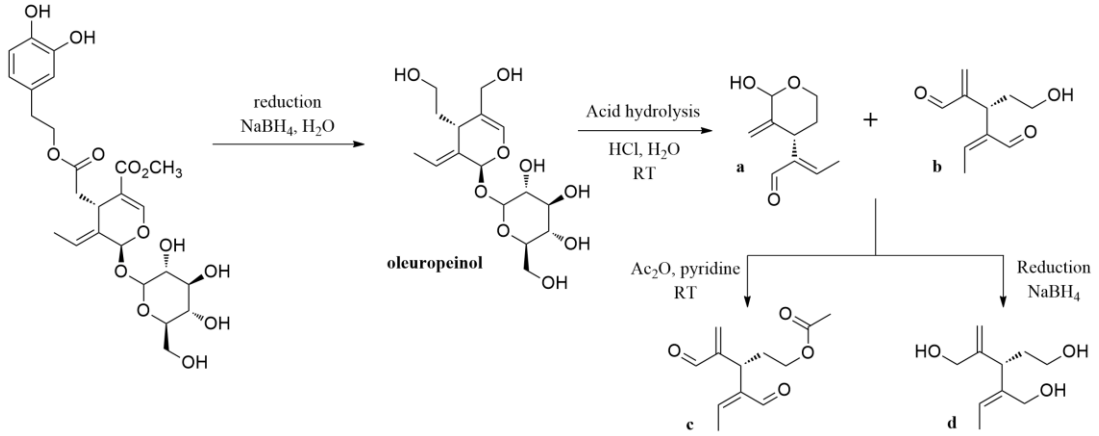

Scheme 1.8. Reduction of oleuropein to oleuropeinol; hydrolysis of oleuropeinol to compounds a and b; acetylation and reduction of the mixture of compounds a and b

The only reported modification of oleuropein in methanol was the transesterification of hydroxytyrosol ester to a methyl ester. In contrast, the acid rearrangement of oleuropeinol in methanol gave two major products. Compound *e* results from the formation of a cyclic hemiacetal moiety between the primary alcohol function and the aldehyde function, which affords the cyclic acetal (40 %). Compound *f* probably arises from the open aldehyde form. ^{1}H NMR showed four signals characteristic of the methoxy groups present. This reaction was left for several hours, giving compound *e* as a major product, and suggesting the existence of an equilibrium between compounds *e* and *f*, which slowly converts into the more stable *e* (Scheme 1.9). (90)

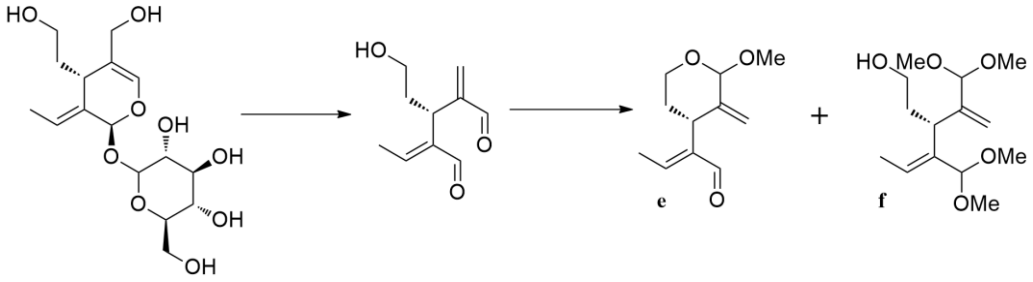

Scheme 1.9. Acid rearrangement of oleuropeinol in methanol.

Vougogiannopoulou *et al*. developed an efficient procedure for a one step semi synthesis of oleacein from oleuropein, under Krapcho decarbomethoxylation. The possible conversion of oleuropein to oleacein involved goes through a three-step procedure: cleavage of the glucose moiety, secoiridoid ring-opening followed by the formation of the two aldehyde groups and decarbomethoxylation. Krapcho reaction was successfully applied in order to perform these three steps in one pot (Scheme 1.10). (91)

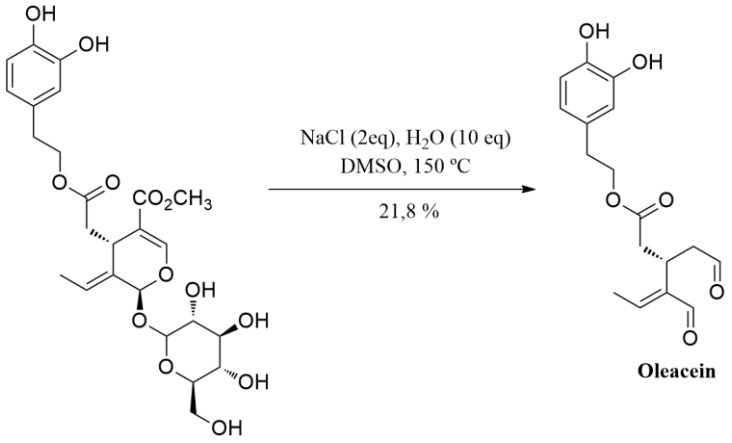

Scheme 1.10. Krapcho decarbomethoxylation of oleuropein to produce oleacein.

1.7. Biological activity of oleuropein and its derivatives

The study of biological and pharmacological activity has revealed that secoiridoids exhibit a wide range of bioactivity.[28]

Oleuropein has potent biological and pharmacological properties. Its main pharmacological activities are anticancer, cardioprotective, neuroprotective, gastroprotective, hepato-protective, anti-diabetes, anti-obesity and radioprotective. These properties are in large part attributed to its antioxidant and anti-inflammatory effects.[92] Oleuropein derivatives were also found to have biological and pharmacological properties.

The accumulation of free radicals on cellular membrane lipids play a major role in various pathological disorders, including atherosclerosis, cancer, aging, rheumatoid arthritis and inflammation. [93] It is known that compounds sharing an orthodiphenolic (catecholic) structure possess antioxidant activity and the main reason of high antioxidant capacity of oleuropein is the existence of catechol structure, having the ability to scavenge free radicals that were possibly formed.[19]

The health benefits associated to olive leaf extracts, oleuropein and its derivatives are presented in Table 1.2. For this, several studies were performed *in vivo* and *in vitro* in animal models, cell lines and human volunteers.

Table 1.2. Health benefits of olive leaf extracts, oleuropein and its derivatives.

Studies	Compounds	Subjects/Cell models	Effects
In vivo Animal studies	Olive leaf extract	Adult male Swiss mice; whole-body irradiated with a single dose of 48 cGy	Antioxidant and radioprotective effects; hydroxyl radical scavenging capacity [94]
	Oleuropein	Adult male Spargue-Dawley rats; oleuropein plus ethanol (12 mg/Kg body weight; 10 days)	Antioxidant effect by scavenging of ROS, produced by ethanol that initiate lipid peroxidation [95]
	Oleuropein and Hydroxytyrosol	Adult male Wistar rats; diabetes induced with alloxan	Anti-diabetic and antioxidant effects [79]
	Hydroxytyrosol and its triacetylated derivative	Wistar rats fed a standard laboratory diet or cholesterol-rich diet	Lipid-lowering and antioxidant effects [10]
	Olive leaf extract	Wistar rats exposed to cold restraint stress; olive leaf extract (80 mg/Kg daily) dissolved in distilled water	Modulation of cold restraint stress oxidative changes in rat liver by inhibition of lipid peroxidation [96]
	Olive leaf extract	Sprague-Dawley rats receiving gentamycin (25 mg/Kg, 50 mg/Kg or 100 mg/Kg daily, 12 days)	Amelioration of gentamycin nephrotoxicity by inhibition of lipid peroxidation [97]

	Oleuropein	Female C57BL/6 mice; azoxymethane (AOM)/dextran sulphate sodium (DSS)-induced colorectal cancer; oleuropein (50 mg/Kg or 100 mg/Kg) dissolved in distilled water	Protection from AOM/DSS-induced colorectal cancer associated with acute colitis; suppression of the growth and multiplicity of colonic tumours [98]
	Hydroxytyrosol	Adult male Wistar rats; C6 glioma cell implantation; subcutaneous injections of 100 µg oleuropein, 100 µg hydroxytyrosol or both daily, for 5 days	Only hydroxytyrosol inhibited tumour growth [99]
	Oleuropein	Visceral leishmaniasis model *L. donovani*-infected BALB/c mice; intraperitoneal injection of oleuropein 14 times	Oleuropein and hydroxytyrosol selectivity for L. donovani; Oleuropein gave parasite depletion of >95% in liver and spleen after 6 weeks [100]
In vivo Human studies	Oleuropein	10 healthy female 20-30 years having skin Fitzpatrick types II and III	Soothing effect in the treatment of UVB-induced erythema [101]
In vitro Animal studies	Oleuropein	Normal mouse hepatocyte FL83B cells; HepG2 and FL83B cells	Decrease of the number size of lipid droplets in free fatty acid-treated cells and reduced intracellular triglyceride accumulation [102]
	Olive leaf extract	*Bacillus cereus* CECT 148; *B. subtilis* CECT 498; *Staphylococcus aureus* ESA 7; *Escherichia coli* CECT 101; *Pseudomonas aeruginosa* CECT 108; *Klebsiella pneumoniae* ESA 8. *Candida albicans* CECT 1394; *Cryptococcus neoformans* ESA 3.	Antimicrobial effects observed with contribution of oleuropein and hydroxytyrosol [48]
In vitro Human studies	Oleuropein	Whole blood of 11 healthy male volunteers	Inhibition of platelet activation by scavenging of H_2O_2 produced in arachidonic acid metabolism cascade that leads to platelet aggregation [103]
	Oleuropein and Hydroxytyrosol	Human breast cancer cell line MCF-7	Apoptotic cell death of human breast cancer MCF-7 cells [104]

	Oleuropein and its semi-synthetic peracetylated derivatives	Human breast cancer cell lines (MCF-7 and T-47D)	Anti-proliferative and antioxidant effects; the peracetylated compounds exerted higher antiproliferative effects than oleuropein [105]
	Hydroxytyrosol rich extract	MCF-7 human breast cancer cells	A dose-dependent growth inhibition of MCF-7 cells [106]
	Olive leaf extract	Peripheral blood leukocytes from six healthy volunteers	Protective effect on the peripheral blood leukocytes against adrenaline induced DNA damage [107]
	Olive leaf extract	Human endothelial cells from bovine brain, MCF-7 cells and T-24 cells (human urinary bladder carcinoma)	Antiproliferative effect against cancer and endothelial cells [108]
	Olive leaf extract (oleuropein and apigenin-7-glucoside)	Human HL-60 cells	Apigenin-7-glucoside of the olive leaf extract was mainly responsible for the HL-60 differentiation and oleuropein showed to exert an influence over this differentiation [109]
	Oleacein	Human recombinant 5-lipooxygenase (5-LO)	Inhibition of 5-LO (IC_{50} = 2 µM), acting as anti-inflammatory agent [91]

Having all these biological properties, oleuropein and its derivatives are promising compounds to be used for pharmaceutical and even cosmetic purposes. Then, it is important to stimulate research from different areas to enhance the content of compounds of interest.

2. Objectives

The lack of research on the synthetic transformations of oleuropein, lead to the purpose of this work to explore some of the reactions already reported, and a complete study of the methanolysis of oleuropein in acidic conditions.

The work started by the extraction and isolation of oleuropein from olive leaves, followed by the study of several reactions in order to remove the problematic glucose and hydroxytyrosol moieties, including methanolysis. For the optimization of methanolysis reaction, several conditions were screened including protic acids, acidic resins and the effect of temperature, which also gave us some mechanism insight of the reaction. A continuous flow approach of the methanolysis of oleuropein was also studied.

The objective of these reactions was the use of an abundant and easily obtained natural product with known biological properties, that can be used as a scaffold in the synthesis of new derivatives with additional interest, such as new potential pharmaceutical properties, by taking advantage of its chemical features.

3. Results and Discussion

3.1. Extraction and isolation of oleuropein from olive leaves

The first part of the work consisted on the extraction and isolation of oleuropein from olive leaves, which are known as an excellent bio-renewable source of oleuropein, that can be found in high amounts in Mediterranean countries, namely Portugal.

In order to find the best conditions to obtain oleuropein from the leaves, different extraction methods were performed, as shown on Table 3.1.

Table 3.1. Extraction and purification conditions of oleuropein from dried olive leaves.

Entry	Air drying conditions	Extraction conditions	Purification conditions	Yield (mg/g)[2]
1	No moisture	30 g olive leaves + 150 mL CH_3OH/H_2O (4:1) RT, stirring overnight Filtration → solvent evaporation	Column Flash Chromatography Büchi CH_2Cl_2 (0-2 min); ↓ % CH_2Cl_2 (2-5 min); CH_2Cl_2/CH_3OH 9:1 (5-10 min); ↓ % CH_2Cl_2 (10-13 min); CH_2Cl_2/CH_3OH 8:2 (13-20 min)	13,4
2		10 g olive leaves + 100 mL H_2O Reflux, stirring overnight Filtration → H_2O evaporation → redissolution acetone → filtration → acetone evaporation	NA	Small amount ND
3		8 g olive leaves + 80 mL H_2O MW 300 W, 100 ˚C, stirring 15 min Filtration → H_2O evaporation → redissolution acetone → filtration → acetone evaporation	Column Flash Chromatography CH_2Cl_2/CH_3OH (9:1)	4,25

[2] Yield expressed has mass of oleuropein (mg) per mass of olive leaves dry weight (g).
NA – purification not performed.
ND – not determined; NP – not present.

4		200 g olive leaves + 2 L H_2O + domestic microwave, 20 min, medium/high Filtration → H_2O evaporation → redissolution acetone → filtration → acetone evaporation	Column Flash Chromatography Combi 0 % CH_3OH (0 - 2,1 min) → 0 – 10 % CH_3OH (2,1 – 4 min) → 10 % CH_3OH (4 – 7,1 min) → 10 – 20 % CH_3OH (7,1 – 10,1 min) → 20 – 20,2 % CH_3OH (10,1 – 33,4 min).	15
5	Moisture	10 g olive leaves + 100 mL H_2O RT, stirring, 2 days Solvent evaporation	NA	ND
6		10 g olive leaves + 80 mL H_2O + domestic microwave, 20 min, medium/high Filtration → H_2O evaporation → redissolution acetone → filtration → acetone evaporation	Preparative TLC CH_2Cl_2/MeOH (9:1)	NP
7		100 g milled olive leaves (from box) + 500 mL CH_3OH + agitation, RT, 3 days Filtration → MeOH evaporation → redissolution acetone/H_2O (1:1) → extraction with *n*-hexane → organic phase recovery → extraction with CH_2Cl_2 → organic phase recovery → solvents evaporation	*n*-hexane fraction redissolved in CH_2Cl_2 → chlorophylls removed with activated charcoal → filtration with celite Column flash chromatography: CH_2Cl_2	NP

Two different lots of olive leaves were used, both dried under room conditions, being the only difference the presence or absence of atmospheric moisture. This factor revealed to be crucial, affecting the amount of oleuropein in olive leaves, as discussed in Section 1.5.2.

As showed on Table 3.1. **(entries 5 to 7)**, oleuropein was not detected in leaves dried in the presence of moisture. This may happen due to the activation of endogenous enzymes, such as *β*-glucosidase, responsible for the transformation of oleuropein into apolar compounds by removal of the glucose moiety, and so decreasing the amount of oleuropein in the leaves dried in these conditions.[59, 110]

For leaves dried without atmospheric moisture **(entries 1 to 4)**, significant amounts of oleuropein were isolated, except for the conditions on **entry 2**. The reflux for such long time, probably lead to some degradation of oleuropein, resulting in a smaller amount.

The best reproduced extraction method was the one proposed by Procopio *et al.* [80] The extraction was assisted by a domestic microwave (MAE), using water as solvent **(entry 4)**,

resulting in a yield of 15 mg of oleuropein per gram of olive leaves dry weight. The MAE allowed an efficient and fast extraction of olive leaves' byphenols, compared to solid-liquid extractions involving agitation **(entry 1)** and high temperatures **(entry 2)**. The short time of extraction avoided a long-time exposure of the compounds to high temperatures and, subsequently, degradation. However the use of the microwave apparatus (QLabo CEM Discover) **(entry 3)**, resulted in smaller yield of oleuropein compared to the domestic microwave.

Being appropriated for microwave use, water was a good solvent for extraction, in which oleuropein exhibited good solubility. Acetone was used to exclude some compounds with more polarity from the mixture obtained by water extraction. Oleuropein **1** was isolated by column flash chromatography in Combi Flash apparatus, through a multi-step gradient elution method, using a variable mixture of methanol and dichloromethane as mobile phase.

The structure of oleuropein **1** was confirmed by NMR spectroscopy and LC-MS-ESI experiments, proving that oleuropein was successfully isolated with high purity (Appendix I). In ^{1}H NMR spectrum (Figure 3.1), the hydroxytyrosol moiety was represented by the signals appearing in the aromatic region (H7', H4' and H8'), by a multiplet at 4.08-4.26 ppm (H1'), and a signal in aliphatic region for H2'. The singlet at 7.52 ppm was characteristic of oleoside type secoiridoids (H3). Together with other signals, such as the ones for H8 and H10 for the exocyclic olefin, the aliphatic diastereotopic protons (H_a6 and H_b6) and H5, as well as the singlet at 3.72 ppm for the carbomethoxy group (H12), corroborating the presence of the monoterpenic unit. The glucose moiety was also represented by the doublet for H1'' at lower field, the signals for H_a6'' and H_b6'', and the multiplet corresponding to H2'', H3'', H4'' and H5''.

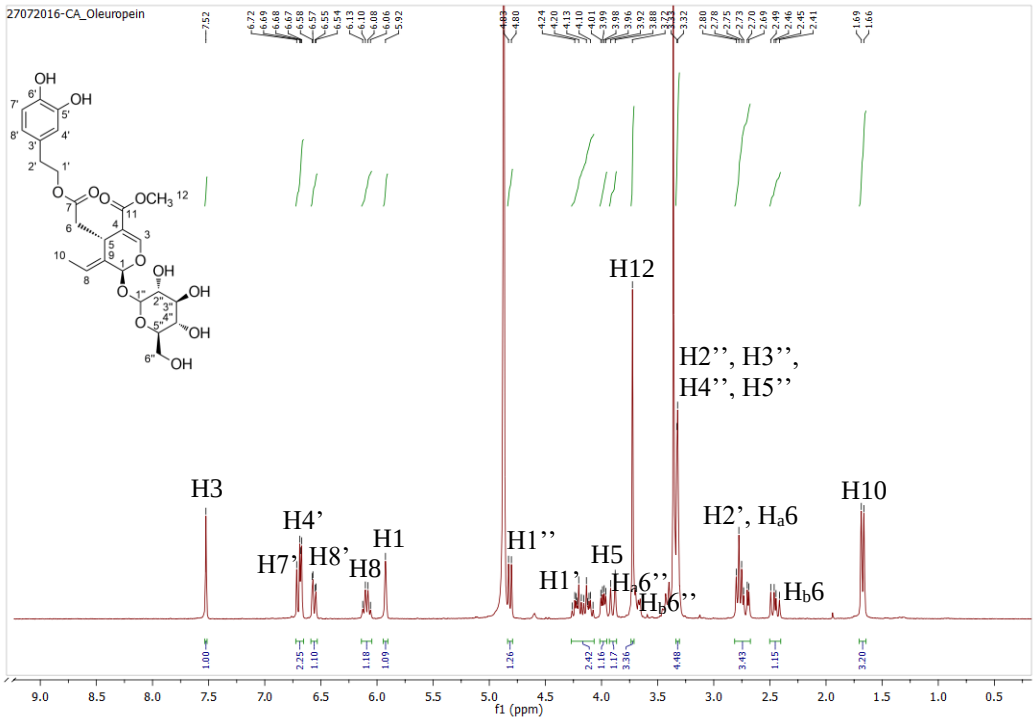

Figure 3.1. ^{1}H NMR spectrum of oleuropein 1, in CD_3OD.

The correlations at the homonuclear (COSY) and heteronuclear (HSQC and HMBC) 2D NMR spectra allowed to make all the correct assignments, which were in concordance with the literature.[111]

LC-MS-ESI experiments were performed in negative and positive mode. Knowing that the exact mass of oleuropein is 540.2, two main fragmentations were observed in negative mode. The pseudo molecular ion was observed at 539.2 *m/z*, corresponding to the loss of a proton $[M-H]^-$. The base peak was observed at 575.2 *m/z*, corresponding to oleuropein and a chlorine $[M+Cl]^-$. In positive mode, a peak was detected at 563 *m/z*, characteristic of an adduct of the molecule and a sodium cation $[M+Na]^+$.

3.2. Semi-synthetic transformations of oleuropein

After extraction and isolation, we proceeded to the study of semi-synthetic transformations of oleuropein **1**. Several reactions were attempted in order to remove the glucose and hydroxytyrosol moieties and produce more handlable compounds.

*3.2.1 Krapcho decarbomethoxylation of oleuropein **1***

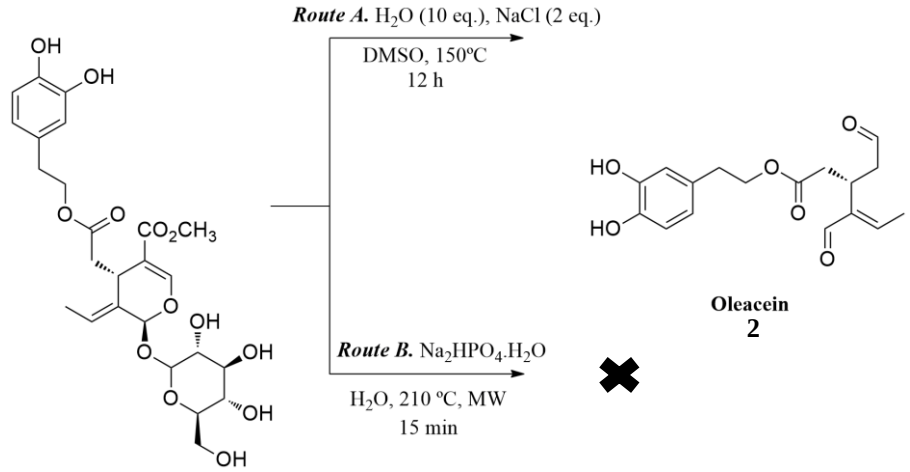

Scheme 3.1. Two routes for Krapcho decarbomethoxylation of oleuropein 1.

The Krapcho decarbomethoxylation was performed to remove the glucose moiety of oleuropein and produce oleacein **2** (Scheme 3.1), the decarboxylated open dialdehyde form of the monoterpene unit, coupled with the hydroxytyrosol moiety.

We reproduced the reported standard conditions (**Route A**),[91] obtaining oleacein **2** in 0,3% yield. The low value, compared with the reported one of 21,5 %, could be explained by the formation of other sub-products and problems with the isolation, contributing to some losses.

The presence of oleacein **2** was supported by comparison between the reported and experimental ^{1}H NMR spectra (Figure 3.2.). The signals characteristic of the two aldehydes were observed at 9.65 ppm (H3) and at 9.20 ppm (H1). Signals visible at the aromatic region confirmed the unaltered hydroxytyrosol unit. The poor resolution of the spectrum is due to the low concentration of the sample, which did not allow to identify clearly the other signals.

Other conditions were carried out to overcome the problem of DMSO evaporation (**Route B**). We used the microwave-assisted Krapcho decarbomethoxylation, performed by Mason *et al*. for alkyl malonate derivatives,[112] using oleuropein as substrate and the salt $Na_2HPO_4.H_2O$, identified as the best catalyst. However, no product was observed, and so other approaches were explored.

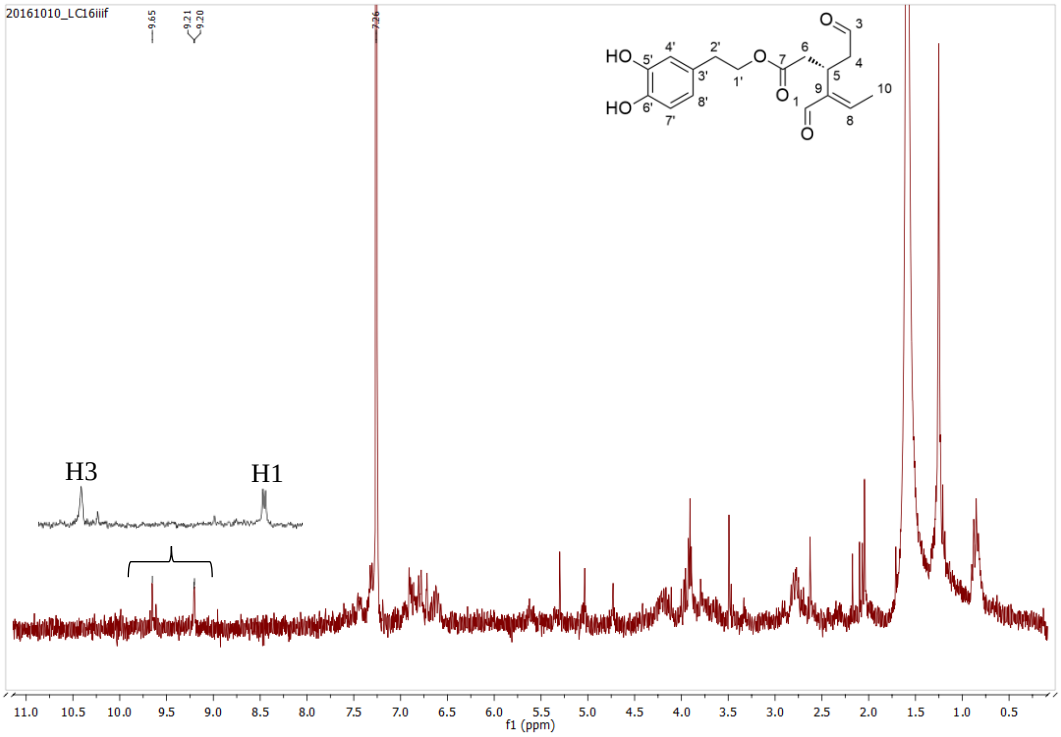

Figure 3.2. ^{1}H NMR spectrum of oleacein 2, in $CDCl_3$.

3.2.2 Hydrolysis of the glucose moiety by β-glucosidase

Since the Krapcho decarbomethoxylation did not give the desired product in high yields other approaches were explored. The enzymatic hydrolysis of oleuropein with *β*-glucosidase was attempted to remove the glucose moiety.

The conditions proposed by Romero-Segura *et al.*[110] were reproduced and the sugar was successfully removed. The reaction had not full conversion and more than one product was formed. The monoterpene unit without the glucose unit seems to be unstable, and different aglycone compounds could be formed, such as a dialdehyde form that is in equilibrium with the corresponding enolic form, and also compounds resulting from intramolecular 1,2 or 1,4 - additions (Scheme 3.2.).

The major compound formed was isolated in 2,8 % yield, by preparative TLC using EtOAc/Hexane (4:1) as mobile phase, and analysed by ^{1}H NMR (Figure 3.3.). The doubling of all signals indicated the presence of two diastereoisomers in an approximated 1:1 ratio. The chemical shifts were in concordance with the literature,[75] indicating the formation of two isomers obtained by the intramolecular rearrangement through a 1,4 - addition (Scheme 3.2.). However, more studies needed to be done to confirm the molecular structure and the absolute configuration at C-1 and C-9. In addition, some integrations were not accurate due to the impurities of the sample.

Nevertheless, this methodology was dropped due to the low yields obtained.

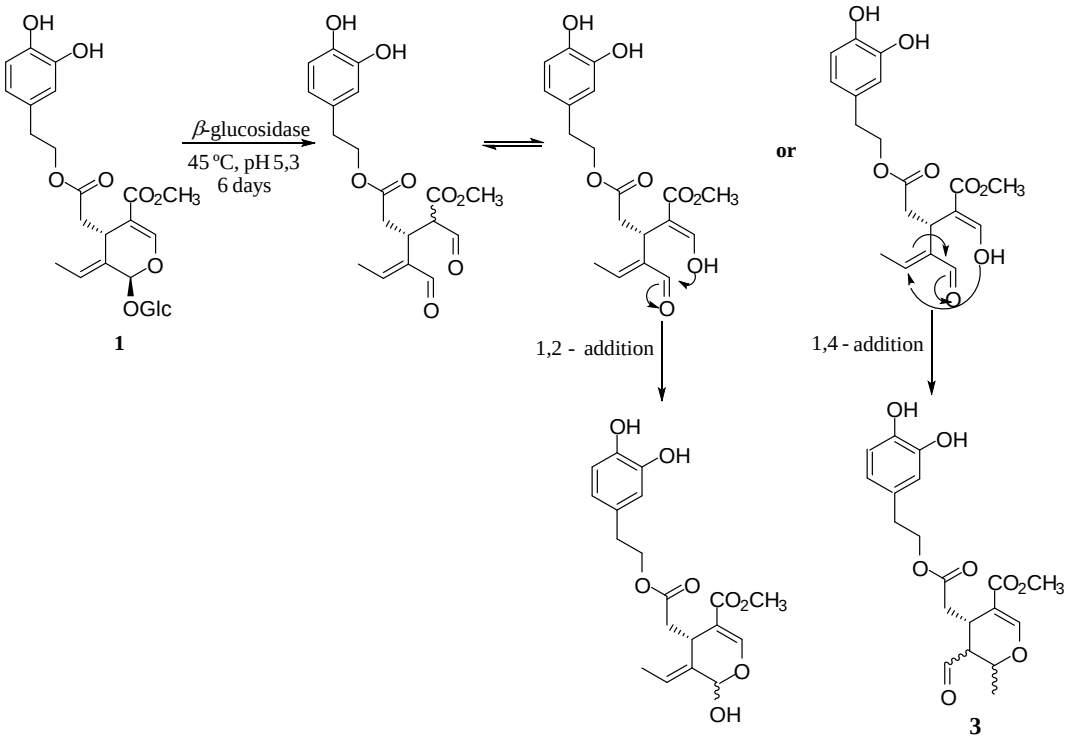

Scheme 3.2. Proposed transformations of oleuropein 1 by *β*-glucosidase.

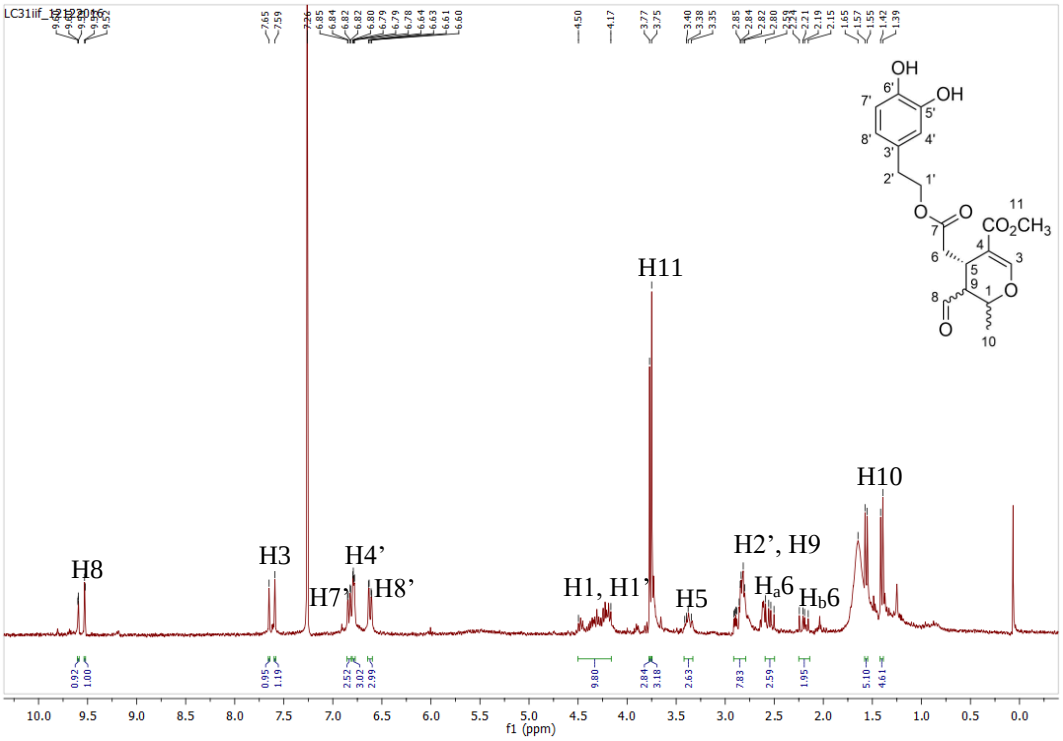

Figure 3.3. ^{1}H NMR spectrum of compounds 3, in $CDCl_3$.

3.2.3 Reduction of hydroxytyrosol and methyl esters

Bianco *et al.*[90] used sodium borohydride to synthesize oleuropeinol by the reduction of hydroxytyrosol and methyl esters of oleuropein (**Route A**), represented in Scheme 3.3.

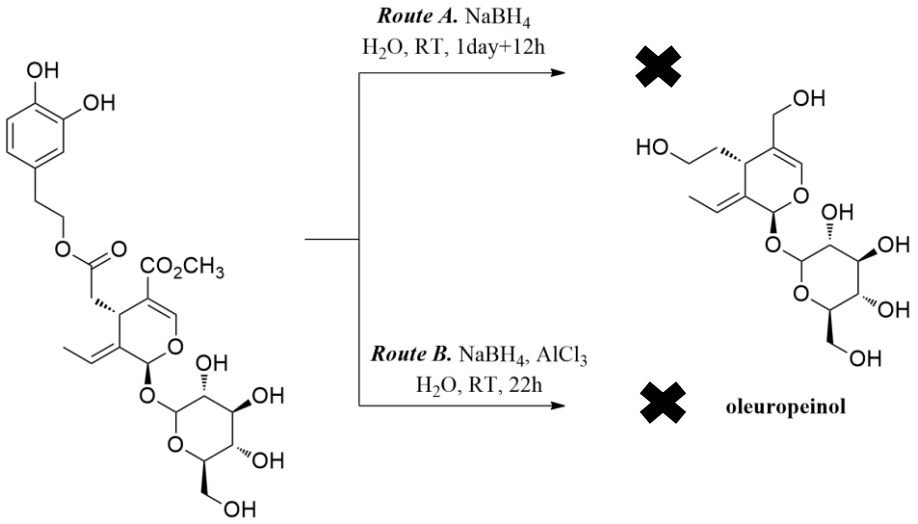

Scheme 3.3. Reduction of oleuropein 1 with $NaBH_4$ to produce oleuropeinol.

We tried to reproduce the described conditions but no oleuropeinol was obtained.

The analysis of the NMR spectra revealed that none of the esters were reduced. The methyl ester remained intact, as indicated by the singlet at 3.74 ppm integrating to three protons in ^{1}H NMR spectrum (Figure 3.4.). ^{13}C NMR spectrum also confirms the existence of the methyl ester with signals appearing at 169.5 ppm (carbonyl group) and 51.8 ppm (carbomethoxy group). ^{1}H NMR spectrum showed no evidence of the phenolic part, meaning that some transformation occurred at the hydroxytyrosol ester. In ^{13}C NMR spectrum was visible a signal at 180.0 ppm, characteristic of carboxylic acids, although no signal of the labile proton was visible in ^{1}H NMR spectrum, due to exchange with deuterium. These observations lead to the conclusion that the hydroxytyrosol ester have suffered hydrolysis. The structure of the new compound, known as jaspolyside **4**,[28] was confirmed by 2D NMR experiments (Appendix II).

ESI-LC-MS experiments, on both positive and negative modes, were performed. In positive mode, a peak appears at 427 *m/z* corresponding to an adduct of the molecule with a sodium cation, $[M+Na]^{+}$. In negative mode, two peaks were observed at 403 *m/z*, by loss of a proton $[M-H]^{-}$ and at 808 *m/z* corresponding to $[2M-H]^{-}$.

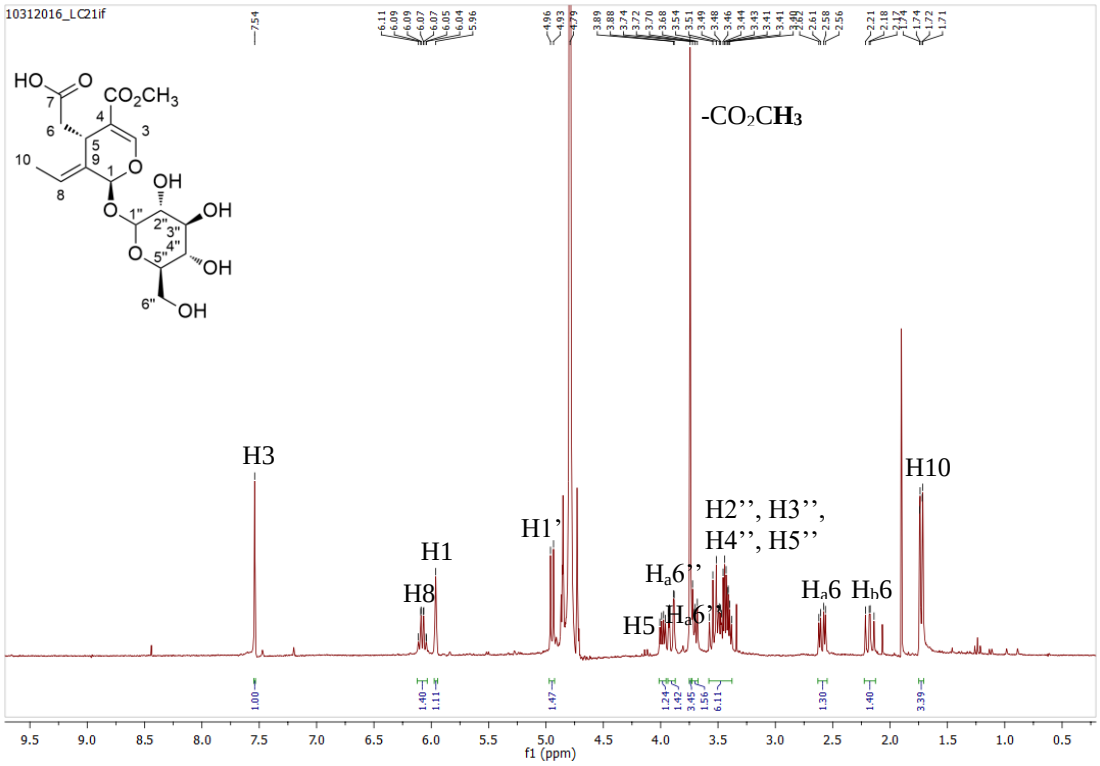

Figure 3.4. ^{1}H NMR spectrum of jaspolyside 4, in D_2O.

Since the conditions of **Route A** failed the purpose to synthesize oleuropeinol, we used a Lewis acid ($AlCl_3$) to catalyse the reduction by $NaBH_4$ (**Route B**), through the activation of the carbonyl groups of both esters. However, this attempt also failed and no product was observed.

Concluding, jaspolyside **4** was obtained in 50 % yield using conditions **A**.[90] In our attempt the reducing agent $NaBH_4$ did not reduce any of the esters to their respective primary alcohols, instead it lead to the hydrolysis of the hydroxytyrosol ester. A stronger reducing agent, such as lithium aluminium hydride ($LiAlH_4$), might be necessary to reduce both esters.

3.2.4 Hydrolysis of hydroxytyrosol ester

The compound jaspolyside **4** obtained from the previous reaction (Section 3.2.3.) was obtained by accident, so we reproduced the conditions of basic hydrolysis reported by Hanessian *et al.*[88] to synthesize this compound, which we isolated in 63 % yield (Scheme 3.4) The presence of the compound was confirmed by ^{1}H NMR by comparison with the previous proton spectrum.

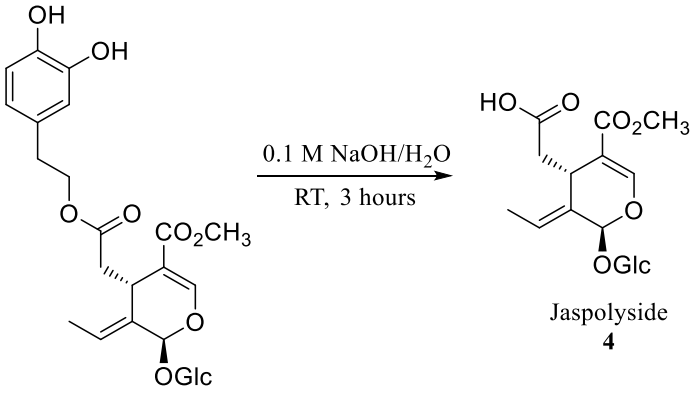

Scheme 3.4. Basic hydrolysis of hydroxytyrosol ester of oleuropein 1 to produce jaspolyside 4.

For the same transformation, an enzymatic approach was also performed, using the enzyme CAL-B with KH_2PO_4/KOH buffer (pH 8,5) at 45 ˚C, for 6 days.

CAL-B is a lipase used for kinetic enzymatic resolution by hydrolysis of racemic esters and transesterification of racemic alcohols. It is known that CAL-B is stereospecific, depending on the substrate, and usually, the slow-reacting enantiomer has *(S)* configuration.(113)

We used CAL-B to perform the hydrolysis of the hydroxytyrosol ester of oleuropein, but the reaction did not occur, probably because oleuropein did not fit well on the enzyme pocket. The configuration of oleuropein stereocenters, might have prevented the catalytic triad (Ser^{105}, His^{224}, Asp^{187}), responsible for the catalysis of the reaction, from work properly.

*3.2.5 Methanolysis of oleuropein **1** in acidic conditions*

In 1995, hydroxyornoside, a secoiridoid isolated from the plant *Fraxinus ornus*, was submitted to an acid methanolysis (16 % H_2SO_4, 4 h), with formation of an acetal compound in 15 % yield. This product results from a transformation in the monoterpene unit, similar to the one found in oleuropein's **1** structure (Scheme 3.5.).(114)

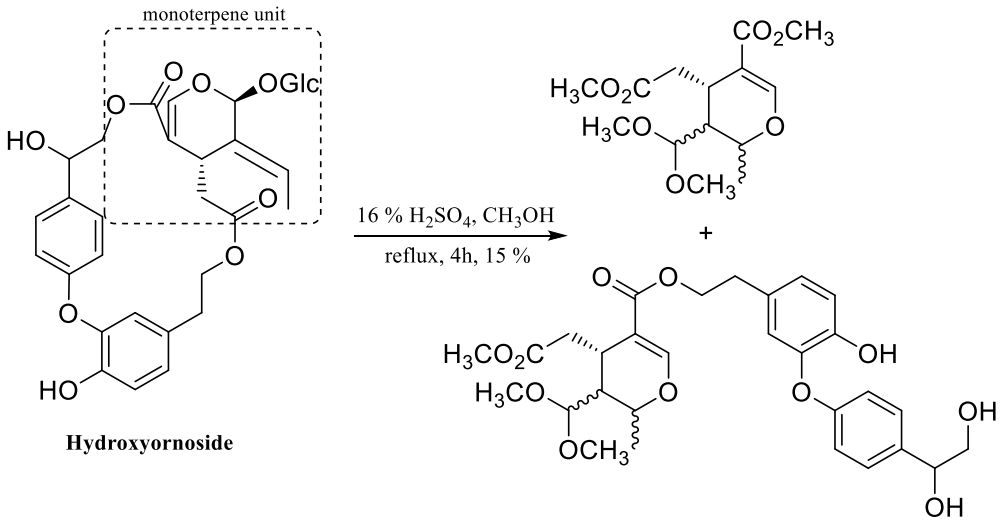

Scheme 3.5. Acid methanolysis of hydroxyornoside.

Considering this precedent literature transformation as a starting point, oleuropein **1** was subjected to a methanolysis reaction using hydrochloric acid (1M, 70 ˚C, 20 h). The elenolic acid derivative **6** (Figure 3.5.) was isolated as a (1:1) diastereomeric mixture in 25 % yield, after purification by column chromatography.

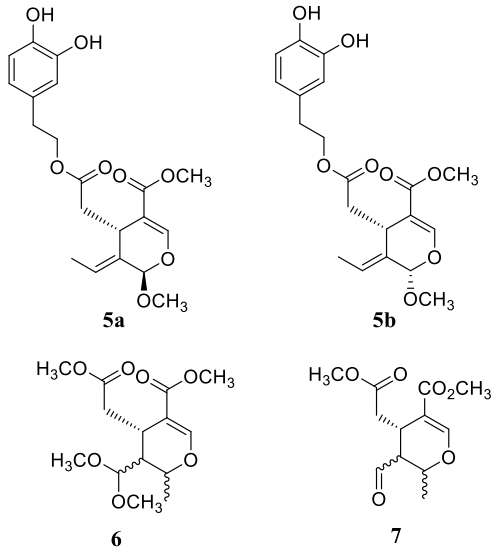

Figure 3.5. Structures of the compounds 5-7 resulted from the methanolysis of oleuropein 1.

The obtained NMR and LC-MS-ESI data (Appendix IV) supported the molecular structures of **6**, and were in agreement with those described in literature.[114] The doubling of all signals indicated the presence of two diastereoisomers in a nearly 1:1 ratio.

In ^{1}H NMR spectrum (Figure 3.6.), the proton (H3) characteristic for oleoside type secoiridoids appeared at 7.58 and 7.53 ppm as singlets, for the two diastereoisomers. The signals of the four methoxy groups (H12 and H13) were visible as two singlets at 3.36 and 3.34 ppm,

each one integrating to three protons, and two superimposed singlets at 3.31 ppm integrating to six protons, suggesting the presence of the acetal group. The signals of the protons of the carbomethoxy groups on methyl esters appeared as singlets at 3.70 and 3.67 ppm (H14), and 3.69 and 3.68 ppm (H15), each integrating to three protons. The chemical shifts related to the methyl group (H10) appears as doublets at 1.43 (J = 9 Hz) and 1.39 ppm (J = 6 Hz). The diastereotopic protons (H6) appeared at 2.82 (J = 9 Hz, 18 Hz) and 2.63 (J = 3 Hz, 15 Hz) ppm (H_a6) and 2.38 (J = 3 Hz, 15 Hz) and 2.23 (J = 9 Hz, 18 Hz) ppm (H_b6) as doublets of doublets.

The stereochemistry at C-1 and C-9 could not be assigned due to the complexity of the spectra.

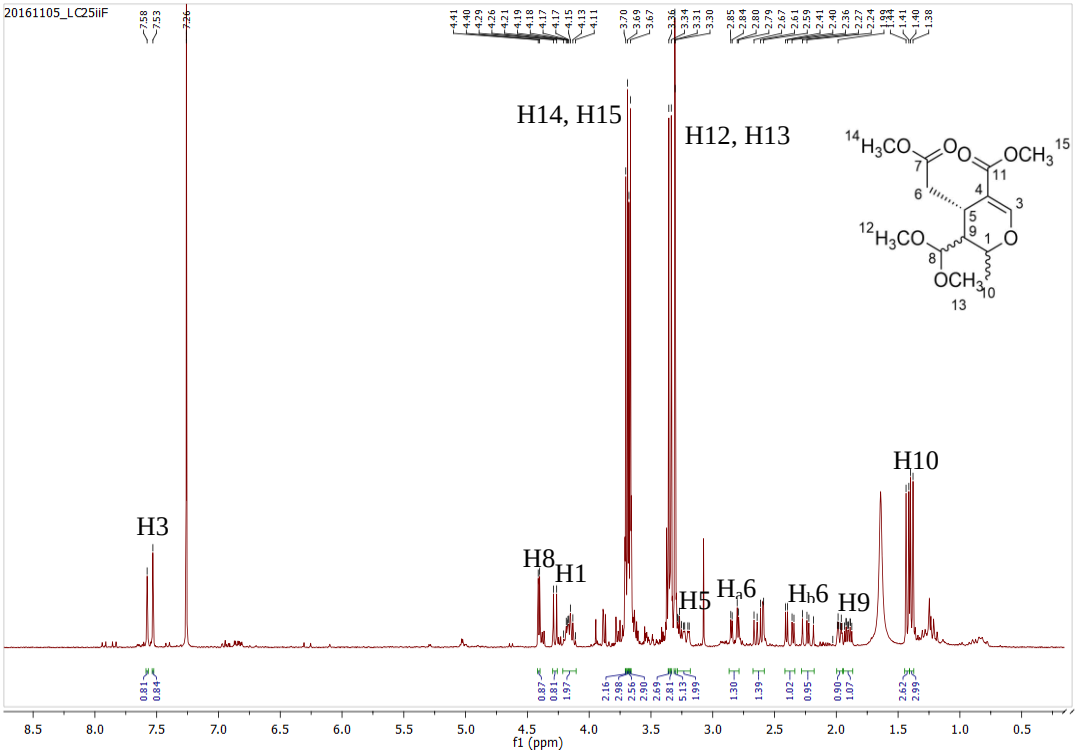

Figure 3.6. ^{1}H NMR spectrum of compounds 6, in $CDCl_3$.

Next, this transformation was tested under heterogeneous conditions, using the strong acidic resin Amberlyst® 15 dry as promoter (1M, 70 ˚C, 2 hours). A mixture (4:1) of two diastereoisomers **5a** and **5b** (Figure 3.5.) was isolated by preparative TLC in 24 % yield, confirmed by the doubling of all signals in NMR spectra (Appendix III).

In ^{1}H NMR spectrum (Figure 3.7.), the olefinic protons (H3) characteristic of the monoterpene moiety were observed at 7.51 and 7.50 ppm, as singlets, for the two diastereoisomers. Signals were observed in the aromatic region, corroborating the fact that the hydroxytyrosol ester remained intact. The presence of the methyl ester was confirmed through two singlets at 3.78 and 3.76 ppm characteristic of the carbomethoxy group (H12). Two singlets were visible at 3.47 and 3.44 ppm, belonging to the protons of the substituent methoxy group at C-1. The exocyclic olefinic protons (H8) were observed as a quartet for the major isomer and as doublet of quartets

for the minor one. The signals of the protons of the methyl group (H10) appeared at 1.67 (J = 6 Hz) and 1.58 (J = 9 Hz) ppm as doublets. There were no evidences of the formation of compound **6**.

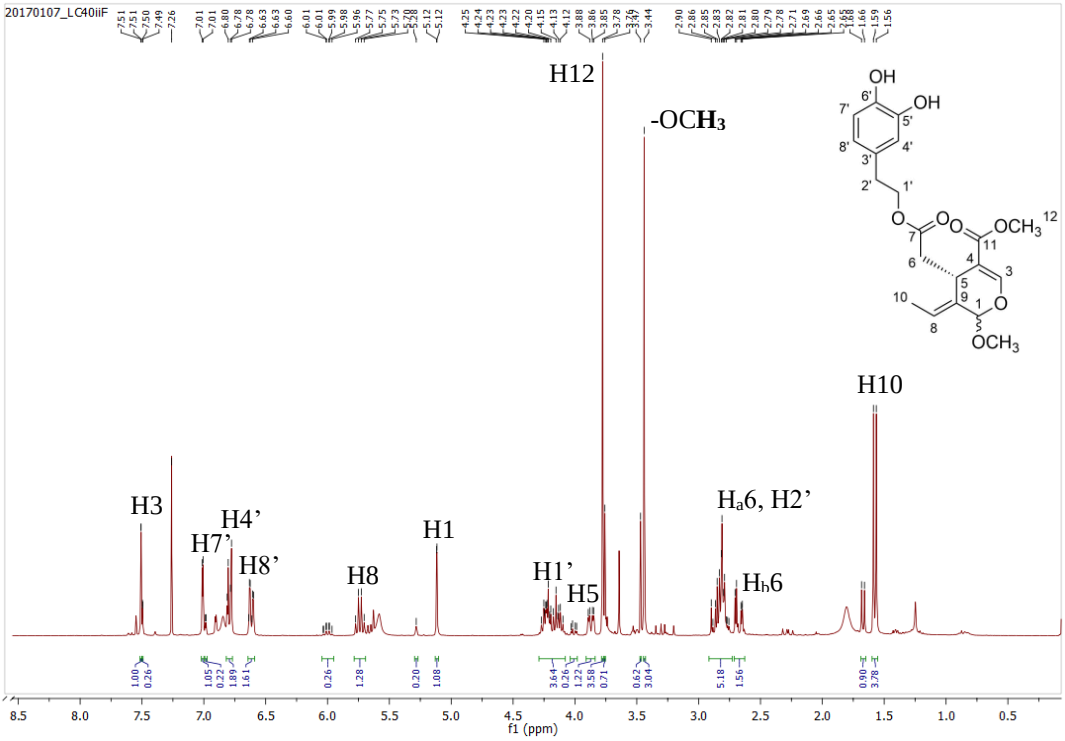

Figure 3.7. ^{1}H NMR spectrum of compounds 5, in $CDCl_3$.

The stereochemistry at C-1 for the major diastereoisomer was not possible to identify through NOESY experiments, due to the complexity of the spectra.

ESI-MS experiments in positive mode were performed and a peak was identified at 415 *m/z*, corresponding to $[M+Na]^+$ (Appendix III).

The different results obtained indicated that the methanolysis reaction of oleuropein might be influenced by the type of acid. With this in mind, a range of protic acids (HCl, *p*TsOH.H_2O, triflic acid, TFA, *p*TsOH.H_2O and triflic acid immobilized in silica) and acidic resins in hydrogen form (Amberlyst® 15 dry, Amberlyst® 16 wet, Amberlyst® 36 wet, Amberlite® IRC86 and Amberlite® IR120) were screened. The reactions were analyzed along the time by analytical reversed-phase HPLC-UV, at 230 nm. For quantitative purpose, calibration curves were performed for all the compounds, with $R^2 > 0.99$. The retention times of oleuropein **1**, compounds **5a** and **5b**, and the mixture of **6** were 20,6 min, 34,6 min, 34,4 min and 32,1 min, respectively (Appendix VI).

In Table 3.2. is presented a selection of the conditions for different acid promoters that allowed the formation of each oleuropein derivative **5a**, **5b** and **6** in high yield.

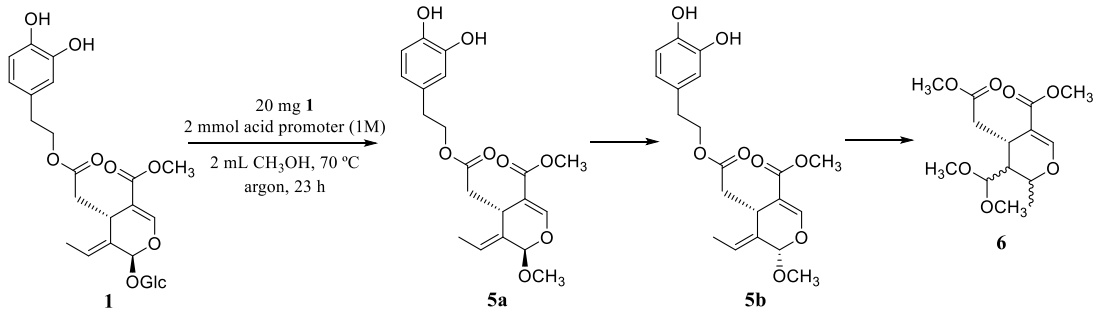

Table 3.2. Conversion and best yields obtained with different acid promoters; time is shown in parenthesis.

Entry	Acid	Conversion (%)	5a (%)	5b (%)	6 (%)
1	HCl *in situ*	100 (15 min)	0	2 (15 min)	24 (6 h)
2	*p*TsOH.H_2O	100 (5 min)	87 (5 min)	63 (45 min)	**57 (6 h)**
3	*p*TsOH.H_2O/SiO_2	100 (4 h)	65 (1 h)	8 (6 h)	0
4	Triflic acid	100 (5 min)	91 (15 min)	**71 (20 min)**	60 (23 h)
5	Triflic acid/SiO_2	100 (5 min)	**92 (5 min)**	20 (2 h)	3 (2 h)
6	(CF_3COOH) TFA	99 (6 h)	65 (6 h)	6 (6 h)	9 (6 h)
7	Amberlyst® 15 dry	100 (2 h)	**100 (1h)**	15 (4 h)	0
8	Amberlyst® 16 wet	100 (6h)	32 (4 h)	1,5 (4 h)	0
9	Amberlyst® 36 wet	100 (23 h)	34 (4 h)	2 (4 h)	2 (2 h)
10	Amberlite® IRC86	20 (15 min)	0	0	0
11	Amberlite® IR120	59 (2 h)	54 (2 h)	2 (2 h)	0

The overall results showed that the type of acid influenced the reaction profile and, in general, the reaction worked better in homogeneous conditions.

Using triflic acid, the acetal **6** was obtained in 60 % yield after 23 hours. However, similar yield (59 %) was obtained after only 6 hours when *p*TsOH.H_2O was used, being this acid the best to obtain **6**. Compounds **5a** and **5b** were also formed in good yields using this acid at 5 minutes and 45 minutes respectively. When *p*TsOH.H_2O was adsorbed in silica, the yields obtained were smaller for each product. The hydrogen bonds between the labile proton and the silanol groups of silica could difficult its role in protonation in some steps of the reaction, explaining the worst results.

Compound **5b** was formed in 71 % yield after 20 minutes using triflic acid. When adsorbed in silica, this acid provides compound **5a** faster in 92 % yield, although compounds **5b** and **6** were not formed in high yields.

Regarding the acidic resins, Amberlyst® 15 dry showed to be the best to obtain the diastereoisomer **5a** with nearly 100 % yield after 1 hour. Nevertheless, none of the resins provided the acetal **6**. Amberlite® IRC86 was the only resin that did not catalyze the reaction, maybe due to its weak acidic properties.

As an example, Figure 3.8. represents the profile of the methanolysis reaction when *p*TsOH.H_2O was used.

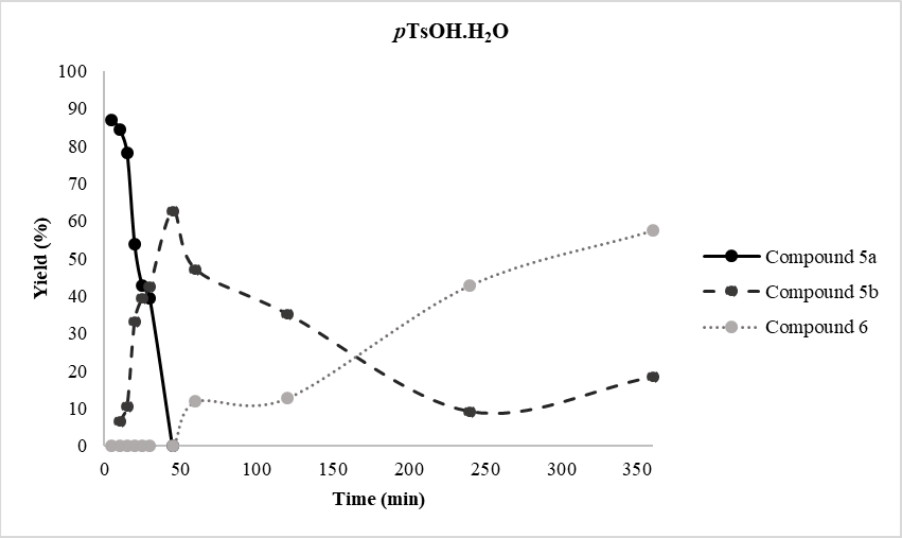

Figure 3.8. Methanolysis reaction profile using *p*TsOH.H_2O, at 70 ºC.

The diastereoisomer **5a** was the first being formed with a maximum yield of 87 % at 5 minutes. It started to decay while the diastereoisomer **5b** was being formed. Compound **5b** reached a maximum (63 % yield) after 45 minutes, corresponding to the time when **5a** disappeared. Then, a decrease of **5b** was observed, matching with the formation of the acetal **6**. These results indicated that compounds **5a** and **5b** were intermediates, interconverting into each other, culminating in the final product **6**. In order to identify the structure of each diastereoisomer **5a** and **5b**, DFT energy calculations (B3LYP/6-31G(d)) of the truncated molecules (substitution of hydroxytyrosol ester by a methyl ester) were performed, indicating that the *cis* product was the most stable diastereoisomer (Δ 0.9 Kcal/mol). Thus, it can be extrapolated that diastereoisomer **5b** is the thermodynamic product and, subsequently, the second to be formed (Figure 3.9). However, further studies need to be done to assign the right configuration of the stereocenter at C-1.

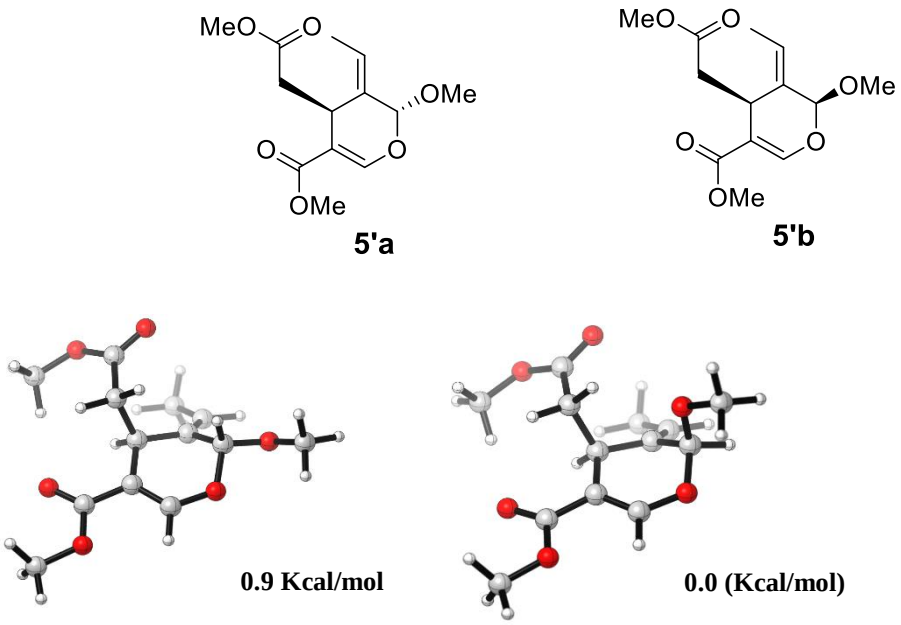

Figure 3.9. Structures and relative free energies of truncated diastereoisomers 5a and 5b computed at a B3LYP/6-31G(d) level of theory.

The profiles using other acids were similar. However, the formation and decay of the products happened at different rates, which could be related with the pK_a of the acids. For example, triflic acid was the stronger acid employed, and was observed that the decay of **5a** and the formation of **5b** were much faster than with other acids. In contrast, with TFA, the rate of the reaction was clearly much slower, since this is a weaker acid than the previous ones. The full conversion of oleuropein was observed only at 6 hours of reaction, and after 23 hours the major compound observed was still **5a**, explaining the role of the pK_a of the acids in the reaction (Appendix VI).

The effect of temperature was also studied at 60 ˚C, 70 ˚C and 80 ˚C, using *p*TsOH.H_2O that, in general, the best performing acid.

At 60 ˚C the decay of **5a**, the formation of **5b**, and further decay of **5b**, were slower than at higher temperatures. However, at this temperature compounds **5a** and **5b** reach their maximum yields of 98% (5 minutes) and 45 % (1 hour), respectively (Figure 3.10. and Figure 3.11.).

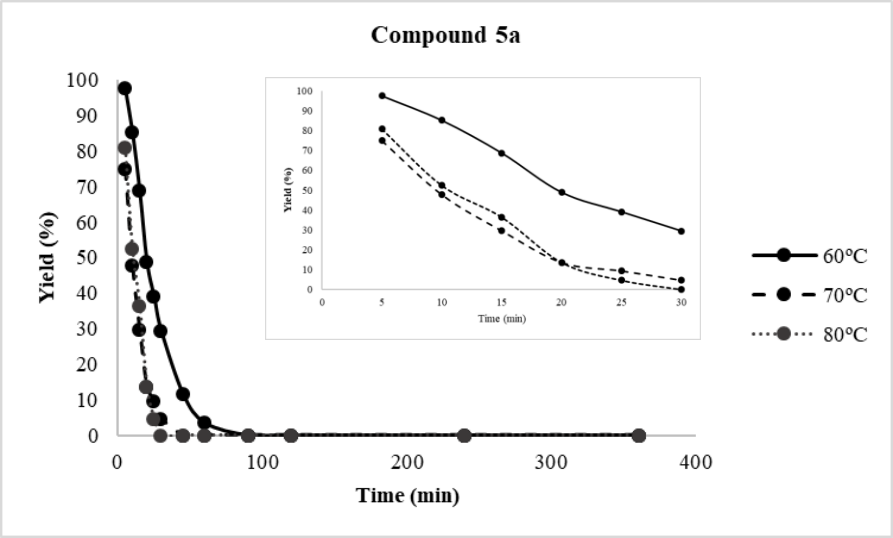

Figure 3.10. Methanolysis reaction profile for compound 5a, at different temperatures, using *p*TsOH.H_2O; Graphic ampliation until 30 minutes.

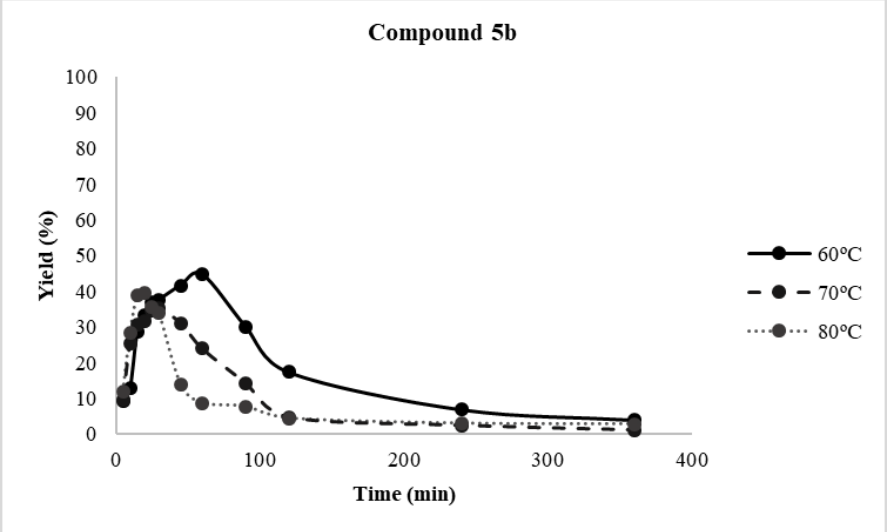

Figure 3.11. Methanolysis reaction profile for compound 5b, at different temperatures, using *p*TsOH.H_2O.

To obtain compound **6**, the best temperature was 80 ˚C, in which it was obtained in nearly 100 % yield after 2 hours. Beyond 2 hours, it was visible a decay in the yield, due to degradation (Figure 3.12.). At 70 ˚C, compound **6** reached a maximum of 81 % yield after 6 hours. When the reaction was performed at 60 ˚C, the maximum yield (39 %) was obtained after 2 hours, reaching a stationary phase.

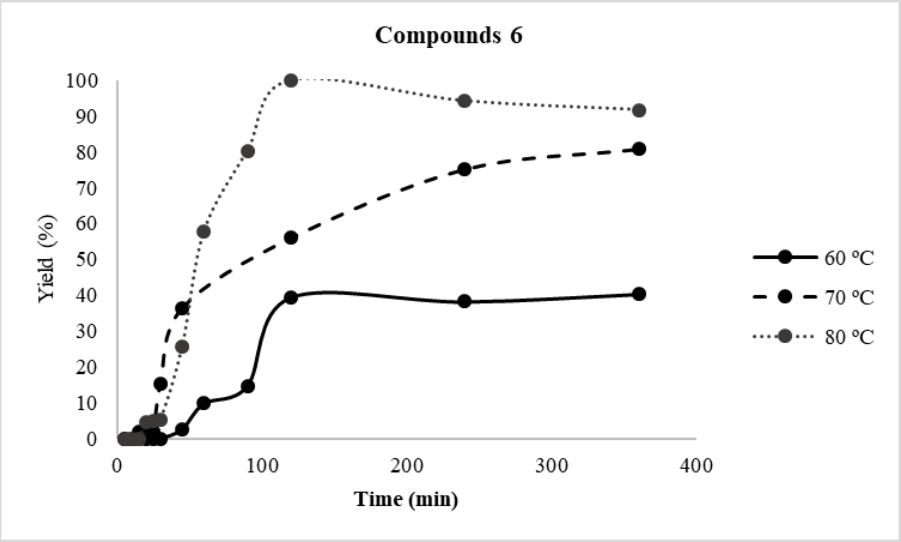

Figure 3.12. Methanolysis reaction profile for compounds 6, at different temperatures, using *p*TsOH.H$_2$O.

The elenolic acid dimethyl ester **7** was obtained, although in low yield (9 %) by adsorbing the crude reaction containing the acetal **6** in silica at 40 ˚C and running the reaction under the previously optimized conditions (80 ˚C, 1M *p*TsOH.H$_2$O, 6 hours) (Scheme 3.6.).

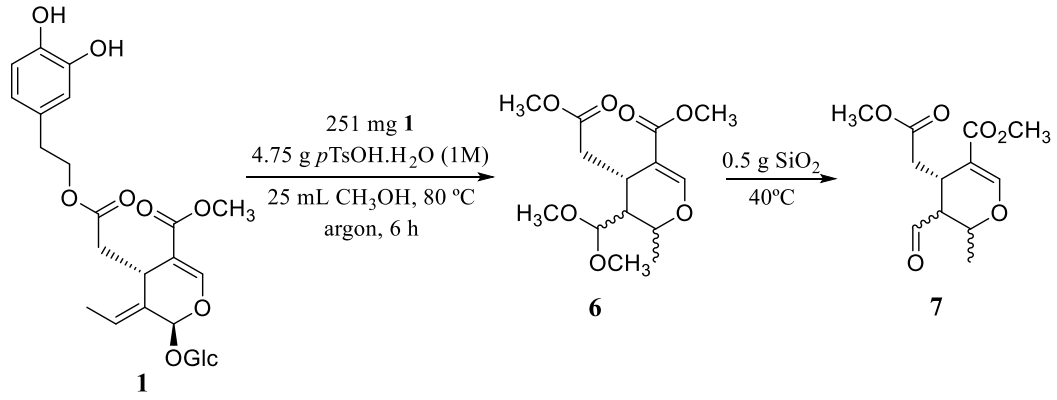

Scheme 3.6. Methanolysis reaction under optimum conditions, to obtain compound 7.

It was expected to isolate **6**, although a signal characteristic of the aldehyde at 9.63 ppm (H8) was visible in the ^{1}H NMR spectrum. The procedure of adsorption in silica might be the reason why compound **7** was isolated instead of **6**, because the presence of water in the surface of silica and its acidic properties, together with the absence of methanol at this stage allowed the deprotection of the aldehyde.

Compound **7** was isolated as a mixture of four diastereoisomers in a ratio of approximately 3:1:1:0,5, and characterized by NMR and ESI-MS experiments (Appendix V), however only the signals for the major isomers were assigned.

In the ^{1}H NMR spectrum (Figure 3.13.) the signal of the endocyclic olefinic proton (H3) in the elenolic core appeared at 7.64 ppm. The signals of the carbomethoxy groups were visible as singlets, each integrating to three protons at 3.69 (H15) and 3.73 (H14) ppm. The signal of the proton H9, adjacent to the aldehyde proton, appeared at 2.64 ppm as a multiplet. H1 adjacent to an oxygen atom, appeared as a doublet of quartets at 4.20 ppm. Finally, the signal of the proton (H10) appeared at 1.57 ppm, as a doublet. These assignments proved the general structure of compound **7**, which are in line with the reported data.[115]

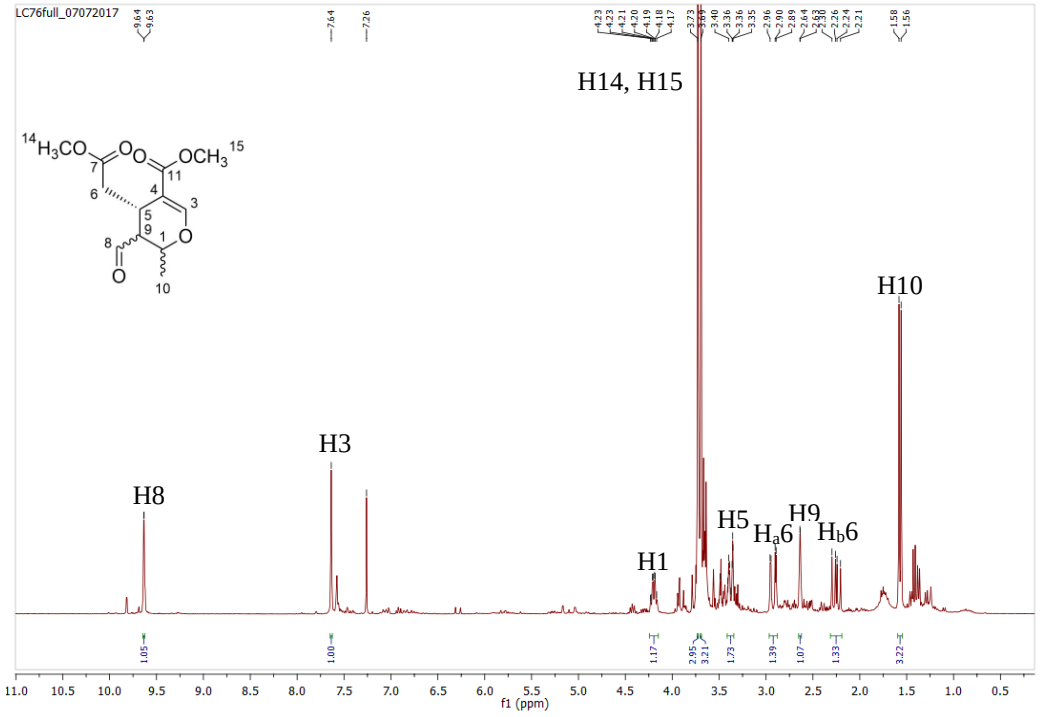

Figure 3.13. ^{1}H NMR spectrum of compounds 7, in $CDCl_3$.

The stereocenters configuration for the major diastereoisomer of **7** obtained from this reaction were difficult to assign by comparison with the reported spectral data for the diastereoisomers (1*S*,5*S*,9*S*) and (1*S*,5*S*,9*R*) of **7.**[115, 116] Therefore, NOESY experiments (Figure 3.15.) allowed to confirm the relative stereochemistry of the asymmetric centers C-1 and C-9, for the major diastereoisomer. Since the stereochemistry at C-5 was already well assigned from the substrate oleuropein, the absolute stereochemistry was defined for the other stereogenic centers. No correlation was observed between H5 and H9, meaning that the relative position between these protons must be *anti*. Thus the aldehyde was in the front of the plan. There was correlation between H1 and H9, suggesting that their relative position was *syn* meaning that the methyl group was in the front of the plan. H9 also had correlations with H_a6 corroborating the proposed configuration for the stereogenic centers, indicating the (1*S*,5*S*,9*S*) diastereoisomer (Figure 3.14.).

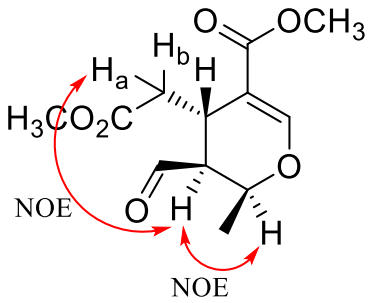

Figure 3.14. Correlations at distance of the major diastereoisomer of 7.

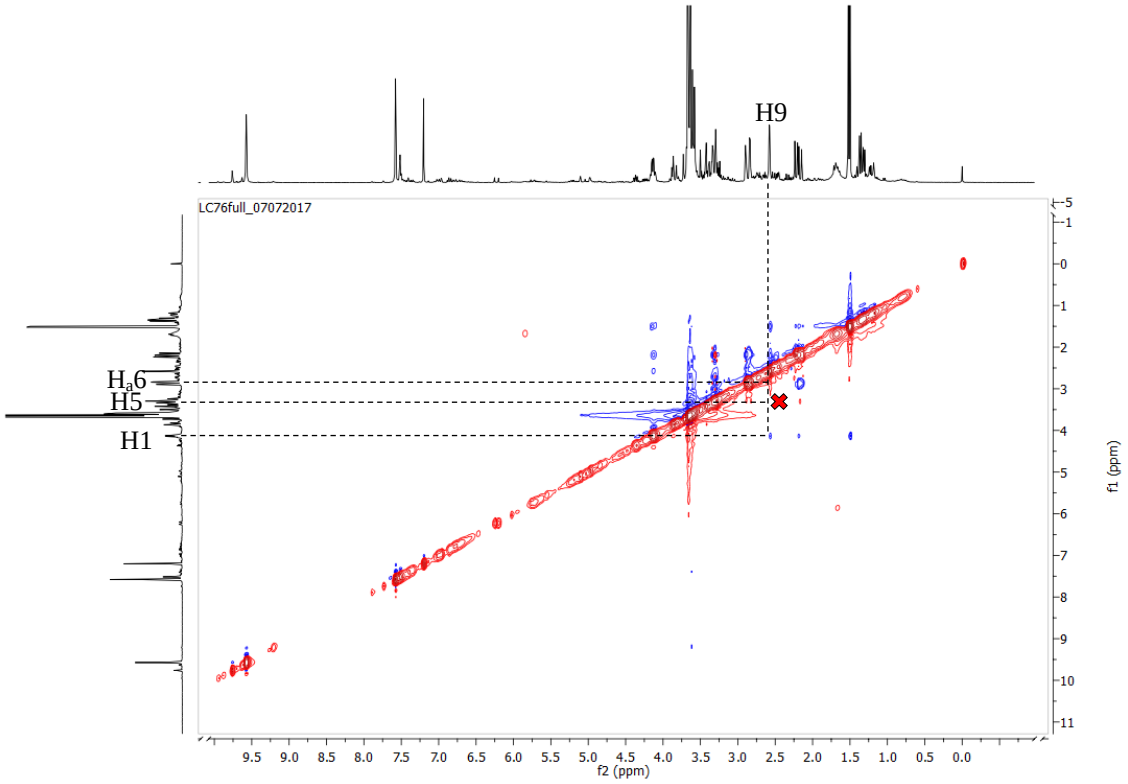

Figure 3.15. NOESY spectrum of compound 7, in $CDCl_3$.

Finally, a mechanism for the methanolysis of oleuropein in acidic conditions was proposed, as shown in Scheme 3.7. The glucose moiety was first hydrolyzed, followed by nucleophilic attack of methanol to form the intermediate **5a**, which interconvert into the more stable **5b**. Then a transesterification of the hydroxytyrosol ester takes place, to form a methyl ester **A**. The opening of the monoterpene ring lead to an intramolecular 1,4 - addition of the nucleophilic oxygen to the exocyclic double bond yielding intermediate **B**. In acidic conditions, the formation of the methoxy acetal **6** was preferred and the aldehyde form **7** can be obtained by adsorption in silica with heat, with formation of a major diastereoisomer.

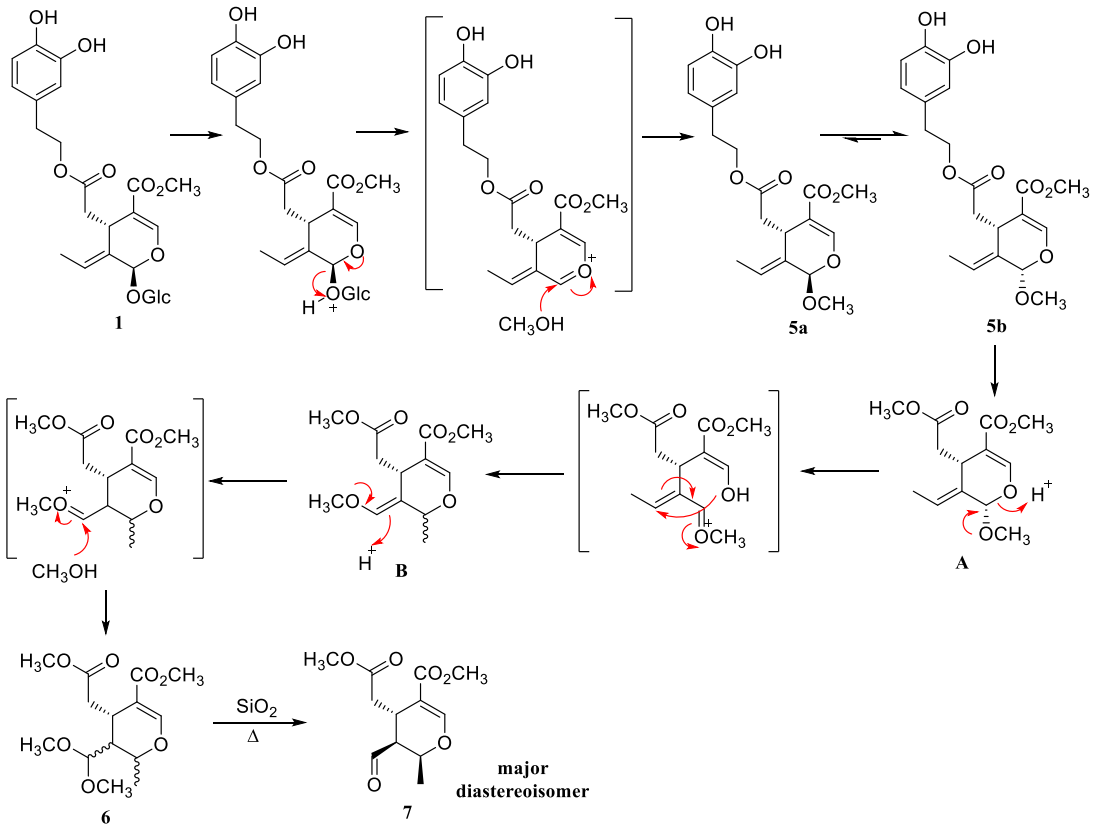

Scheme 3.7. Proposed mechanism for the methanolysis of oleuropein 1 in acidic conditions.

Continuous flow approach of the methanolysis of oleuropein 1

In order to obtain the diastereoisomer **5a** in *batch* conditions, we choose dry Amberlyst® 15, that gave the best yield of this product (see entry 7, Table 3.2.), and a continuous flow approach of the methanolysis of oleuropein **1**.

Continuous flow processes are very advantageous since they allow to speed up the reaction and achieve better fine control due to efficient heat and mass transfer, and so improving the productivity and reducing the side reactions. Furthermore, some of the reaction parameters such as temperature, pressure and residence time, can be easily set up and monitored, making the process more reliable and reproducible. The short residence time of substrates and formed products in the system can decrease or eliminate the formation of side products. Also, this approach requires small amounts of solvents which makes it a simple and cost-effective system, compared to the *batch* approach. The flow process can be applied to heterogeneous catalysis by immobilization of the catalyst in a small reactor, providing the important advantage of increasing the catalyst/substrate ratio.[117]

For the continuous flow methodology an empty HPLC column (i.d. = 4.6 mm; L = 3 cm) was filled with Amberlyst® 15 and oleuropein dissolved in methanol was injected at constant flow using a syringe pump.

Three residence times were studied (1, 5 and 10 min), and the optimum conditions were of 5 minutes of residence time, with a flow of 86 µL/min giving **5a** in a yield of 53 % (Table 3.3.). The reaction was almost complete and only small amounts of **5b** (4 %) were detected.

Table 3.3. Results for compound 5a from continuous flow experiments.

Residence Time (min)	Flow (µl/min)	5a (%)
1	314	30
5	86	53
10	37	32

To obtain the product **5a**, the reactor needed to be washed with 1 mL of methanol, in all cases, except for the experience of 1 minute of residence time. The high flow used (314 µL/min) was enough to remove the product trapped inside the resin spheres without further wash.

To evaluate the robustness of the resin, another experiment was performed where oleuropein was sequentially injected (4 × 1 mL; 5 min of residence time), and samples were collected (≈ 100 µL/sample) and analyzed by TLC. Unexpectedly, the presence of **5a** was just observed after the third injection and was still visible after a final wash of the reactor with 1 mL of methanol. The product seemed to be retained inside the resin spheres and was liberated only when some degree of saturation happened.

The samples in which the product was detected by TLC were combined and analyzed by NMR. The ^{1}H NMR spectrum of the crude sample was very similar to the isolated **5**, suggesting that the released glucose moiety was retained in the resin and the reaction was complete and very clean (Appendix VII). In addition, this spectroscopic analysis and the DFT calculations allowed to identify the major diastereoisomer of **5** previously isolated from batch as being **5a**.

Unfortunately, the HPLC analysis of the crude sample obtained in flow process was only possible to perform after 1 month. Nevertheless, 31 % global yield of **5a** was obtained, but some degradation products were identified in the chromatogram. This experiment will be repeated to confirm the yield of **5a**. In conclusion, this approach can be used to obtain the diastereoisomer **5a** in good yields, faster and without many impurities detected in *batch* experiments. In addition, the resin seems to tolerate some cycles of injections giving the desired product in good yields.

Acid methanolysis of the olive leaves extract

The crude mixture rich in oleuropein, directly extracted from olive leaves, could also be used as substrate for the methanolysis reaction. In this way, it would be possible to avoid the oleuropein purification step and proceed to production in larger scale. Having this in mind, the methanolysis of crude was tested (1M *p*TsOH.H_2O, 70 ˚C) and analyzed along the time by HPLC-UV at 230 nm (Appendix VI). The acetal **6** was obtained in a nearly 100 % yield after 23 hours, regarding the amount of oleuropein in crude (55 mg/g), meaning that the amount of acetal **6** obtained was 31 mg/g of crude. Figure 3.16. represents the methanolysis reaction profile of the crude mixture.

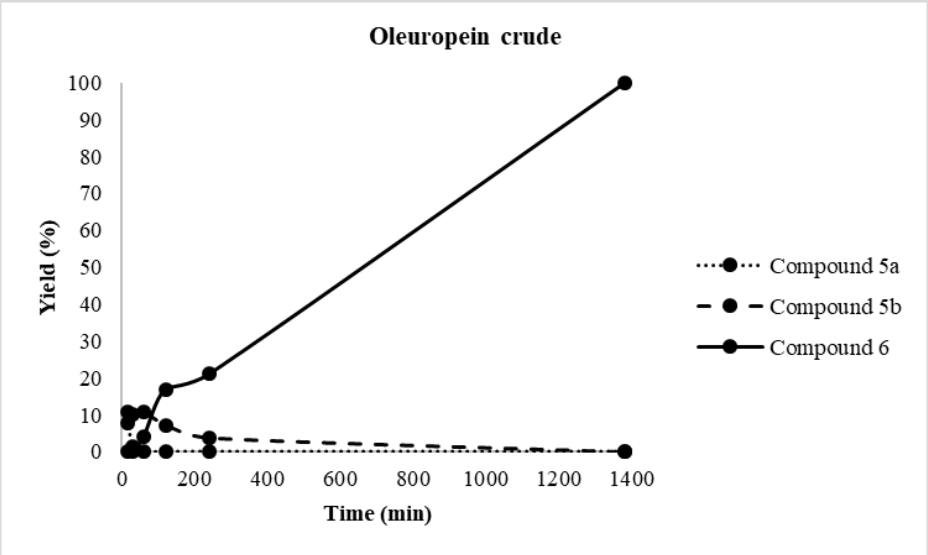

Figure 3.16. Methanolysis reaction profile of crude mixture using *p*TsOH.H_2O, at 70 ºC.

4. Conclusions

Oleuropein **1** was obtained easily in high amounts from olive leaves. Its chemical features made it an important scaffold to obtain novel compounds with potential pharmacological properties.

The study of the methanolysis reaction in acidic conditions was a step further in the research on the transformations of oleuropein, allowing to remove the problematic glucose and hydroxytyrosol moieties and modify the monoterpene core, in one pot and with relative good yields (57 % **6**). The (-)-methyl elenolate **7** (Figure 4.1) obtained from this reaction is known to have a range of antiviral activity and synthetic utility as a precursor of the antihypertensive ajmalicine, making it a desirable target.[118] In addition, this compound has several functional groups (esters, double bonds, aldehyde), that can be further explored for the synthesis of new compounds with additional importance.

The use of continuous flow revealed to be a good and fast method to obtain **5a** in good yields, compound that might also be used as a building block to obtain new derivatives.

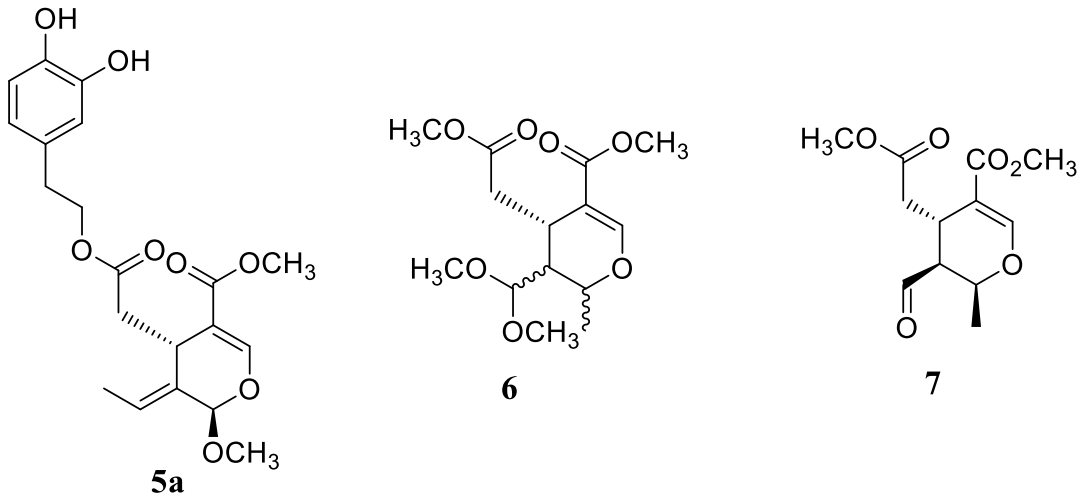

Figure 4.1. Molecular structures of compounds 5a, 6 and the major diastereoisomer of 7.

5. Materials and methods

5.1. General Remarks

Plant material: Olive leaves from *Olea europaea* were collected from different regions in Portugal, over the year. They were dried and stored at room temperature under atmospheric conditions.

Reagents and solvents: All solvents were distilled from commercial grade sources. The specific used anhydrous solvents were prepared according usual procedures.[119] Reagents were used without any purification with >98% purity (Alfa Aesar, Fluka, Sigma Aldrich). Acetonitrile (ChemLab) for analytical purpose was of HPLC grade with >99,9% purity. Water for analytical purpose was obtained by distillation, followed by a filtration under vacuum using a cellulose acetate membrane (0,45 µm, 47 mm).

Stationary phases: Silica gel 60A (P2050017, Carlo Erba) and (TA2045967, Merk) were used respectively for column chromatography and preparative TLC. Analytical TLCs were performed in silica gel 60 F_{254} plates (HX69787354, Merck).

Analytical reversed-phase HPLC: HPLC analysis were performed on a Thermo Scientific Dionex Ultimate 3000 apparatus with a LPG-3400SD Pump, a UV MWD-3000(RS) detector and an autosampler ACC-3000 equipped with a 20 µL loop, using a reversed-phase EC 250/4 Nucleodur 100-5 C18ec column (250×4 mm; 5 µm), Thermo Scientific™ Dionex™. The data were obtained from the Thermo Scientific™ Dionex™ Chromeleon™ 7 chromatography data system software, version 7.2 SR4.

NMR spectroscopy: ^{1}H NMR spectra were obtained in a Bruker Fourier 300 spectrometer, that operates at 300 MHz. ^{13}C NMR spectra were obtained in the same apparatus at 100 MHz. The chemical shifts are indicated in ppm, related to TMS, and the *J* coupling constants are indicated in Hz. Geminal protons are referred with “a” and “b” indexes. Splitting patterns are indicated as s, singlet; d, doublet; t, triplet; q, quartet; m, multiplet.

Mass spectrometry: Low resolution ESI mass spectra were carried on an ion trap mass analyser (Thermo Scientific LCQ Fleet Ion Trap LC/MS) equipped with an electrospray interface. Pro Mass for Xcalibur (Version 2.8) was used as software.

Computational calculations: Density functional theory (DFT) calculations were performed with Gaussian 09[120] and structural representations were generated with *CYLview*.[121] Geometry optimizations were carried out at the B3LYP level of theory with the 6-31G(d) basis set. Optimized geometries were verified by frequency computations as minima (zero imaginary

frequencies). Thermal corrections and entropic contributions were calculated at the same level of theory (B3LYP/6-31G(d)) on the optimized geometries.

5.2. Extraction and isolation of oleuropein 1

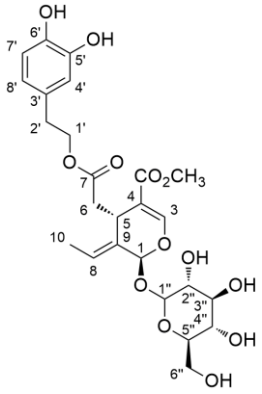

1

Milled dried olive leaves (200 g) were suspended in 2 L of distilled water inside a pyrex beaker and heated in a domestic microwave at medium/high potency, for 15 minutes. Leaves were removed by filtration, followed by water evaporation under reduced pressure. Acetone (100 mL) was added to the brown oily mixture and stirred overnight at room temperature. The insoluble material was filtered and the solvent removed under vacuum yielding a brown oil.[80] Oleuropein **1** was isolated by column chromatography in Combi Flash® Rf Teledyne Isco apparatus using as mobile phase a mixture of CH_2Cl_2 (**A**)/CH_3OH (**B**) in a multi-step gradient – 0 %B (0 - 2,1min); 0 – 10 %B (2,1 – 4 min); 10 %B (4 – 7,1 min); 10 – 20 %B (7,1 – 10,1 min); 20 - 20,2 %B (10,1 – 33,4 min). Oleuropein **1** (3 g) was obtained as a yellow amorphous solid in 1.5 % (w/w dried olive leaves).

R_f (CH_2Cl_2/CH_3OH - 9:1) = 0,49; (R_f (CH_2Cl_2/CH_3OH - 8:1) = 0,5)[87].

^{1}H NMR (300 MHz, CD_3OD): δ 7.52 (s, 1H, H3); 6.72– 6.67 (m, 2H, H7', H4'); 6.56 (dd, *J* = 8.0, 1.8 Hz, 1H, H8'); 6.09 (q, *J* = 6.9 Hz, 1H, H8); 5.92 (s, 1H, H1); 4.73 (d, *J* = 7.6 Hz, 1H, H1''); 4.26– 4,08 (m, 2H, H1'a, H1'b); 3.99 (dd, *J* = 9.0, 4.4 Hz, 1H, H5); 3.90 (d, *J* = 12.1 Hz, 1H, H_a6''); 3.72 (s, 3H, H12); 3.70 - 3.66 (m, 1H, H_b6''); 3.33 – 3.30 (m, 4H, H2'', H3'', H4'', H5''); 2.80 - 2.69 (m, 3H, H2', H_a6); 2.46 (dd, *J* = 14.1, 9.1 Hz, 1H, H_b6); 1.68 (d, *J* = 7.0, 3H, H10) ppm.

^{13}C NMR (100 MHz, CD_3OD): δ 173.2 (C7); 168.7 (C11); 155.2 (C3); 146.2 (C5'); 144.9 (C6'); 130.7 (C9); 130.5 (C3'); 124.7 (C8) 121.3 (C8'); 117.1 (C4'); 116.4 (C7'); 109.4 (C4); 100.9 (C1''); 95.1 (C1); 78.4 (C3''); 77.9 (C5''); 74.8 (C2''); 71.5 (C4''); 66.9 (C1'); 62.7 (C6''); 51.9 (C12); 41.3 (C6); 35.4 (C2'); 31.8 (C5); 13.6 (C10) ppm.

LC-MS-ESI: *ESI (+):* $[M+Na]^+$ = 563 *m/z*; *ESI (-):* $[M-H]^-$ = 539 *m/z*; $[M+Cl]^-$ = 575 *m/z*.

5.3. Semi synthetic transformations of oleuropein 1

Oleacein (**2**)

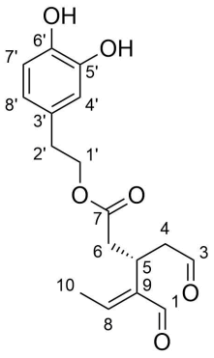

2

Route A (following reported conditions).[91] To a solution of oleuropein **1** (0.267 g, 0.49 mmol) dissolved in DMSO (7.2 mL), in a 25 mL round bottom flask, equipped with a condenser was added a solution of NaCl (59.9 g, 2 eq.) in distilled water (88 µL, 10 eq.). The reaction was stirred at ≈150 ˚C for 12 hours, followed by TLC using CH_2Cl_2/MeOH (9:1) as mobile phase. After cooling down the reaction mixture, the solvent was evaporated the mixture was redissolved in CH_2Cl_2, filtered and concentrated. Oleacein **2** was isolated in 0,3 % yield (0.5 mg) by preparative TLC using AcOEt/Hexane (4:1) as mobile phase. $\mathbf{R_f}$ (CH_2Cl_2/CH_3OH - 9:1) = 0.76. The proposed structure of **2** was assigned by comparing the spectral ^1H NMR data with literature.[91]

Route B (experiment adapted from a reported method for other substrate).[112] $Na_2HPO_4.H_2O$ (7.6 mg, 0.05 mmol) was added to a solution of oleuropein **1** (0.023 g, 0.04 mmol) in distilled water (200 µL). After heating this mixture in a microwave (QLabo CEM Discover), at 300 W for 10 minutes to reach 210 ºC, the reaction was stirred 5 minutes more at this temperature to obtain a black residue. The reaction was followed by TLC using a mixture of CH_2Cl_2/CH_3OH (9:1) as mobile phase. Only degradation products were detected by TLC of the crude reaction.

Compound (**3**)

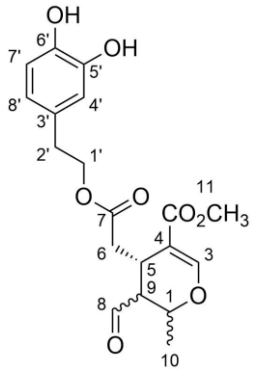

3

(Experimental procedure based on reported method) [110] A solution of *β*-glucosidase (1.3 mg) in sodium acetate/acetic acid buffer (100 µL) was added to oleuropein **1** (0.1395 g, 0.26 mmol) dissolved in the same buffer (3 mL) at pH 5,3. The reaction was heated at 45 ˚C, for 7 days. *β*-glucosidase (1,3 mg) was added again and the reaction continued, at the same conditions, for 1 more day. The reaction was followed by TLC using as mobile phase CH_2Cl_2/CH_3OH (4:1). The aqueous buffer was evaporated and the mixture dissolved in methanol. Compound **3** was isolated in 2.9 % yield (2.8 mg) by preparative TLC (EtOAc/Hexane (4:1) as mobile phase).

R_f (CH_2Cl_2/CH_3OH – 9:1) = 0.76. 1H NMR spectrum in accordance with literature.[75]

^{1}H NMR (300 MHz, $CDCl_3$): *δ* 9.60 – 9.59 (m, 1H, H8 minor); 9.53 (d, *J* = 3 Hz, 1H, H8 major); 7.65 (s, 1H, H3 minor); 7.59 (s, 1H, H3 major); 6.83 (dd, *J* = 3 Hz, 6 Hz, 2H, H7'); 6.79 (dd, *J* = 3 Hz, 18 Hz, 3H, H4'); 6.62 (dd, *J* = 3 Hz, 9 Hz, 3H, H8'); 4.50 – 4.17 (m, 10H, H1, H1'); 3.77 (s, 3H, H11 minor); 3.75 (s, 3H, H11 major); 3.41- 3.35 (m, 2H, H5); 2.91 – 2.80 (m, 7H, H2', H9); 2.55 (dd, *J* = 9 Hz, 15 Hz, 2H, H_a6); 2.20 (dd, *J* = 9 Hz, 15 Hz, 2H, H_b6); 1.56 (d, *J* = 6 Hz, 5H, H10 major); 1.41 (d, *J* = 9 Hz, 5H, H10 minor) ppm.

Jaspolyside (**4**)

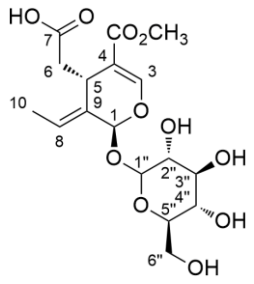

4

(Experimental procedure following reported method)[88] Oleuropein **1** (30 mg, 0.06 mmol) was added to a aqueous solution of NaOH (0.1M, 1.1 mL), and the reaction was stirred at room temperature for 5h30min. The reaction was followed by TLC (CH_2Cl_2/CH_3OH – 4:1). After

cooling down the reaction, it was acidified to ≈ pH 5, using a solution of HCl 10 %, followed by water evaporation. Jaspolyside **4** was isolated as a brown amorphous solid in 63 % yield (14.1 mg), by column flash chromatography using CH_2Cl_2/CH_3OH (4:1) → CH_3OH as mobile phase. Spectral data comparable to reported.[28]

^{1}H NMR (300 MHz, D_2O): δ 7.54 (s, 1H, H3); 6,08 (dq, *J* = 3 Hz, 6 Hz, 1H, H8); 5.96 (t, *J* = 3 Hz, 1H, H1); 4.95 (d, *J* = 9 Hz, 1H, H1'); 3.98 (dd, *J* = 6 Hz, 12 Hz, 1H, H5); 3.91 (dd, *J* = 3 Hz, 12 Hz, 1H, H_a6''); 3.74 (s, 3H, -$CO_2C\mathbf{H_3}$); 3.70 (dd, *J* = 3 Hz, 6 Hz, 1H, H_b6''); 3.57-3.38 (m, 6H, H2', H3', H4', H5'); 2.60 (dd, *J* = 3 Hz, 12 Hz, 1H, H_a6); 2.18 (dd, *J* = 9 Hz, 12 Hz, 1H, H_b6); 1.73 (dd, *J* = 3 Hz, 6 Hz, 3H, H10) ppm.

^{13}C NMR (100 MHz, D_2O): δ 180.0 (C7); 169.5 (-$\mathbf{C}O_2CH_3$); 153.8 (C3); 128.9 (C9); 124.1 (C8); 109.4 (C4); 99.6 (C1''); 95.0 (C1); 76.4 (C3''); 75.6 (C5''); 72.6 (C2''); 69.4 (C4''); 60.5 (C6''); 51.8 (-$CO_2\mathbf{C}H_3$); 43.6 (C6); 31.3 (C5); 12.8 (C10) ppm.

ESI-MS: *ESI(+):* 427 $[M+Na]^+$; *ESI(-):* 403 $[M-H]^-$; 808 $[2M-H]^-$.

Compound (**5**)

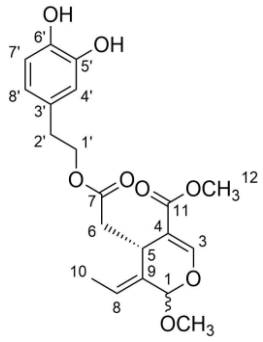

5

Amberlyst® 15 dry (43.6 mg, 2 eq.) was placed in a previous flame dried and degassed pressure tube (15 mL, L×OD 10.2×25.4 cm, Ref. Z181099-1EA Aldrich. A solution of oleuropein **1** (53.1 mg, 0.1 mmol), in dry CH_3OH (2 mL), was added to the tube. The reaction was heated at 70 ˚C, for 2 hours. The resin was removed by filtration, the solvent was evaporated under reduced pressure, and compound **5** was isolated by preparative TLC – CH_2Cl_2:CH_3OH (9:1) - in 24 % yield (9.1 mg) after desorption from silica with dichloromethane.

R_f (CH_2Cl_2/CH_3OH – 9:1) = 0.77.

Major - **^{1}H NMR (300 MHz, $CDCl_3$):** 7.51 (s, 1H, H3); 7.01 (d, *J* = 1.98 Hz, 1H, H7'); 6.79 (d, *J* = 6 Hz, 1H, H4'); 6.62 (dd, *J* = 3 Hz, 9 Hz, 2H, H8' both); 5.74 (q, *J* = 6 Hz, 1H, H8); 5.12 (d, *J* = 0,86 Hz, 1H, H1); 4.28 – 4.09 (m, 2H, H1'); 3.87 (dd, *J* = 3 Hz, 9 Hz, 1H, H5); 3.78 (s, 3H, H12); 3.44 (s, 3H, -OC**H$_3$**); 2.90 – 2.75 (m, 6H, H_a6, H2' both); 2.71 – 2.65 (m, 2H, H_b6 both); 1.58 (d, *J* = 9 Hz, 3H, H10) ppm; **^{13}C NMR (100 MHz, $CDCl_3$):** δ 172.1 (C7); 168.4 (C11); 153.4 (C3); 143.4 (C5'); 143.2 (C6'); 130.6 (C3'); 130.0 (C9); 128.9 (C8); 121.3 (C8'); 117.1 (C7');

115.0 (C4'); 108.7 (C4); 104.8 (C1); 65.2 (C1'); 56.3 (-OCH_3); 51.9 (C12); 38.7 (C6); 34.3 (C2'); 28.7 (C5); 13.3 (C10) ppm.

Minor - **^{1}H NMR (300 MHz, $CDCl_3$):** δ 7.50 (s, H3); 6.98 (d, *J* = 2 Hz, H7'); 6.79 (d, *J* = 9 Hz, H4'); 6.00 (dq, *J* = 3 Hz, 9 Hz, H8); 5.28 (t, H1); 4.28 – 4.09 (m, 2H, H1'); 4.01 (dd, *J* = 3 Hz, 9 Hz, H5); 3.76 (s, H12); 3.47 (s, -OC**H$_3$**); 1.67 (d, *J* = 6 Hz, H10); **^{13}C NMR (100 MHz, $CDCl_3$):** δ 172.3 (C7); 168.1 (C11); 152.8 (C3); 143.2 (C5'); 143.1 (C6'); 130.7 (C3'); 130.5 (C9); 129.3 (C8); 121.2 (C8'); 116.8 (C7'); 115.1 (C4'); 109.0 (C4); 99.2 (C1); 65.5 (C1'); 56.5 (-OCH_3); 51.8 (C12); 39.2 (C6); 34.6 (C2'); 30.6 (C5); 13.2 (C10) ppm.

ESI-MS: *ESI(+):* $[M+Na]^+$ = 415 *m/z.*

Compound (**6**)

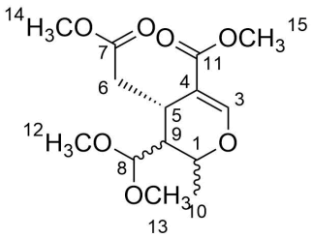

6

To a previously flame dried and degassed round bottom flask equipped with a condenser, was added dry CH_3OH (3 mL). Then, acetyl chloride (292 µL, 4 mmol) was slowly added under stirring, and the reaction was stirred for 5 minutes at room temperature. A solution of oleuropein **1** (0.120 g, 0.22 mmol) in dry methanol (1.2 mL) was added to the previous mixture and stirred for 20 hours at 70 ºC. The reaction was followed by TLC - CH_2Cl_2/CH_3OH (9:1). The acid was neutralized with an aqueous saturated solution of $NaHCO_3$ (3 mL), and extracted with ethyl acetate (4×15 mL). The combined organic phase was dried with anhydrous Na_2SO_4, filtered and the solvent removed under reduced pressure. The obtained residue was purified by column flash chromatography (CH_2Cl_2/CH_3OH - 9:1), yielding acetal **6** (16.5 mg) as a brown oil, in 25 % yield. Spectral data is in accordance with reported.[(114)]

R_f (CH_2Cl_2/CH_3OH - 9:1) = 0.88.

Major – **^{1}H NMR (300 MHz, $CDCl_3$):** δ 7.53 (s, 1H, H3); 4.41 (d, *J* = 3 Hz, 1H, H8); 4.21-4.11 (m, 2H, H1 both); 3.68 (s, 3H, H15); 3.67 (s, 3H, H14); 3.36 (s, 3H, -OC**H$_3$**); 3.34 (s, 3H, -OC**H$_3$**); 3.28 – 3.19 (m, 2H, H5 both); 2.63 (dd, *J* = 3 Hz, 15 Hz, 1H, H_a6); 2.38 (dd, *J* = 3 Hz, 15 Hz, 1H, H_b6); 1,93 – 1,87 (m, 1H, H9); 1.39 (d, *J* = 6 Hz, 3H, H10) ppm; **^{13}C NMR (100 MHz,$CDCl_3$):** δ 173.2 (C7); 172.4 (C11); 156.3 (C3); 109.0 (C4); 106.1 (C8); 71.5 (C1); 55.7 (C12); 54.3 (C13); 51.8 (C14); 51.6 (C15); 43.6 (C9); 37.3 (C6); 28.8 (C5); 19.5 (C10) ppm.

Minor - **^{1}H NMR (300 MHz, $CDCl_3$):** δ 7.58 (s, 1H, H3); 4.28 (d, *J* = 9 Hz, 1H, H8); 4.21-4.11 (m, 2H, H1 both); 3.70 (s, 3H, H14); 3.69 (s, 3H, H15); 3.31 (d, *J* = 3 Hz, 6H, -OCH_3); 3.28 – 3.19 (m, 2H, H5 both); 2.82 (dd, *J* = 9 Hz, 18 Hz, 1H, H_a6); 2.23 (dd, *J* = 9 Hz, 18 Hz, 1H, H_b6);

1.98 (dt, *J* = 3 Hz, 9 Hz, 1H, H9); 1.43 (d, *J* = 9 Hz, 3H, H10) ppm; **^{13}C NMR (100 MHz, $CDCl_3$):** *δ* 167.7 (C7); 167.6 (C11); 155.2 (C3); 107.6 (C4); 101.5 (C8); 71.1 (C1); 55.4 (C12); 51.6 (C13); 51.4 (C14); 51.3 (C15); 41.2 (C9); 39.7 (C6); 29.1 (C5); 18.8 (C10) ppm.
ESI-MS: *ESI(+)*: $[M+Na]^+$ = 325 *m/z*; $[2M+Na]^+$ = 627 *m/z*.

Compound (**7**)

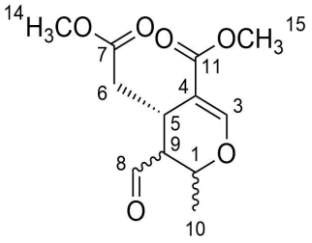

7

*p*TsOH.H_2O (4,75 g, 1M) was added to a solution of oleuropein **1** (0.251 g, 0.5 mmol) in dry CH_3OH (25 mL) in a round bottom flask equipped with condenser under argon atmosphere. The reaction was stirred for 6 hours, at 80 ºC. The reaction mixture was neutralized with a solution of $NaHCO_3$ (sat.), followed by solvent evaporation under vacuum. The obtained residue was redissolved in water (5 mL) and extracted with ethyl acetate (4×15 mL). The organic phase was dried with Na_2SO_4 (anhyd.) filtered and the solvent evaporated under reduced pressure. The crude mixture was adsorbed in silica (0.5 g) at 40 ˚C under reduced pressure, followed by column flash chromatography (CH_2Cl_2/EtOAc – 3:1), providing compound **7** (10.6 mg, 9 %) as a mixture of diastereoisomers in a ratio of 3:1:1.0.5.
R_f (CH_2Cl_2/EtOAc – 3:1) = 0,85.
Major diastereoisomer – **^{1}H NMR (300 MHz, $CDCl_3$):** *δ* 9.64 (d, *J* = 3 Hz, 1H, H8); 7.64 (s, 1H, H3); 4.20 (dq, *J* = 3 Hz, 6 Hz, 1H, H1); 3.73 (s, 3H, H14); 3.69 (s, 3H, H16); 3.39 (m, 1H, H5); 2.93 (dd, *J* = 3 Hz, 18 Hz, 1H, H_a6); 2.64 (m, 1H, H9); 2.25 (dd, *J* = 12 Hz, 18 Hz, 1H, H_b6); 1.57 (d, *J* = 6 Hz, 3H, H10) ppm.
^{13}C NMR (100 MHz, $CDCl_3$): *δ* 199.6 (C8); 171.7 (C11); 167.0 (C7); 156.7 (C3); 106.5 (C4); 69.5 (C1); 51.9 (C15); 51.5 (C14); 50.8 (C9); 38.4 (C6); 28.0 (C5); 17.9 (C10) ppm.
ESI-MS: *ESI(+)*: $[M+H]^+$ = 257 *m/z*; $[M+Na]^+$ = 279 *m/z*.

Screening of acids and temperature effect studies in methanolysis reaction

To a previous flamed pressure tube (15 mL, L×OD 10.2×25.4 cm, Ref. Z181099-1EA Aldrich), under inert atmosphere (argon), was added oleuropein **1** (20 mg, 0.04 mmol) dissolved in dry CH_3OH (2 mL), followed by addition of the acid promoter (2 mmol, 1M). the reaction was stirred during 23 hours at 70 ˚C, and followed by HPLC analysis. At each specific time, the reaction was cooled down, aliquots (65 µL) were taken and diluted in HPLC grade acetonitrile to 0,4 mM concentrated and analyzed by reversed-phase HPLC-UV, at 230 nm. A mixture of (**A**) H_2O/1% TFA and (**B**) ACN/1% TFA was used as mobile phase in a multistep gradient: 5% B – 28% B (0-19 min); 28% B – 35% B (19-25 min); 35%, B – 75% B (25-45 min). The retention times of oleuropein **1**, compounds **5a** and **5b**, and the mixture of **3** were 20,6 min, 34,6 min, 34,4 min and 32,1 min, respectively.

For the study of temperature effect, the same conditions were adopted, at different temperatures of 60 ˚C, 70 ˚C and 80 ˚C, using the promoter *p*TsOH.H_2O.

Continuous flow experiments under heterogeneous conditions

An empty HPLC column (i.d.=4.6 mm; L=3 cm) was filled with resin (Amberlyst® 15 dry, aprox. 313 mg, for the specific amount used in each experiment, see Appendix VII) and equilibrated by injecting methanol (aprox. 370 µL, for the specific volume used in each experience, see Appendix VII). It was submersed in a water bath at 70 ˚C while 10 mg of oleuropein **1** dissolved in 1 mL of CH_3OH were passing through the reactor at a specific flow (New Era Pump Systems, Inc.) corresponding to 1 min, 5 min or 10 min of residence time. Except for 1 min of residence time, the reactor was washed with 1 mL of methanol to remove the product. The samples were analyzed by HPLC-UV at the same conditions reported before.

To evaluate the resin robustness, 10 mg of oleuropein in 1 mL of methanol were injected 4 times using the same resin and at optimum conditions (5 min residence time). At the end, the reactor was washed with 1 mL of methanol to release the product. 55 samples (≈ 100 µL/sample) were collected and analyzed by TLC (CH_2Cl_2/CH_3OH – 9:1). The samples that showed evidence of compound **5a** were joined and analyzed by ^{1}H NMR. This sample was analyzed by HPLC only after 1 month, aiming a global yield of 31 % of **5a**, with formation of other products due to degradation.

Methanolysis reaction of crude mixture

The crude extract from leaves (20 mg) was dissolved in dry methanol (2 mL) and placed in a pressure tube (15 mL, L×OD 10.2×25.4 cm, Ref. Z181099-1EA Aldrich), under argon atmosphere. The reaction was stirred at 70 ˚C and analyzed by HPLC-UV along the time, as described before.

6. References

1. Schmitt EK, Moore CM, Krastel P, Petersen F. Natural products as catalysts for innovation: a pharmaceutical industry perspective. *Current Opinion in Chemical Biology*. **2011**;*15*(4):497-504.
2. DeCorte BL. Underexplored Opportunities for Natural Products in Drug Discovery. *Journal of Medicinal Chemistry*. **2016**;*59*(20):9295-304.
3. Cutler SJ, Cutler HG. *Biologically Active Natural Products: Pharmaceuticals*: CRC-Press; **1999**.
4. Apostolakis A, Grigorakis S, Makris DP. Optimisation and comparative kinetics study of polyphenol extraction from olive leaves (Olea europaea) using heated water/glycerol mixtures. *Separation and Purification Technology*. **2014**;*128*:89-95.
5. Japón-Luján R, Luque-Rodríguez J, De Castro ML. Dynamic ultrasound-assisted extraction of oleuropein and related biophenols from olive leaves. *Journal of Chromatography A*. **2006**;*1108*(1):76-82.
6. Stamatopoulos K, Katsoyannos E, Chatzilazarou A, Konteles SJ. Improvement of oleuropein extractability by optimising steam blanching process as pre-treatment of olive leaf extraction via response surface methodology. *Food chemistry*. **2012**;*133*(2):344-51.
7. Talhaoui N, Taamalli A, Gómez-Caravaca AM, Fernández-Gutiérrez A, Segura-Carretero A. Phenolic compounds in olive leaves: Analytical determination, biotic and abiotic influence, and health benefits. *Food Research International*. **2015**;*77*:92-108.
8. Malik NS, and Joe M. Bradford. Recovery and stability of oleuropein and other phenolic compounds during extraction and processing of olive (Olea europaea L.) leaves. *Journal of Food Agriculture and Environment* **2008**;*6*(2):8-13.
9. Japon-Lujan R, De Castro MDL. Small branches of olive tree: A source of biophenols complementary to olive leaves. *J Agr Food Chem*. **2007**;*55*(11):4584-8.
10. Bouaziz M, Fki I, Jemai H, Ayadi M, Sayadi S. Effect of storage on refined and husk olive oils composition: Stabilization by addition of natural antioxidants from Chemlali olive leaves. *Food Chemistry*. **2008**;*108*(1):253-62.
11. Bouaziz M, Sayadi S. Isolation and evaluation of antioxidants from leaves of a Tunisian cultivar olive tree. *European Journal of Lipid Science and Technology*. **2005**;*107*(7-8):497-504.
12. Guinda Á, Castellano JM, Santos-Lozano JM, Delgado-Hervás T, Gutiérrez-Adánez P, Rada M. Determination of major bioactive compounds from olive leaf. *LWT-Food Science and Technology*. **2015**;*64*(1):431-8.
13. Li C, Zheng Y, Wang X, Feng S, Di D. Simultaneous separation and purification of flavonoids and oleuropein from Olea europaea L.(olive) leaves using macroporous resin. *Journal of the Science of Food and Agriculture*. **2011**;*91*(15):2826-34.
14. Rahmanian N, Jafari SM, Wani TA. Bioactive profile, dehydration, extraction and application of the bioactive components of olive leaves. *Trends in Food Science & Technology*. **2015**;*42*(2):150-72.
15. Şahin S, Şamlı R. Optimization of olive leaf extract obtained by ultrasound-assisted extraction with response surface methodology. *Ultrasonics Sonochemistry*. **2013**;*20*(1):595-602.
16. Kamran M, Hamlin AS, Scott CJ, Obied HK. Drying at high temperature for a short time maximizes the recovery of olive leaf biophenols. *Industrial Crops and Products*. **2015**;*78*:29-38.
17. de Castro ML, Japón-Luján R. State-of-the-art and trends in the analysis of oleuropein and derivatives. *TrAC Trends in Analytical Chemistry*. **2006**;*25*(5):501-10.
18. Soler-Rivas C, Espín JC, Wichers HJ. Oleuropein and related compounds. *Journal of the Science of Food and Agriculture*. **2000**;*80*(7):1013-23.
19. Erbay Z, Icier F. The Importance and Potential Uses of Olive Leaves. *Food Reviews International*. **2010**;*26*(4):319-34.
20. Abaza L, Taamalli A, Nsir H, Zarrouk M. Olive Tree (Olea europeae L.) Leaves: Importance and Advances in the Analysis of Phenolic Compounds. *Antioxidants*. **2015**;*4*(4):682-98.

21. El SN, Karakaya S. Olive tree (Olea europaea) leaves: potential beneficial effects on human health. *Nutrition reviews.* **2009**;*67*(11):632-8.
22. Khan Y, Panchal S, Vyas N, Butani A, Kumar V. Olea europaea: a phyto-pharmacological review. *Pharmacognosy Reviews*. **2007**;*1*(1):114-8.
23. Omar SH. Phcog Rev.: Plant Review Olive: Native of Mediterranean region and Health benefits. *Pharmacognosy Reviews*. **2008**;*2*(3).
24. Tripoli E, Giammanco M, Tabacchi G, Di Majo D, Giammanco S, La Guardia M. The phenolic compounds of olive oil: structure, biological activity and beneficial effects on human health. *Nutrition research reviews.* **2005**;*18*(01):98-112.
25. Dinda B, Chowdhury DR, Mohanta BC. Naturally occurring iridoids, secoiridoids and their bioactivity. An updated review, part 3. *Chemical and Pharmaceutical Bulletin*. **2009**;*57*(8):765-96.
26. Dinda B, Debnath S, Banik R. Naturally occurring iridoids and secoiridoids. An updated review, part 4. *Chemical and Pharmaceutical Bulletin.* **2011**;*59*(7):803-33.
27. Dinda B, Debnath S, Harigaya Y. Naturally occurring iridoids. A review, part 1. *Chemical and pharmaceutical bulletin*. **2007**;*55*(2):159-222.
28. Dinda B, Debnath S, Harigaya Y. Naturally occurring secoiridoids and bioactivity of naturally occurring iridoids and secoiridoids. A review, part 2. *Chemical and pharmaceutical bulletin*. **2007**;*55*(5):689-728.
29. Briante R, La Cara F, Febbraio F, Patumi M, Nucci R. Bioactive derivatives from oleuropein by a biotransformation on Olea europaea leaf extracts. *Journal of Biotechnology*. **2002**;*93*(2):109-19.
30. Malik NS, Bradford JM. Changes in oleuropein levels during differentiation and development of floral buds in 'Arbequina'olives. *Scientia Horticulturae.* **2006**;*110*(3):274-8.
31. Xie P-J, Huang L-x, Zhang C-h, You F, Zhang Y-l. Reduced pressure extraction of oleuropein from olive leaves (Olea europaea L.) with ultrasound assistance. *Food and Bioproducts processing*. **2015**;*93*:29-38.
32. Gikas E, Bazoti FN, Tsarbopoulos A. Conformation of oleuropein, the major bioactive compound of Olea europea. *Journal of Molecular Structure: THEOCHEM.* **2007**;*821*(1):125-32.
33. Obied HK, Prenzler PD, Ryan D, Servili M, Taticchi A, Esposto S, et al. Biosynthesis and biotransformations of phenol-conjugated oleosidic secoiridoids from Olea europaea L. *Natural product reports*. **2008**;*25*(6):1167-79.
34. Ana M. Lobo AML. *Biossíntese de Produtos Naturais*. 1st ed., **2007**.
35. Zun-Qiu W, Gui-Zhou Y, Qing-Ping Z, You-Jun J, Kai-Yu T, Hua-Ping C, et al. Purification, Dynamic Changes and Antioxidant Activities of Oleuropein in Olive (Olea Europaea L.) Leaves. *Journal of Food Biochemistry*. **2015**;*39*(5):566-74.
36. Gutierrez-Rosales F, Romero MaP, Casanovas Ma, Motilva MaJ, Mínguez-Mosquera MaI. Metabolites involved in oleuropein accumulation and degradation in fruits of Olea europaea L.: Hojiblanca and Arbequina varieties. *J Agr Food Chem.* **2010**;*58*(24):12924-33.
37. Amiot M-J, Fleuriet A, Macheix J-J. Accumulation of oleuropein derivatives during olive maturation. *Phytochemistry*. **1989**;*28*(1):67-9.
38. Ramírez E, Medina E, Brenes M, Romero Cn. Endogenous enzymes involved in the transformation of oleuropein in Spanish table olive varieties. *J Agr Food Chem*. **2014**;*62*(39):9569-75.
39. Ryan D, Prenzler PD, Lavee S, Antolovich M, Robards K. Quantitative changes in phenolic content during physiological development of the olive (Olea europaea) cultivar Hardy's Mammoth. *J Agr Food Chem.* **2003**;*51*(9):2532-8.
40. De Leonardis A, Macciola V, Cuomo F, Lopez F. Evidence of oleuropein degradation by olive leaf protein extract. *Food chemistry*. **2015**;*175*:568-74.
41. Le Floch F, Tena M, Rıos A, Valcarcel M. Supercritical fluid extraction of phenol compounds from olive leaves. *Talanta*. **1998**;*46*(5):1123-30.
42. Meirinhos J, Silva BM, Valentão P, Seabra RM, Pereira JA, Dias A, et al. Analysis and quantification of flavonoidic compounds from Portuguese olive (Olea europaea L.) leaf cultivars. *Natural product research*. **2005**;*19*(2):189-95.

43. Mylonaki S, Kiassos E, Makris DP, Kefalas P. Optimisation of the extraction of olive (Olea europaea) leaf phenolics using water/ethanol-based solvent systems and response surface methodology. *Analytical and Bioanalytical Chemistry*. **2008**;*392*(5):977.
44. Ortega-García F, Blanco S, Peinado M, Peragón J. Phenylalanine ammonia-lyase and phenolic compounds in leaves and fruits of Olea europaea L. cv. Picual during ripening. *Journal of the Science of Food and Agriculture*. **2009**;*89*(3):398-406.
45. Ortega-García F, Blanco S, Peinado M, Peragón J, Preedy V, Watson R. *Polyphenol oxidase and Oleuropein in Olives and their changes during olive ripening. Olives and olive oil in health and disease prevention* Academic Press, USA. **2010**:233-8.
46. Paiva-Martins F, Correia R, Félix S, Ferreira P, Gordon MH. Effects of enrichment of refined olive oil with phenolic compounds from olive leaves. *J Agr Food Chem*. **2007**;*55*(10):4139-43.
47. Papoti VT, Tsimidou MZ. Looking through the qualities of a fluorimetric assay for the total phenol content estimation in virgin olive oil, olive fruit or leaf polar extract. *Food Chemistry*. **2009**;*112*(1):246-52.
48. Pereira AP, Ferreira IC, Marcelino F, Valentão P, Andrade PB, Seabra R, et al. Phenolic compounds and antimicrobial activity of olive (Olea europaea L. Cv. Cobrançosa) leaves. *Molecules*. **2007**;*12*(5):1153-62.
49. Petridis A, Therios I, Samouris G, Koundouras S, Giannakoula A. Effect of water deficit on leaf phenolic composition, gas exchange, oxidative damage and antioxidant activity of four Greek olive (Olea europaea L.) cultivars. *Plant physiology and biochemistry*. **2012**;*60*:1-11.
50. Rada M, Guinda Á, Cayuela J. Solid/liquid extraction and isolation by molecular distillation of hydroxytyrosol from Olea europaea L. leaves. *European journal of lipid science and technology*. **2007**;*109*(11):1071-6.
51. Ranalli A, Contento S, Lucera L, Di Febo M, Marchegiani D, Di Fonzo V. Factors affecting the contents of iridoid oleuropein in olive leaves (Olea europaea L.). *J Agr Food Chem*. **2006**;*54*(2):434-40.
52. Ryan D, Antolovich M, Herlt T, Prenzler PD, Lavee S, Robards K. Identification of phenolic compounds in tissues of the novel olive cultivar hardy's mammoth. *J Agr Food Chem*. **2002**;*50*(23):6716-24.
53. Savournin C, Baghdikian B, Elias R, Dargouth-Kesraoui F, Boukef K, Balansard G. Rapid high-performance liquid chromatography analysis for the quantitative determination of oleuropein in Olea europaea leaves. *J Agr Food Chem*. **2001**;*49*(2):618-21.
54. Scognamiglio M, D'Abrosca B, Pacifico S, Fiumano V, De Luca PF, Monaco P, et al. Polyphenol characterization and antioxidant evaluation of Olea europaea varieties cultivated in Cilento National Park (Italy). *Food Research International*. **2012**;*46*(1):294-303.
55. Silva S, Gomes L, Leitao F, Coelho A, Boas LV. Phenolic compounds and antioxidant activity of Olea europaea L. fruits and leaves. *Food Science and Technology International*. **2006**;*12*(5):385-95.
56. Taamalli A, Arráez-Román D, Barrajón-Catalán E, Ruiz-Torres V, Pérez-Sánchez A, Herrero M, et al. Use of advanced techniques for the extraction of phenolic compounds from Tunisian olive leaves: phenolic composition and cytotoxicity against human breast cancer cells. *Food and chemical toxicology*. **2012**;*50*(6):1817-25.
57. Talhaoui N, Gómez-Caravaca AM, León L, De la Rosa R, Segura-Carretero A, Fernández-Gutiérrez A. Determination of phenolic compounds of 'Sikitita'olive leaves by HPLC-DAD-TOF-MS. Comparison with its parents 'Arbequina'and 'Picual'olive leaves. *LWT-Food Science and Technology*. **2014**;*58*(1):28-34.
58. Petridis A, Therios I, Samouris G, Tananaki C. Salinity-induced changes in phenolic compounds in leaves and roots of four olive cultivars (Olea europaea L.) and their relationship to antioxidant activity. *Environmental and Experimental Botany*. **2012**;*79*:37-43.
59. Bilgin M, Şahin S. Effects of geographical origin and extraction methods on total phenolic yield of olive tree (Olea europaea) leaves. *Journal of the Taiwan Institute of Chemical Engineers*. **2013**;*44*(1):8-12.

60. Boudhrioua N, Bahloul N, Slimen IB, Kechaou N. Comparison on the total phenol contents and the color of fresh and infrared dried olive leaves. *Industrial crops and products*. **2009**;*29*(2):412-9.
61. Erbay Z, Icier F. Optimization of drying of olive leaves in a pilot-scale heat pump dryer. *Drying Technology*. **2009**;*27*(3):416-27.
62. Ahmad-Qasem MH, Barrajón-Catalán E, Micol V, Mulet A, García-Pérez JV. Influence of freezing and dehydration of olive leaves (var. Serrana) on extract composition and antioxidant potential. *Food Research International*. **2013**;*50*(1):189-96.
63. Bahloul N, Boudhrioua N, Kouhila M, Kechaou N. Effect of convective solar drying on colour, total phenols and radical scavenging activity of olive leaves (Olea europaea L.). *International journal of food science & technology*. **2009**;*44*(12):2561-7.
64. Aouidi F, Dupuy N, Artaud J, Roussos S, Msallem M, Gaime IP, et al. Rapid quantitative determination of oleuropein in olive leaves (Olea europaea) using mid-infrared spectroscopy combined with chemometric analyses. *Industrial Crops and Products*. **2012**;*37*(1):292-7.
65. Cárcel J, Nogueira RI, García-Pérez J, Sanjuán N, Riera E, editors. Ultrasound effects on the mass transfer processes during drying kinetic of olive leaves (Olea Europea, var. Serrana). *Defect and Diffusion Forum*; **2010**: Trans Tech Publ.
66. Erbay Z, Icier F. Thin-layer drying behaviors of olive leaves (Olea europaea L.). *Journal of Food Process Engineering*. **2010**;*33*(2):287-308.
67. Huang H-W, Hsu C-P, Yang BB, Wang C-Y. Advances in the extraction of natural ingredients by high pressure extraction technology. *Trends in Food Science & Technology*. **2013**;*33*(1):54-62.
68. Xie P, Huang L, Zhang C, You F, Wang C, Zhou H. Boiling extraction of oleuropein at low temperature and reduced pressure. *China journal of Chinese materia medica*. **2012**;*37*(13):1946-51.
69. Luque-Garcıa J, De Castro ML. Ultrasound-assisted soxhlet extraction: an expeditive approach for solid sample treatment: application to the extraction of total fat from oleaginous seeds. *Journal of Chromatography A*. **2004**;*1034*(1):237-42.
70. Dang J, Huang Z, Zhang Z, Feng L, Dun X. Different Extraction of Oleuropein from Olea Europaea Leaves [J]. *Journal of Shenzhen Polytechnic*. **2006**;*4*:010.
71. Mandal V, Mohan Y, Hemalatha S. Microwave assisted extraction—an innovative and promising extraction tool for medicinal plant research. *Pharmacognosy reviews*. **2007**;*1*(1):7-18.
72. Altıok E, Bayçın D, Bayraktar O, Ülkü S. Isolation of polyphenols from the extracts of olive leaves (Olea europaea L.) by adsorption on silk fibroin. *Separation and Purification Technology*. **2008**;*62*(2):342-8.
73. Bayçın D, Altıok E, Ülkü S, Bayraktar O. Adsorption of olive leaf (Olea europaea L.) antioxidants on silk fibroin. *J Agr Food Chem*. **2007**;*55*(4):1227-36.
74. Didaskalou C, Buyuktiryaki S, Kecili R, Fonte CP, Szekely G. Valorisation of agricultural waste with an adsorption/nanofiltration hybrid process: from materials to sustainable process design. *Green Chemistry*. **2017**.
75. Gariboldi P, Jommi G, Verotta L. Secoiridoids from Olea europaea. *Phytochemistry*. **1986**;*25*(4):865-9.
76. Japón-Luján R, Luque-Rodríguez J, De Castro ML. Multivariate optimisation of the microwave-assisted extraction of oleuropein and related biophenols from olive leaves. *Analytical and bioanalytical chemistry*. **2006**;*385*(4):753-9.
77. Japón-Luján R, de Castro ML. Superheated liquid extraction of oleuropein and related biophenols from olive leaves. *Journal of Chromatography A*. **2006**;*1136*(2):185-91.
78. Jemai H, Bouaziz M, Fki I, El Feki A, Sayadi S. Hypolipidimic and antioxidant activities of oleuropein and its hydrolysis derivative-rich extracts from Chemlali olive leaves. *Chemico-biological interactions*. **2008**;*176*(2):88-98.
79. Jemai H, El Feki A, Sayadi S. Antidiabetic and Antioxidant Effects of Hydroxytyrosol and Oleuropein from Olive Leaves in Alloxan-Diabetic Rats. *J Agr Food Chem*. **2009**;*57*(19):8798-804.

80. Procopio A, Alcaro S, Nardi M, Oliverio M, Ortuso F, Sacchetta P, et al. Synthesis, Biological Evaluation, and Molecular Modeling of Oleuropein and Its Semisynthetic Derivatives as Cyclooxygenase Inhibitors. *J Agr Food Chem*. **2009**;*57*(23):11161-7.
81. Xynos N, Papaefstathiou G, Psychis M, Argyropoulou A, Aligiannis N, Skaltsounis A-L. Development of a green extraction procedure with super/subcritical fluids to produce extracts enriched in oleuropein from olive leaves. *The Journal of Supercritical Fluids*. **2012**;*67*:89-93.
82. Xynos N, Papaefstathiou G, Gikas E, Argyropoulou A, Aligiannis N, Skaltsounis A-L. Design optimization study of the extraction of olive leaves performed with pressurized liquid extraction using response surface methodology. *Separation and Purification Technology*. **2014**;*122*:323-30.
83. Paiva-Martins F, Gordon MH. Isolation and characterization of the antioxidant component 3, 4-dihydroxyphenylethyl 4-formyl-3-formylmethyl-4-hexenoate from olive (Olea europaea) leaves. *J Agr Food Chem.* **2001**;*49*(9):4214-9.
84. Paiva-Martins Ft, Pinto M. Isolation and characterization of a new hydroxytyrosol derivative from olive (Olea europaea) leaves. *J Agr Food Chem*. **2008**;*56*(14):5582-8.
85. Guiso M, Marra C. Highlights in oleuropein aglycone structure. *Natural product research*. **2005**;*19*(2):105-9.
86. Kikuchi M, Mano N, Uehara Y, Machida K, Kikuchi M. Cytotoxic and EGFR tyrosine kinase inhibitory activities of aglycone derivatives obtained by enzymatic hydrolysis of oleoside-type secoiridoid glucosides, oleuropein and ligustroside. *Journal of Natural Medicines*. **2011**;*65*(1):237-40.
87. Briante R, La Cara F, Tonziello MP, Febbraio F, Nucci R. Antioxidant activity of the main bioactive derivatives from oleuropein hydrolysis by hyperthermophilic β-glycosidase. *J Agr Food Chem.* **2001**;*49*(7):3198-203.
88. Hanessian S, Mainetti E, Lecomte F. Synthesis and Stereochemical Confirmation of the Secoiridoid Glucosides Nudiflosides D and A. *Organic letters*. **2006**;*8*(18):4047-9.
89. Ranarivelo Y, Magiatis P, Skaltsounis A-L, Tillequin F. Selective Amination of Secoiridoid Glycosides to give Monomeric Pyridine, Dimeric Pyridine, and Naphthyridine Alkaloids. *Natural product letters*. **2001**;*15*(2):131-7.
90. Bianco A, Jensen SR, Olesen J, Passacantilli P, Ramunno A. Acid rearrangement of secoiridoids related to oleuropein and secologanin. *European journal of organic chemistry*. **2003**;*2003*(22):4349-54.
91. Vougogiannopoulou K, Lemus C, Halabalaki M, Pergola C, Werz O, Smith III AB, et al. One-step semisynthesis of oleacein and the determination as a 5-lipoxygenase inhibitor. *Journal of natural products*. **2014**;*77*(3):441-5.
92. Hassen I, Casabianca H, Hosni K. Biological activities of the natural antioxidant oleuropein: Exceeding the expectation–A mini-review. *Journal of Functional Foods*. **2015**;*18*:926-40.
93. Şahin S, Bilgin M, Dramur MU. Investigation of oleuropein content in olive leaf extract obtained by supercritical fluid extraction and soxhlet methods. *Separation Science and Technology*. **2011**;*46*(11):1829-37.
94. Castillo J, Alcaraz M, Benavente-García O. *Antioxidant and radioprotective effects of olive leaf extract. Olives and Olive oil in health and disease prevention* Academic Press, Oxford. **2010**:951-8.
95. Alirezaei M, Dezfoulian O, Neamati S, Rashidipour M, Tanideh N, Kheradmand A. Oleuropein prevents ethanol-induced gastric ulcers via elevation of antioxidant enzyme activities in rats. *Journal of physiology and biochemistry*. **2012**;*68*(4):583-92.
96. Dekanski D, Ristić S, Radonjić NV, Petronijević ND, Dekanski A, Mitrović DM. Olive leaf extract modulates cold restraint stress-induced oxidative changes in rat liver. *Journal of the Serbian Chemical Society*. **2011**;*76*(9):1207-18.
97. Tavafi M, Ahmadvand H, Toolabi P. Inhibitory effect of olive leaf extract on gentamicin-induced nephrotoxicity in rats. *Iranian Journal of Kidney Diseases*. **2012**;*6*(1):25.
98. Giner E, Recio MC, Ríos JL, Cerdá-Nicolás JM, Giner RM. Chemopreventive effect of oleuropein in colitis-associated colorectal cancer in c57bl/6 mice. *Molecular nutrition & food research*. **2016**;*60*(2):242-55.

99. Martínez-Martos JM, Mayas MD, Carrera P, de Saavedra JMA, Sánchez-Agesta R, Arrazola M, et al. Phenolic compounds oleuropein and hydroxytyrosol exert differential effects on glioma development via antioxidant defense systems. *Journal of Functional Foods*. **2014**;*11*:221-34.
100. Kyriazis JD, Aligiannis N, Polychronopoulos P, Skaltsounis A-L, Dotsika E. Leishmanicidal activity assessment of olive tree extracts. *Phytomedicine*. **2013**;*20*(3):275-81.
101. Perugini P, Vettor M, Rona C, Troisi L, Villanova L, Genta I, et al. Efficacy of oleuropein against UVB irradiation: preliminary evaluation. *International journal of cosmetic science*. **2008**;*30*(2):113-20.
102. Hur W, Kim SW, Lee YK, Choi JE, Hong SW, Song MJ, et al. Oleuropein reduces free fatty acid-induced lipogenesis via lowered extracellular signal-regulated kinase activation in hepatocytes. *Nutrition Research*. **2012**;*32*(10):778-86.
103. Singh I, Mok M, Christensen A-M, Turner AH, Hawley JA. The effects of polyphenols in olive leaves on platelet function. *Nutrition, metabolism and cardiovascular diseases*. **2008**;*18*(2):127-32.
104. Han J, Talorete TP, Yamada P, Isoda H. Anti-proliferative and apoptotic effects of oleuropein and hydroxytyrosol on human breast cancer MCF-7 cells. *Cytotechnology*. **2009**;*59*(1):45-53.
105. Bulotta S, Corradino R, Celano M, D'Agostino M, Maiuolo J, Oliverio M, et al. Antiproliferative and antioxidant effects on breast cancer cells of oleuropein and its semisynthetic peracetylated derivatives. *Food Chemistry*. **2011**;*127*(4):1609-14.
106. Bouallagui Z, Han J, Isoda H, Sayadi S. Hydroxytyrosol rich extract from olive leaves modulates cell cycle progression in MCF-7 human breast cancer cells. *Food and chemical toxicology*. **2011**;*49*(1):179-84.
107. Čabarkapa A, Živković L, Žukovec D, Djelić N, Bajić V, Dekanski D, et al. Protective effect of dry olive leaf extract in adrenaline induced DNA damage evaluated using in vitro comet assay with human peripheral leukocytes. *Toxicology in Vitro*. **2014**;*28*(3):451-6.
108. Goulas V, Exarchou V, Troganis AN, Psomiadou E, Fotsis T, Briasoulis E, et al. Phytochemicals in olive-leaf extracts and their antiproliferative activity against cancer and endothelial cells. *Molecular nutrition & food research.* **2009**;*53*(5):600-8.
109. Abaza L, Talorete TP, Yamada P, Kurita Y, Zarrouk M, Isoda H. Induction of growth inhibition and differentiation of human leukemia HL-60 cells by a Tunisian gerboui olive leaf extract. *Bioscience, biotechnology, and biochemistry*. **2007**;*71*(5):1306-12.
110. Romero-Segura C, García-Rodríguez R, Sánchez-Ortiz A, Sanz C, Pérez AG. The role of olive β-glucosidase in shaping the phenolic profile of virgin olive oil. *Food Research International*. **2012**;*45*(1):191-6.
111. Montedoro G, Servili M, Baldioli M, Selvaggini R, Miniati E, Macchioni A. Simple and hydrolyzable compounds in virgin olive oil. 3. Spectroscopic characterizations of the secoiridoid derivatives. *J Agr Food Chem.* **1993**;*41*(11):2228-34.
112. Mason JD, Murphree SS. Microwave-assisted aqueous Krapcho decarboxylation. *Synlett*. **2013**;*24*(11):1391-4.
113. Jaeger K-E, Ransac S, Dijkstra BW, Colson C, van Heuvel M, Misset O. Bacterial lipases. *FEMS microbiology reviews*. **1994**;*15*(1):29-63.
114. Iossifova T, Mikhova B, Kostova I. A secoiridoid dilactone fromFraxinus ornus bark. *Monatshefte für Chemie/Chemical Monthly*. **1995**;*126*(11):1257-64.
115. Christophoridou S, Dais P, Tseng L-H, Spraul M. Separation and identification of phenolic compounds in olive oil by coupling high-performance liquid chromatography with postcolumn solid-phase extraction to nuclear magnetic resonance spectroscopy (LC-SPE-NMR). *J Agr Food Chem.* **2005**;*53*(12):4667-79.
116. Baggiolini EG, Pizzolato G, Uskoković MR. Stereocontrolled synthesis of 19-epiajmalicine from loganin aglucone. *Tetrahedron*. **1988**;*44*(11):3203-8.
117. Porta R, Benaglia M, Puglisi A. Flow chemistry: Recent developments in the synthesis of pharmaceutical products. Org Process Res Dev. **2016**;*20*(1):2-25.
118. Hatakeyama S, Saijo K, Takano S. Enantioselective synthesis of (−)-elenolic acid and (−)-ajmalicine. *Tetrahedron letters*. **1985**;*26*(7):865-8.

119. D. D. Perrin WLFA. *Purification of Laboratory Chemicals*. 3rd ed. Oxford, United Kingdom: Pergamon Press; **1998**.
120. *Gaussian 09* RD, M. J. Frisch, G. W. Trucks, H. B. Schlegel, G. E. Scuseria, M. A. Robb, J. R. Cheeseman, G. Scalmani, V. Barone, B. Mennucci, G. A. Petersson, H. Nakatsuji, M. Caricato, X. Li, H. P. Hratchian, A. F. Izmaylov, J. Bloino, G. Zheng, J. L. Sonnenberg, M. Hada, M. Ehara, K. Toyota, R. Fukuda, J. Hasegawa, M. Ishida, T. Nakajima, Y. Honda, O. Kitao, H. Nakai, T. Vreven, J. A. Montgomery, Jr., J. E. Peralta, F. Ogliaro, M. Bearpark, J. J. Heyd, E. Brothers, K. N. Kudin, V. N. Staroverov, T. Keith, R. Kobayashi, J. Normand, K. Raghavachari, A. Rendell, J. C. Burant, S. S. Iyengar, J. Tomasi, M. Cossi, N. Rega, J. M. Millam, M. Klene, J. E. Knox, J. B. Cross, V. Bakken, C. Adamo, J. Jaramillo, R. Gomperts, R. E. Stratmann, O. Yazyev, A. J. Austin, R. Cammi, C. Pomelli, J. W. Ochterski, R. L. Martin, K. Morokuma, V. G. Zakrzewski, G. A. Voth, P. Salvador, J. J. Dannenberg, S. Dapprich, A. D. Daniels, O. Farkas, J. B. Foresman, J. V. Ortiz, J. Cioslowski, and D. J. Fox, . Gaussian, Inc, Wallingford CT. **2013**.
121. CYLview bL, C. Y., Université de Sherbrooke, **2009** (http://www.cylview.org).

7. Appendices

7.1. Appendix I – NMR spectra and LC-MS-ESI of oleuropein 1

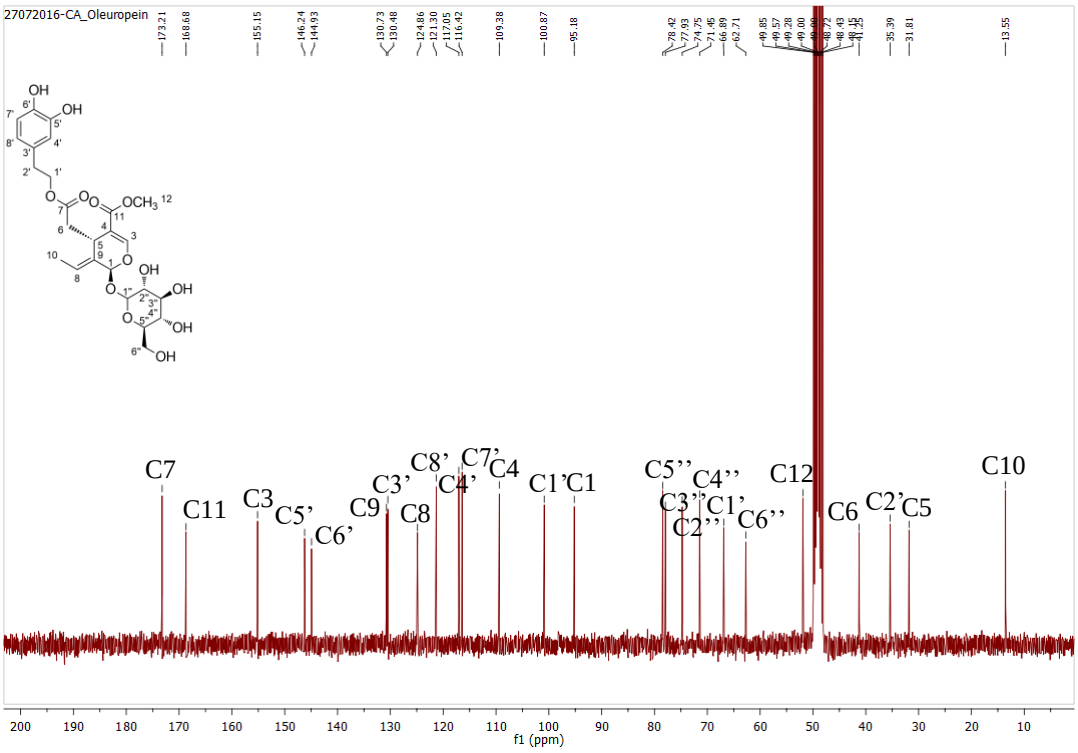

Figure 7.1. ^{13}C NMR spectrum of oleuropein 1, in CD_3OD.

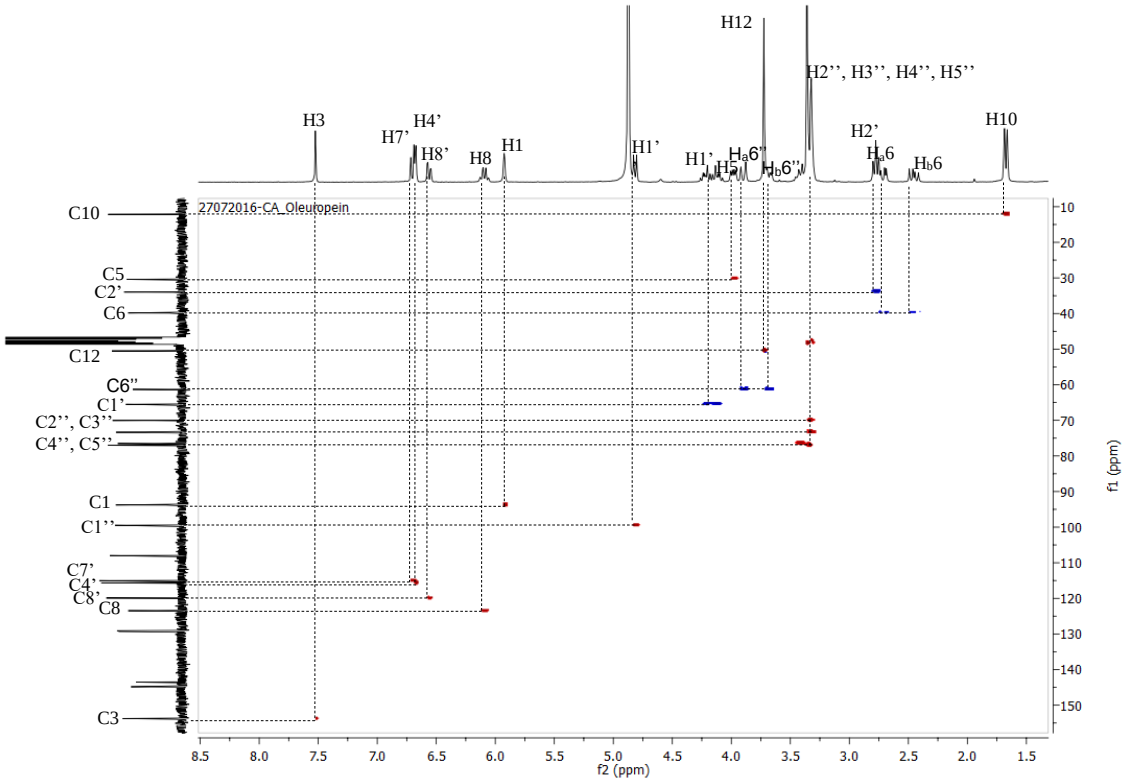

Figure 7.2. HSQC spectrum of oleuropein 1, in CD_3OD.

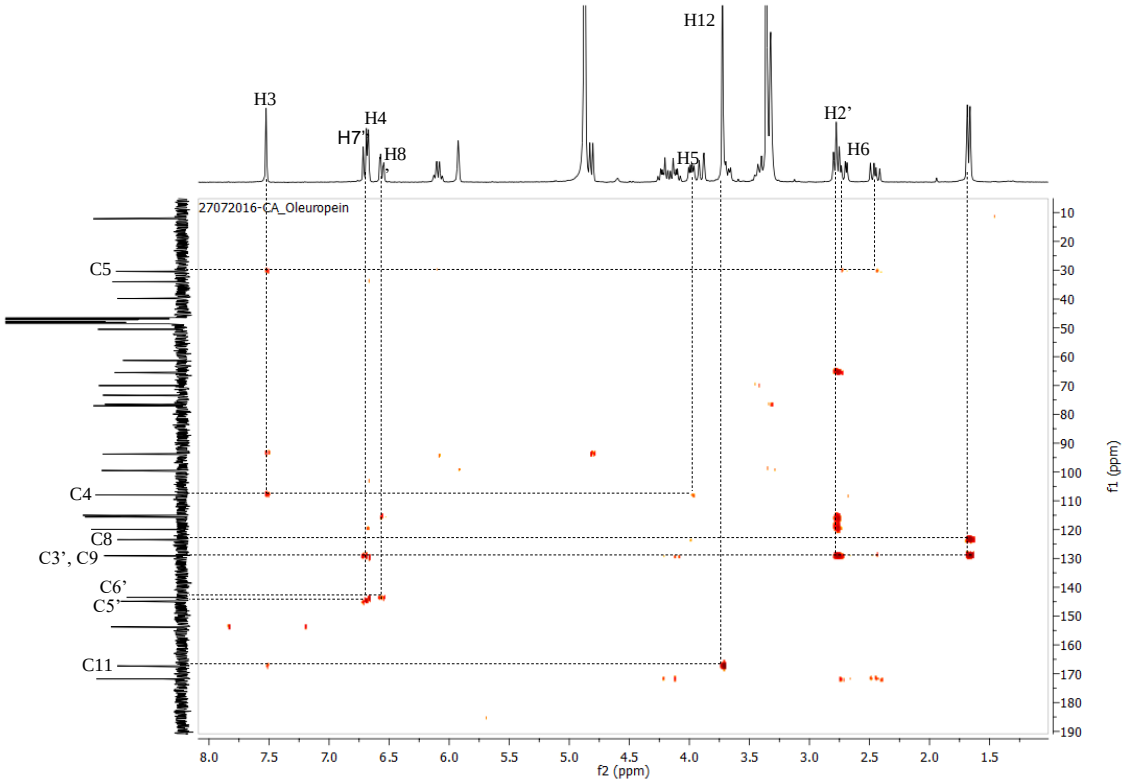

Figure 7.3. HMBC spectrum of oleuropein 1, in CD_3OD.

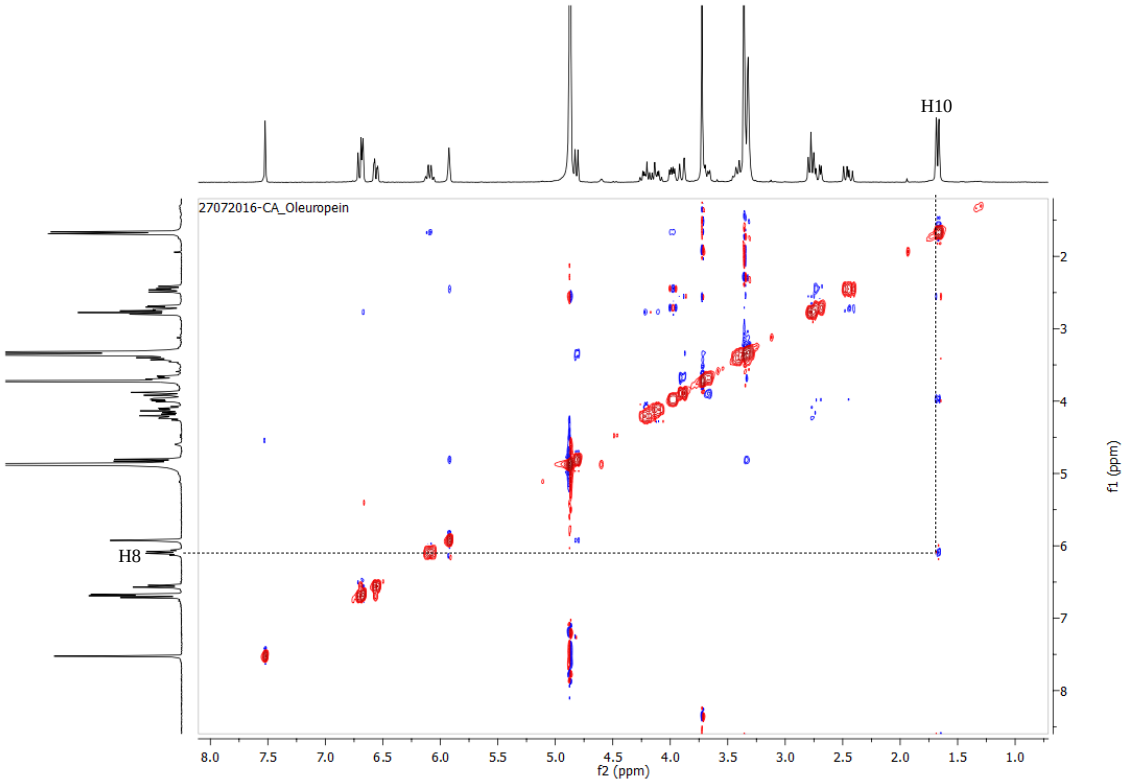

Figure 7.4. COSY spectrum of oleuropein 1, in CD_3OD.

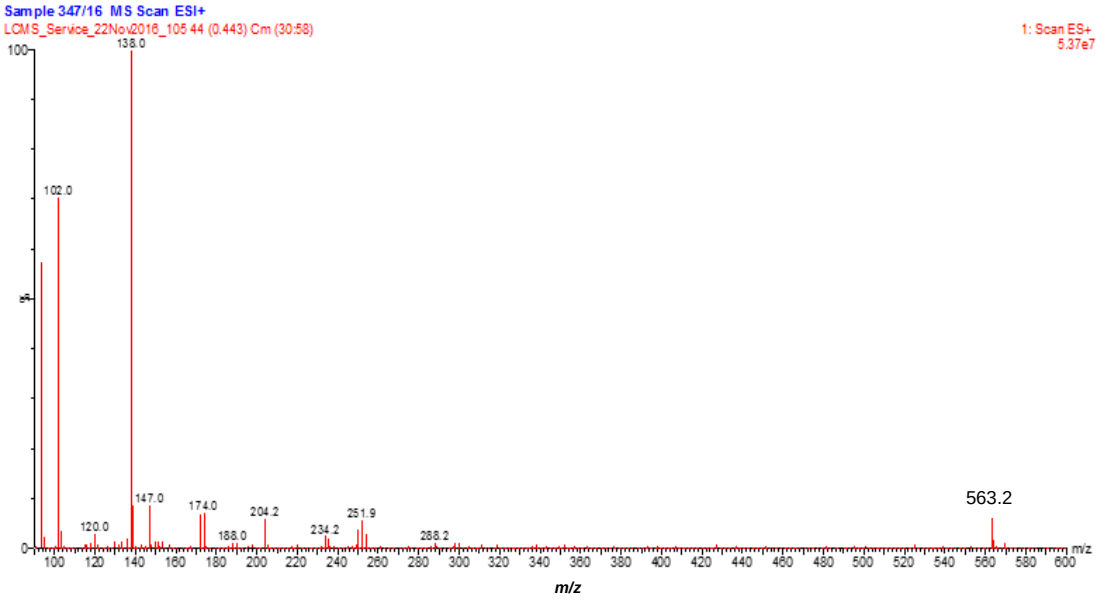

Figure 7.5. LC-ESI-MS of oleuropein 1, in positive mode.

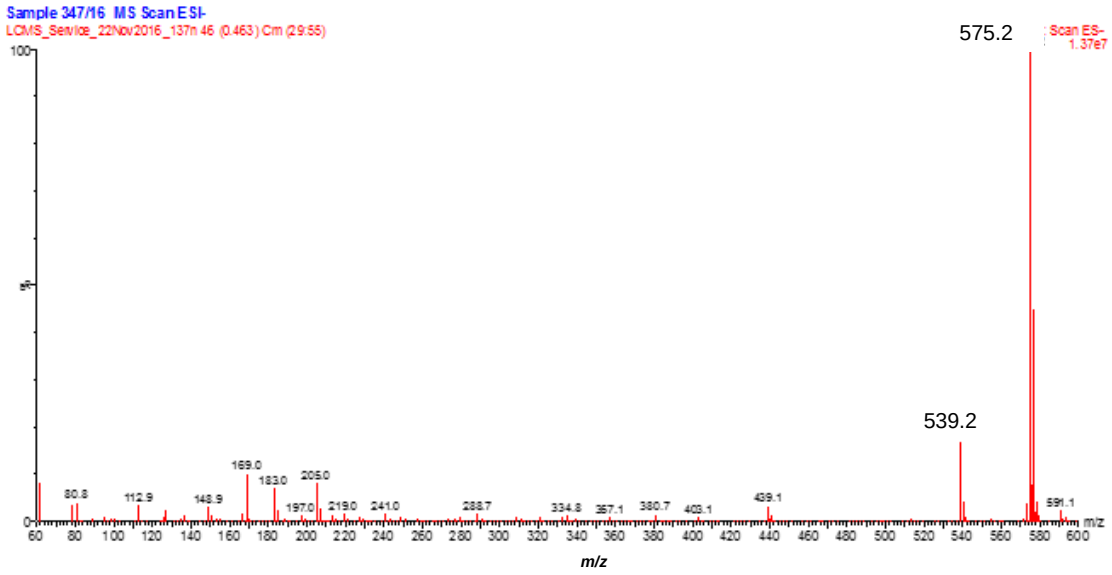

Figure 7.6. LC-ESI-MS spectrum of oleuropein 1, in negative mode.

7.2. Appendix II – NMR spectra and ESI-MS of jaspolyside 4

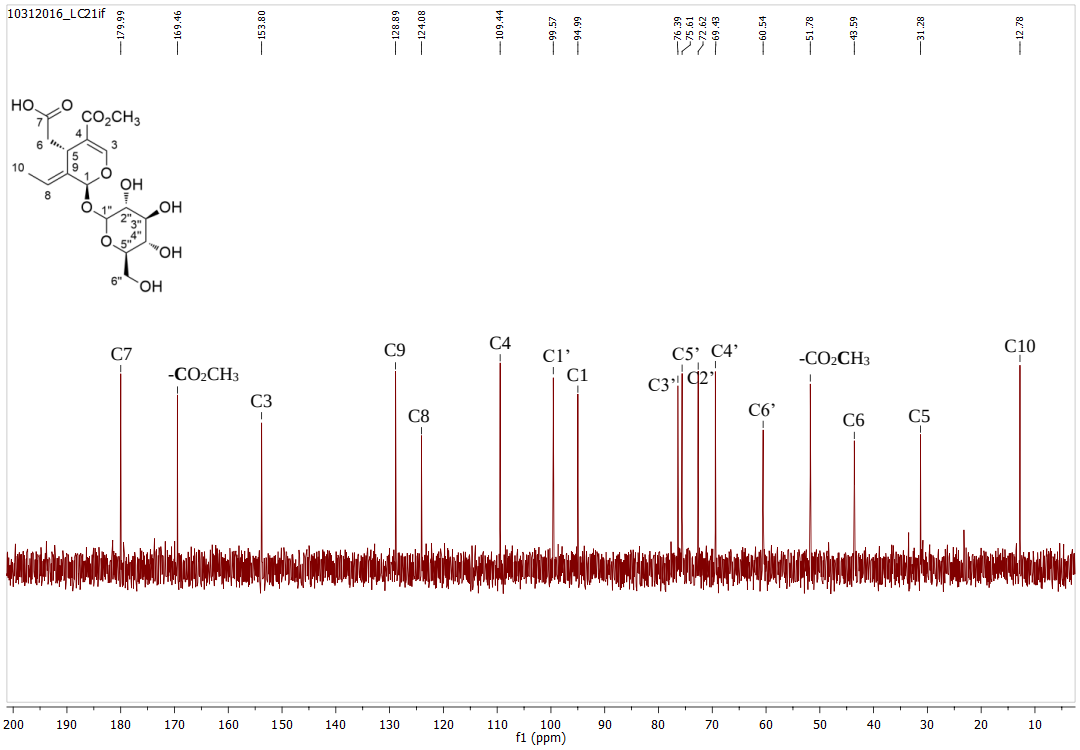

Figure 7.7. ^{13}C NMR spectrum of jaspolyside 4, in D_2O.

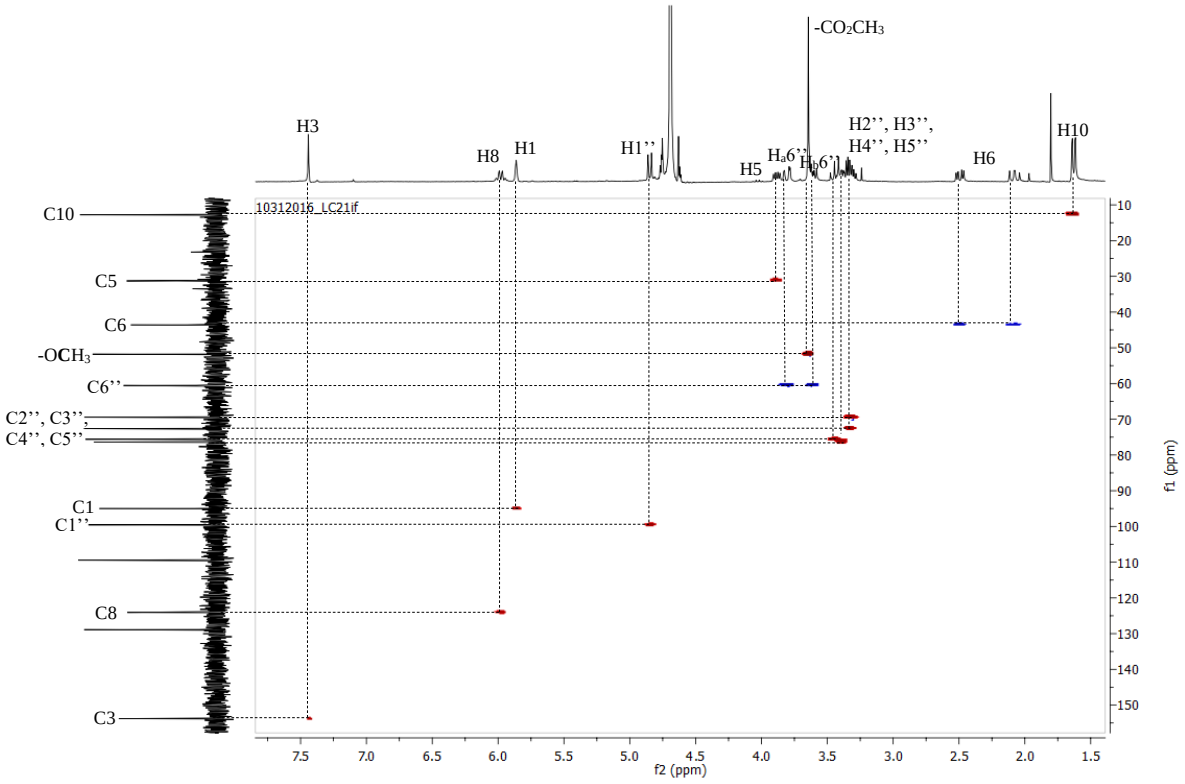

Figure 7.8. HSQC spectrum of jaspolyside 4, in D_2O.

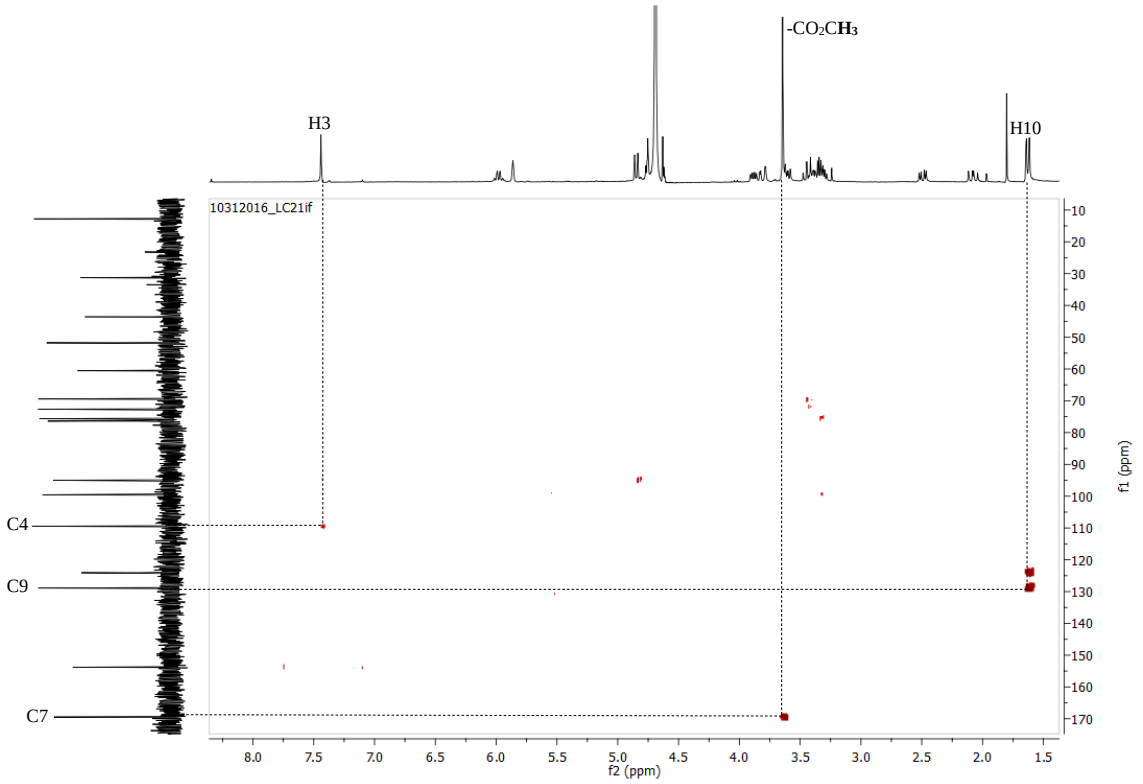

Figure 7.9. HMBC spectrum of jaspolyside 4, in D_2O.

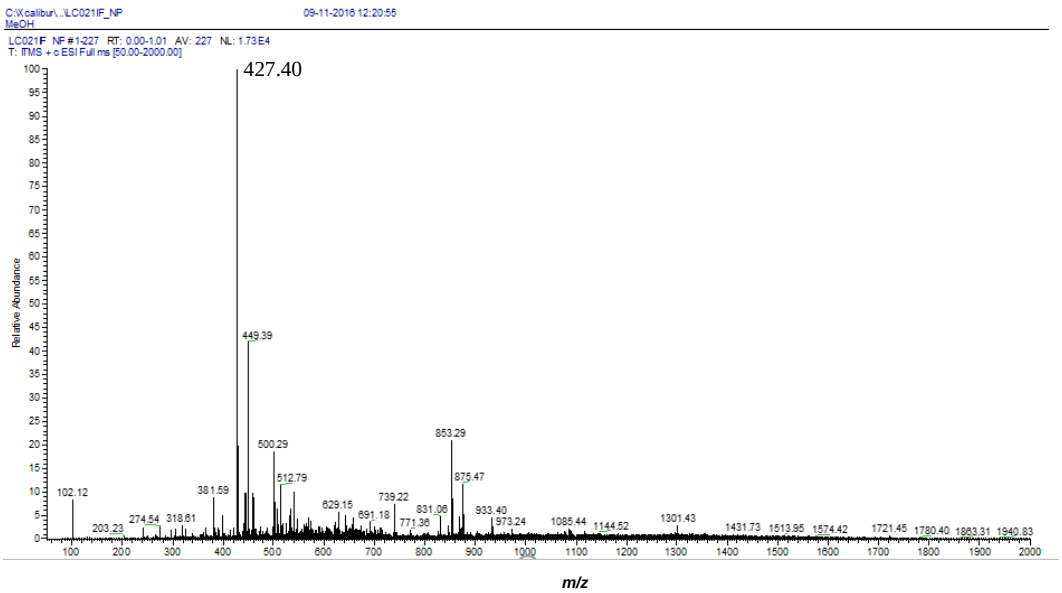

Figure 7.10. ESI-MS spectrum of jaspolyside 4, in positive mode.

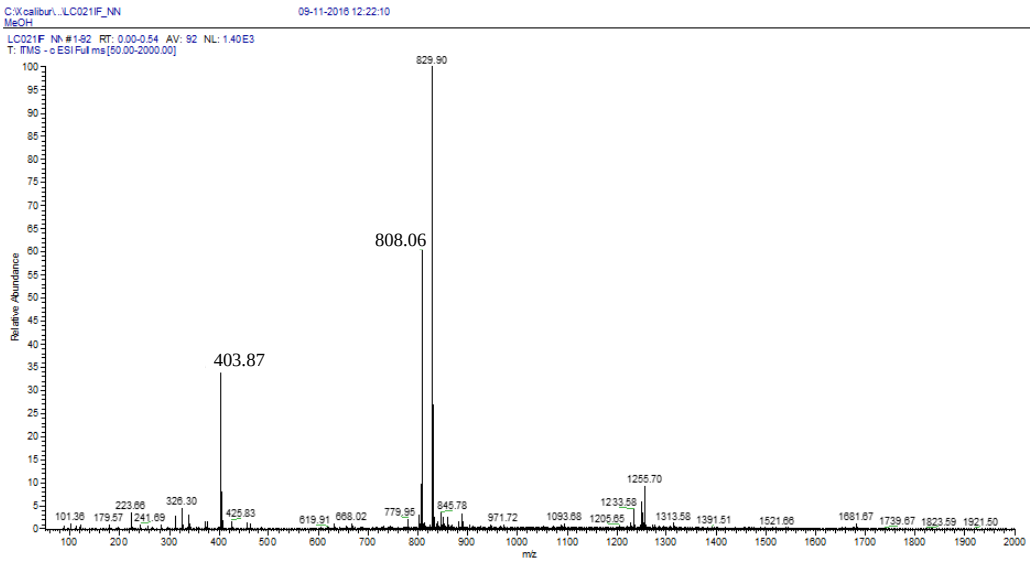

Figure 7.11. ESI-MS spectrum of jaspolyside 4, in negative mode.

7.3. Appendix III– NMR spectra and ESI-MS of compounds 5

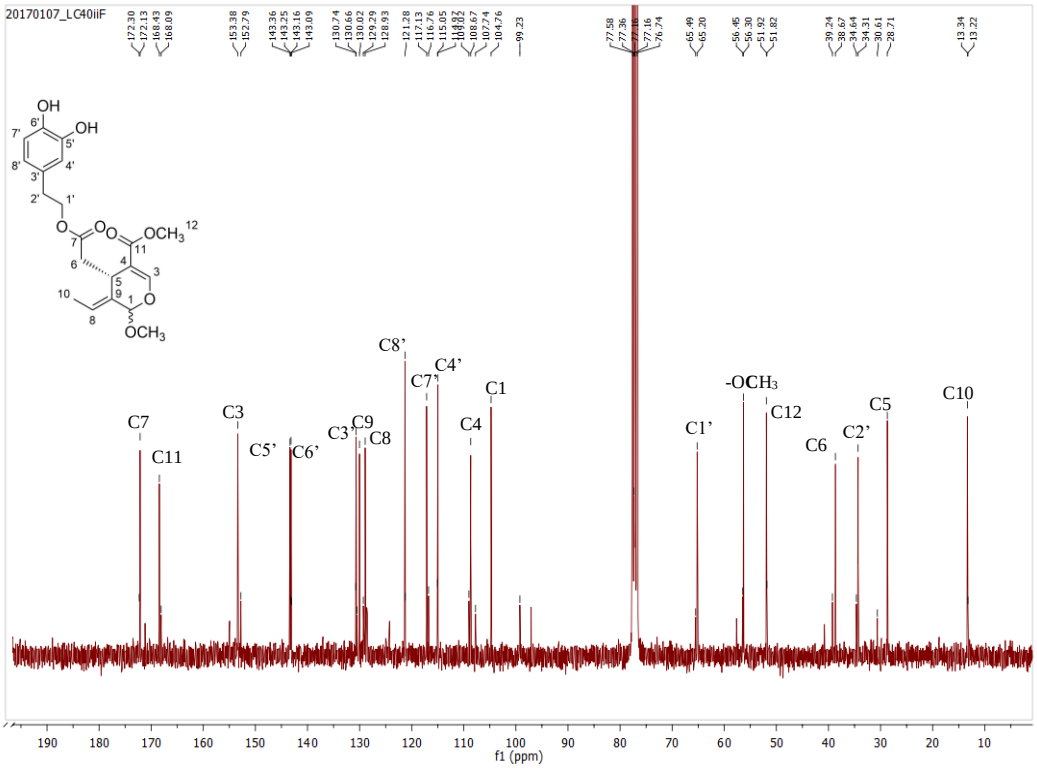

Figure 7.12. ^{13}C NMR spectrum of compounds 5, in $CDCl_3$.

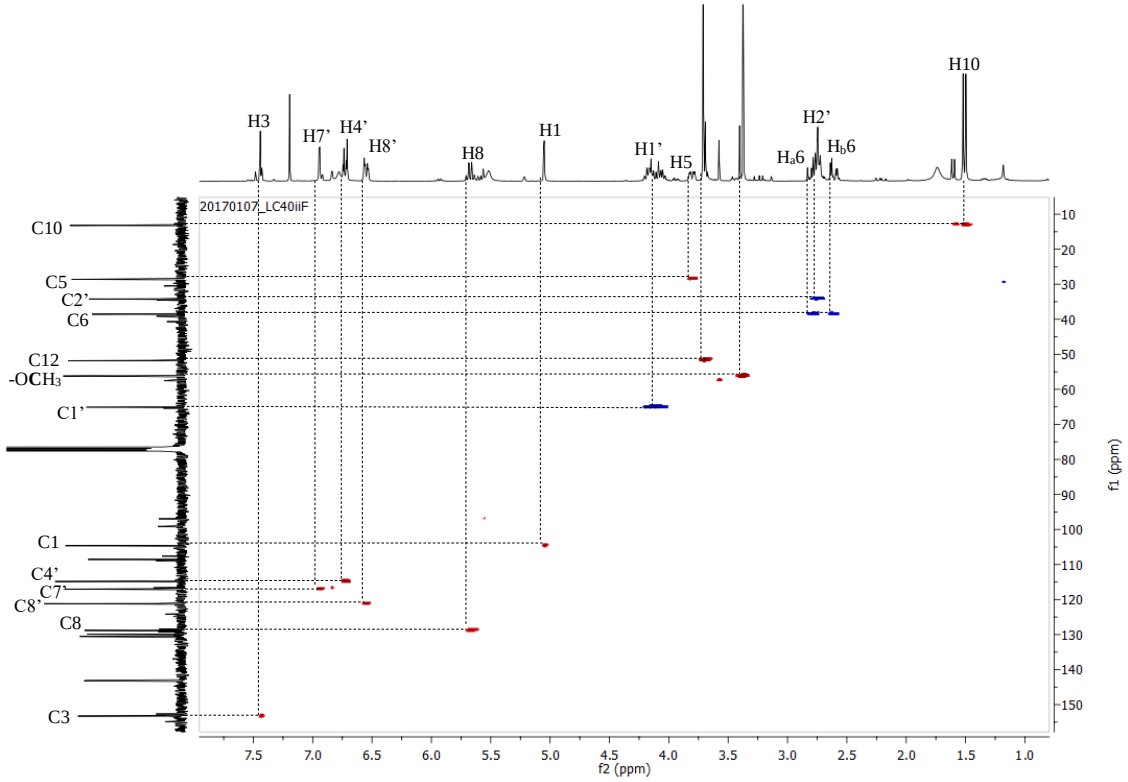

Figure 7.13. HSQC spectrum of compounds 5, in $CDCl_3$.

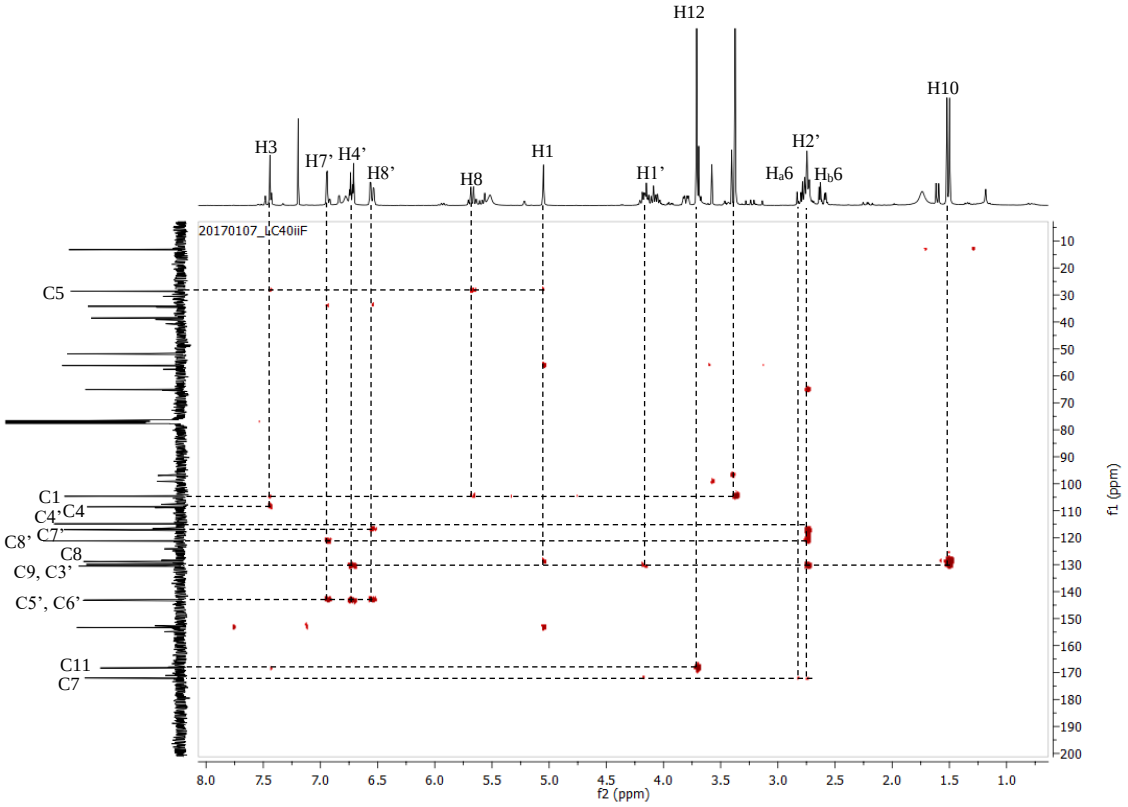

Figure 7.14. HMBC spectrum of compounds 5, in $CDCl_3$.

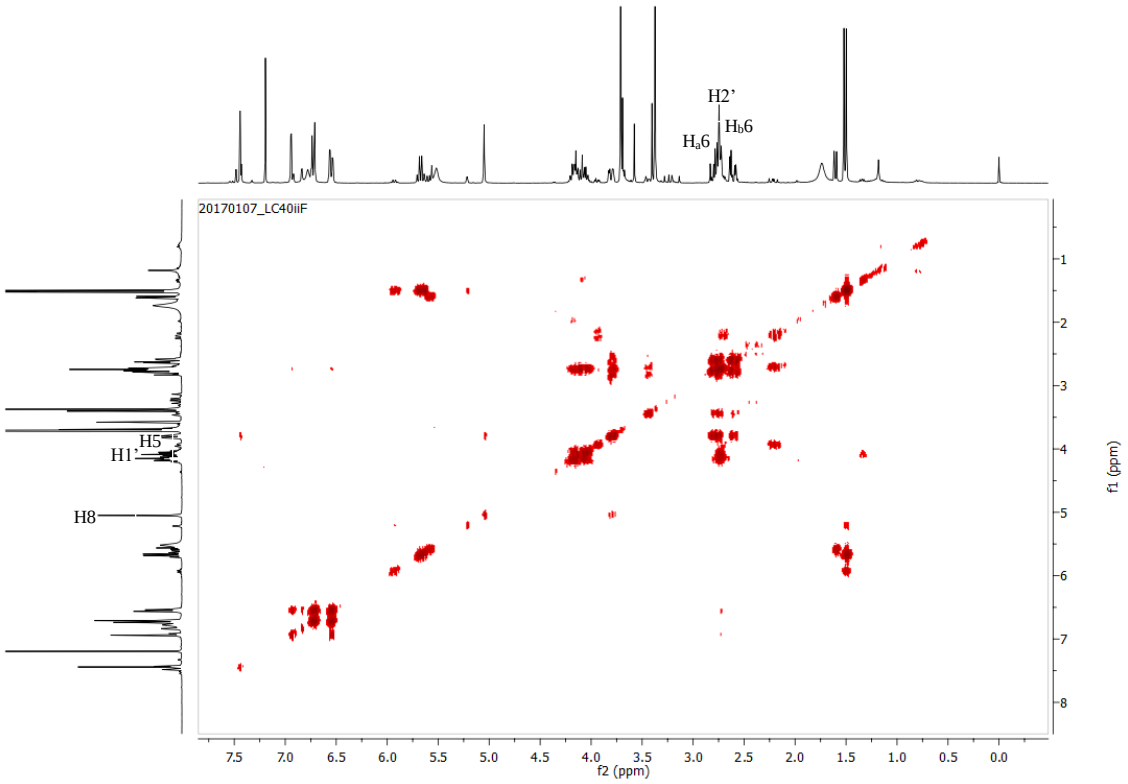

Figure 7.15. COSY spectrum of compounds 5, in $CDCl_3$.

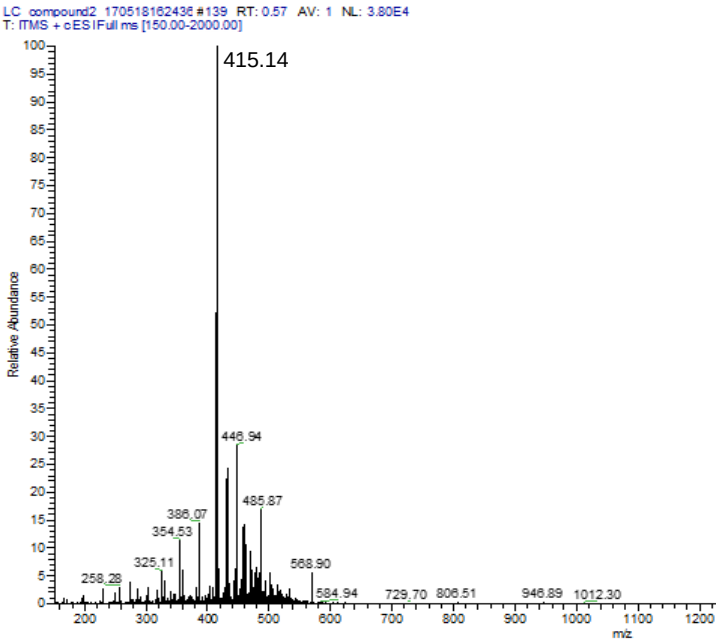

Figure 7.16. ESI-MS spectrum of compounds 5, in positive mode.

7.4. Appendix IV – NMR spectra and ESI-MS of compounds 6

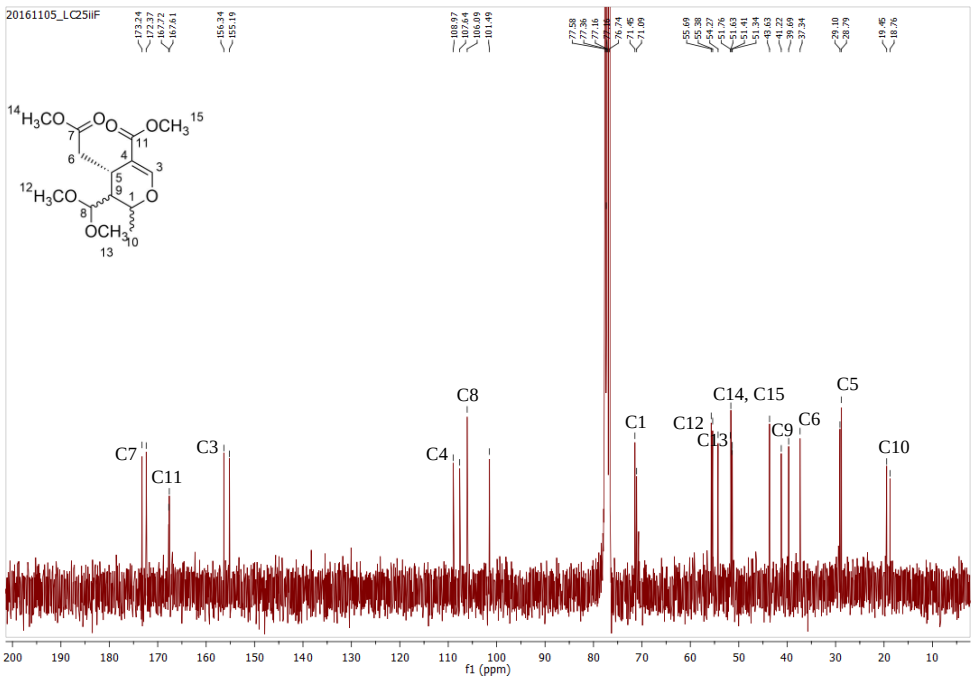

Figure 7.17. ^{13}C NMR spectrum of compounds 5, in $CDCl_3$.

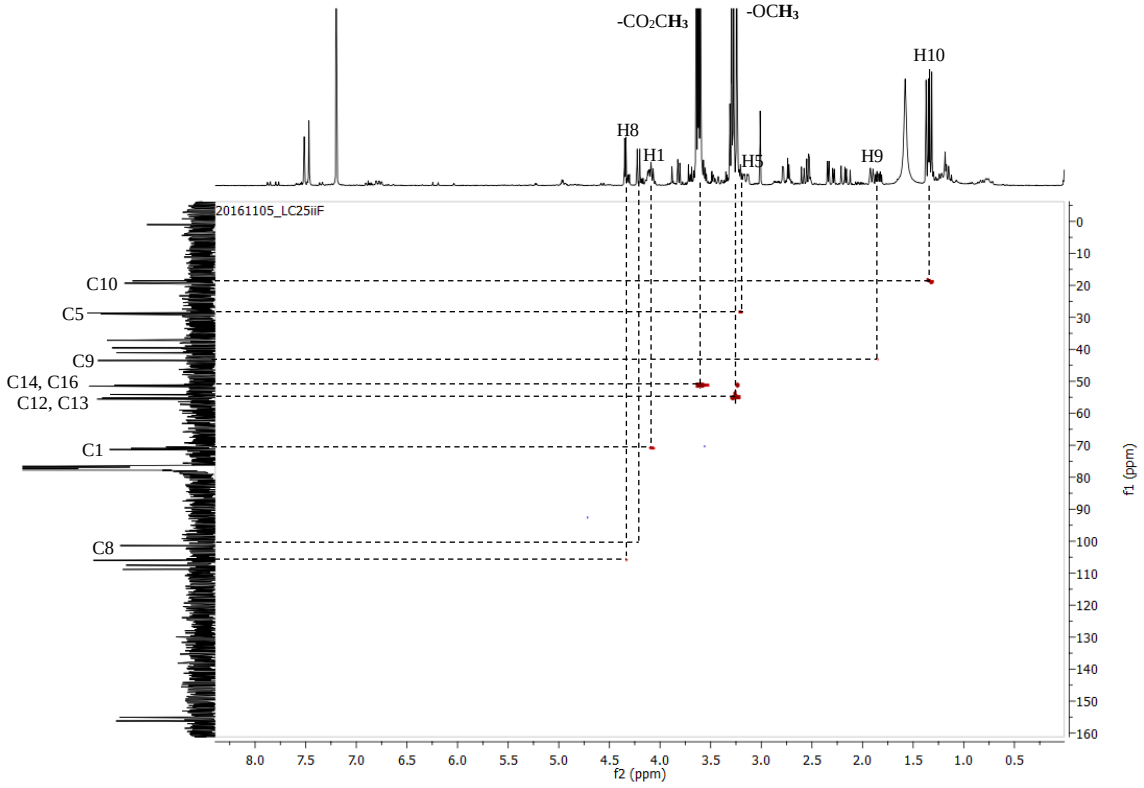

Figure 7.18. HSQC spectrum of compounds 6, in $CDCl_3$.

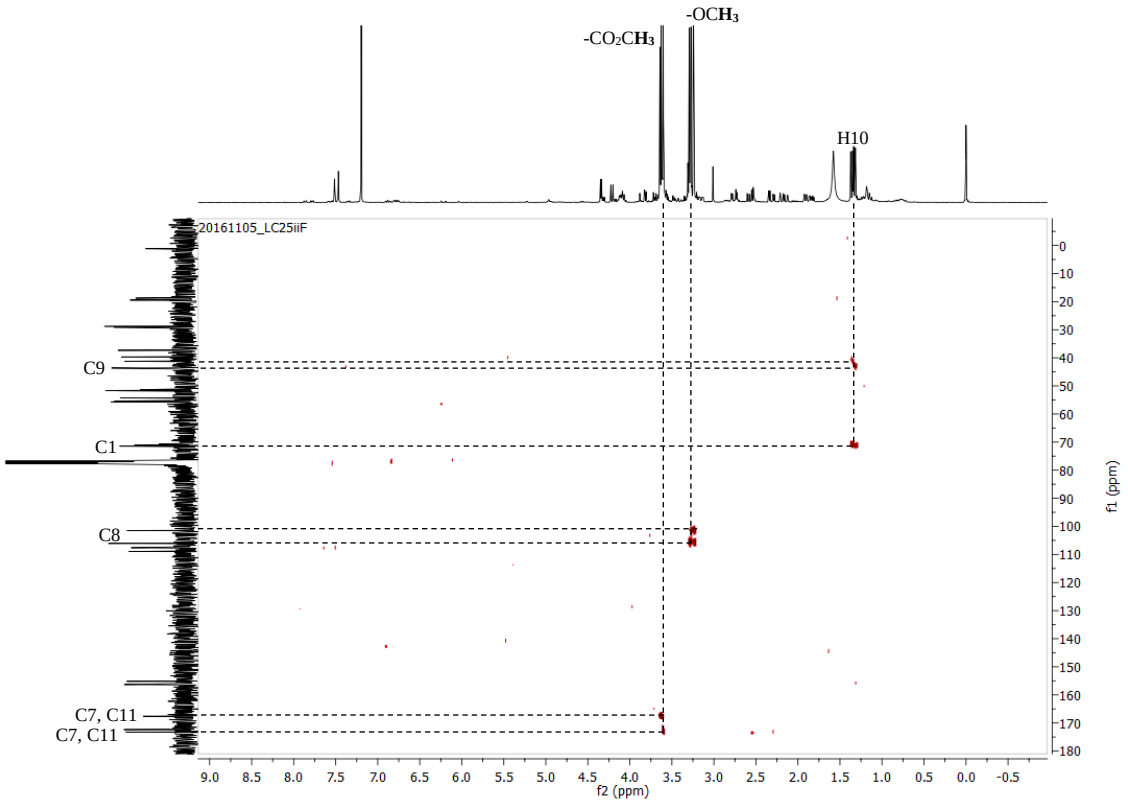

Figure 7.19. HMBC spectrum of compounds 6, in $CDCl_3$.

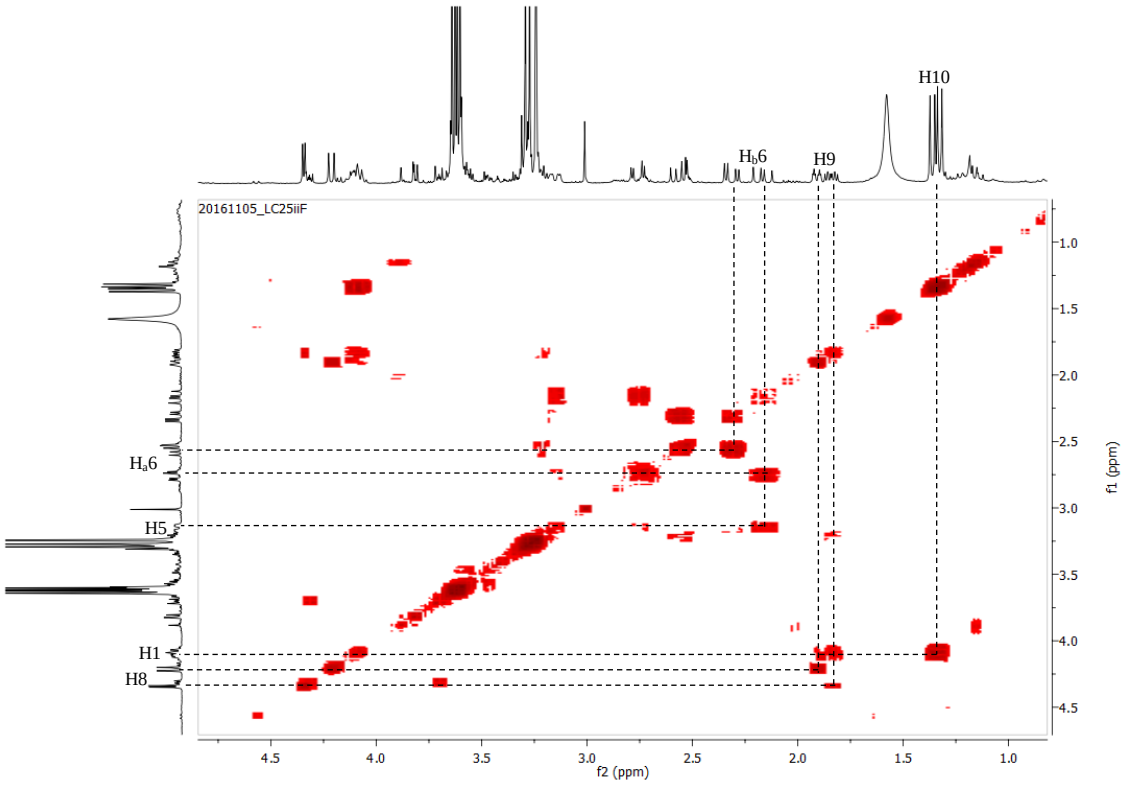

Figure 7.20. COSY spectrum of compounds 6, in $CDCl_3$.

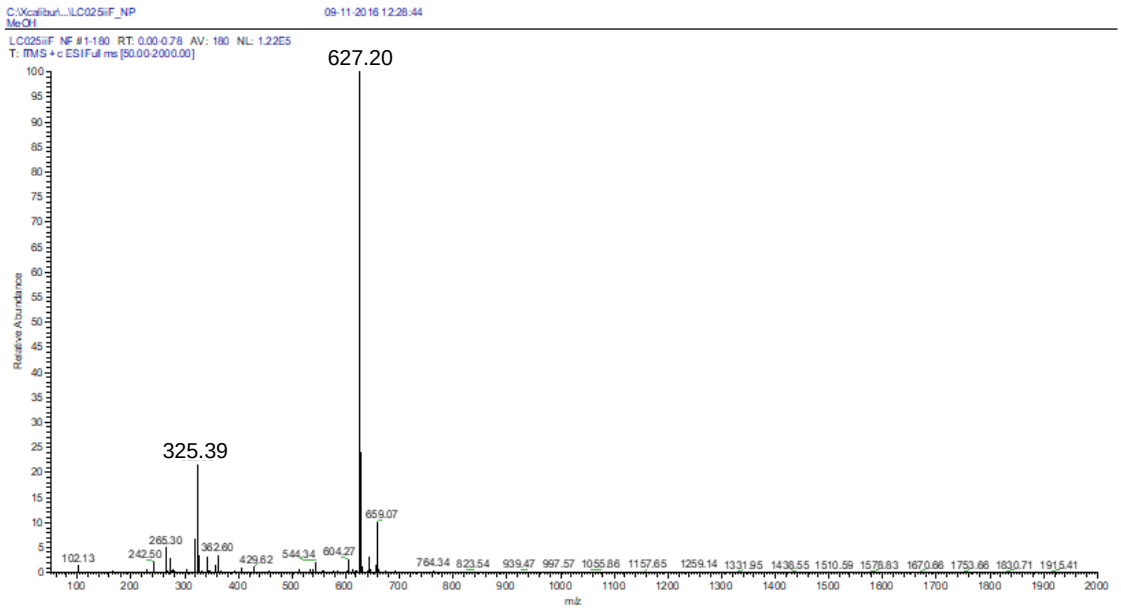

Figure 7.21. ESI-MS spectrum of compounds 6, in positive mode.

7.5. Appendix V – NMR spectra and ESI-MS of compounds 7

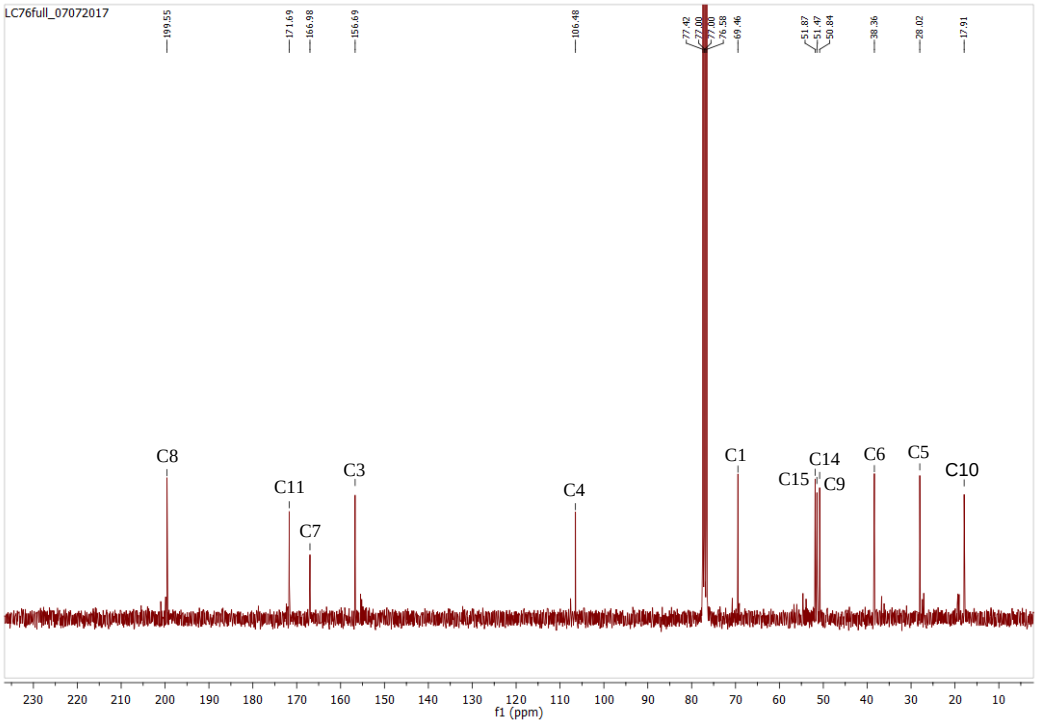

Figure 7.22. ^{13}C NMR spectrum of compounds 7, in $CDCl_3$.

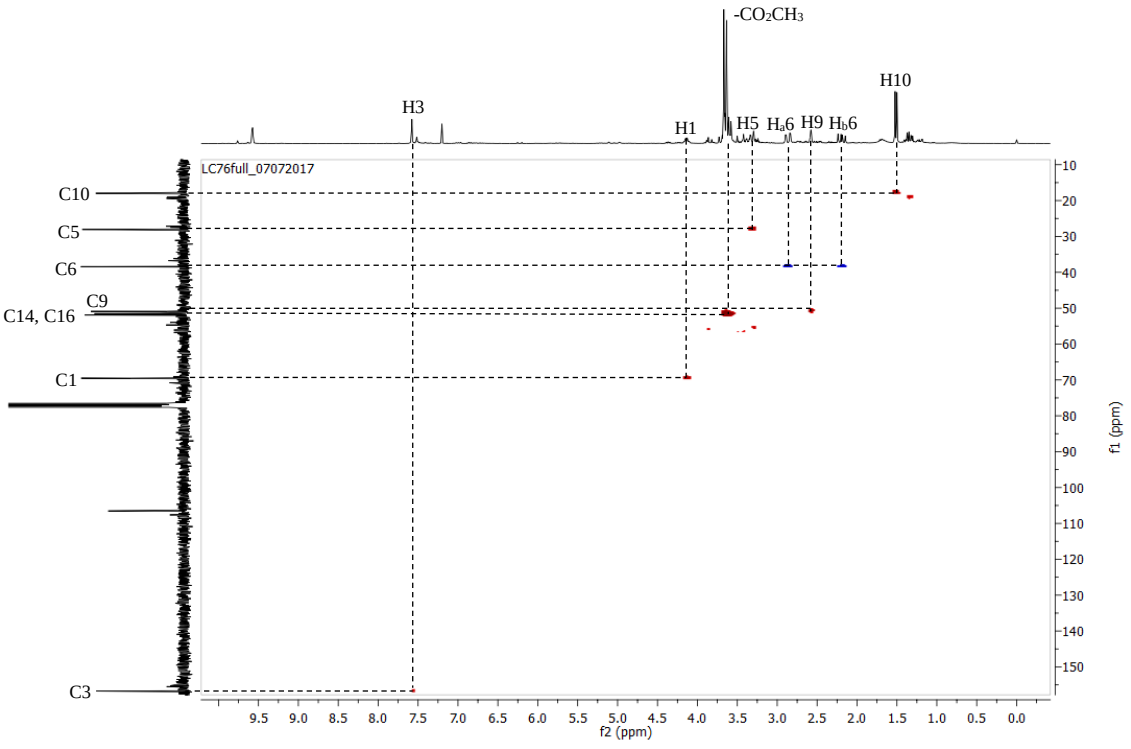

Figure 7.23. HSQC spectrum of compounds 7, in $CDCl_3$.

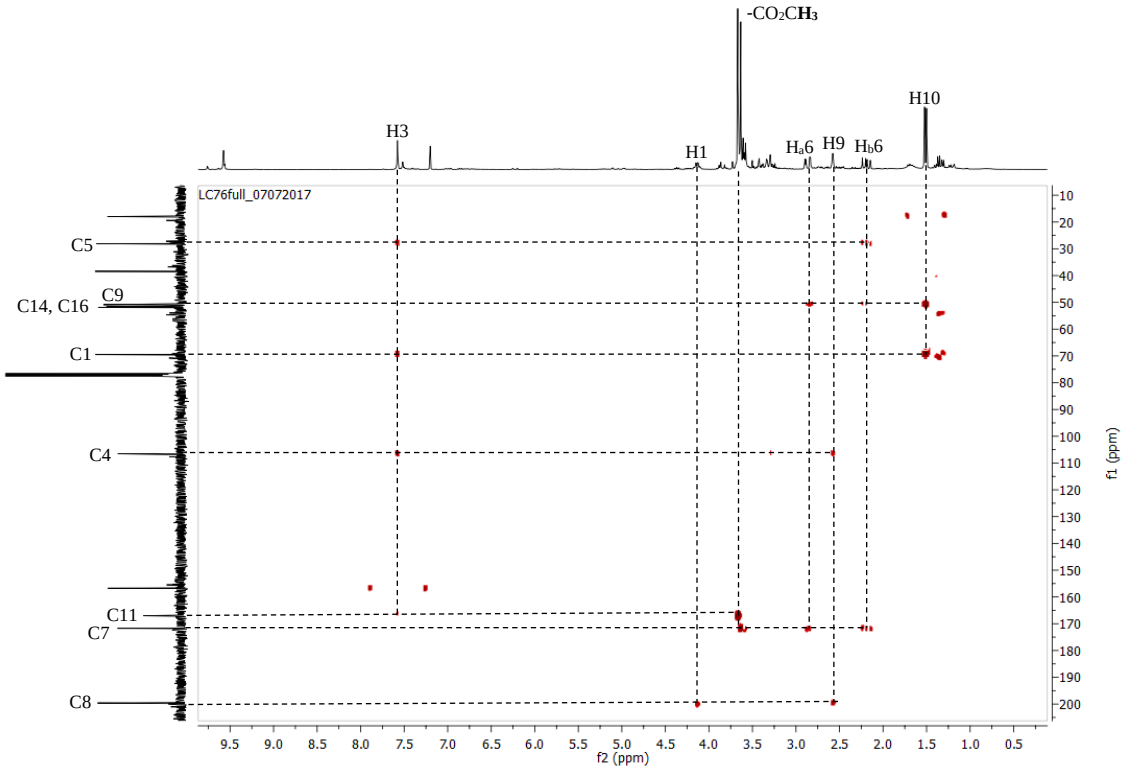

Figure 7.24. HMBC spectrum of compounds 7, in $CDCl_3$.

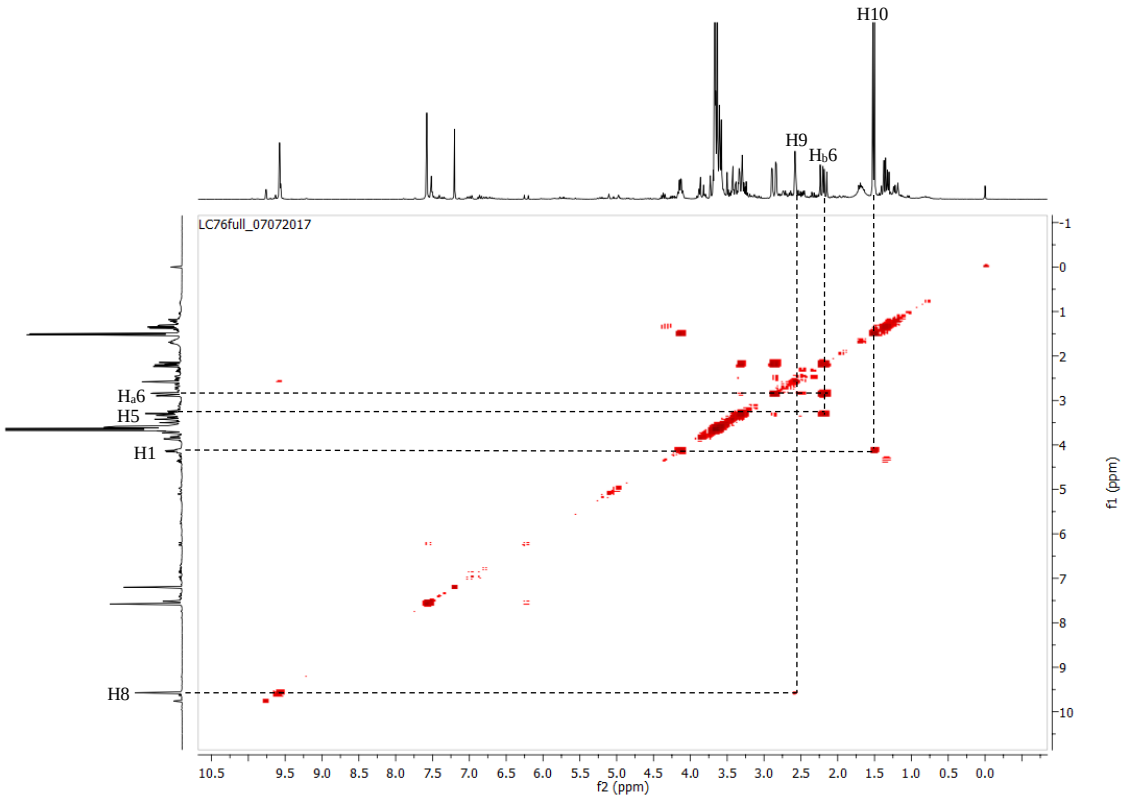

Figure 7.25.COSY spectrum of compounds 7, in $CDCl_3$.

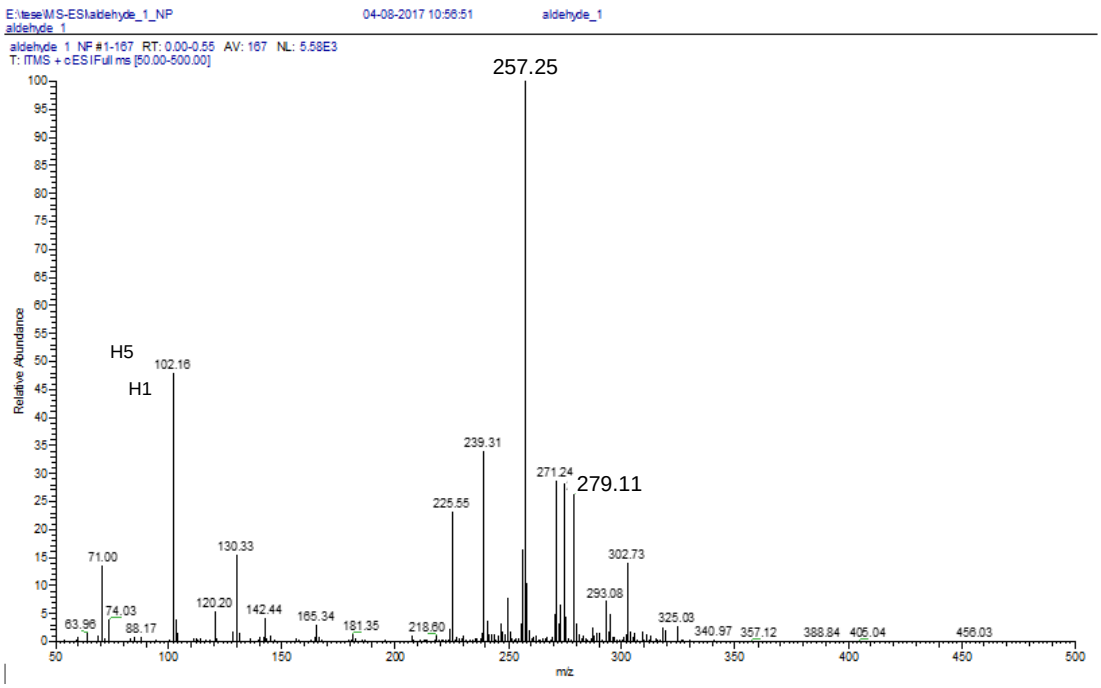

Figure 7.26. ESI-MS spectrum of compounds 7, in positive mode.

7.6. Appendix VI – Screening of acids and acidic resins experiment

Table 7.1. Data for calibration curves of oleuropein 1, compounds 5 and 6.

	Oleuropein **1**			Compounds **5**			Compounds **6**		
Concentration (mM)	Area	Average	RSD (%)	Area	Average	RSD (%)	Area	Average	RSD (%)
0,10	8,2576	8,3737	1,96	13,896	14,111	1,55	3,5908	3,4668	4,12
	8,4897			14,053			3,3665		
	-			14,327			3,3427		
0,15	-			20,648	20,007	3,24	4,5971	4,6574	1,53
				19,860			4,7110		
				19,365			4,7177		
0,20	16,758	16,549	1,94	26,518	26,239	1,18	6,2452	6,2665	1,01
	16,709			26,045			6,1821		
	16,179			25,961			6,2878		
0,30	23,678	22,956	2,76	40,226	40,226	1,18	9,4188	9,4794	1,51
	22,496			40,900			9,2963		
	22,694			40,226			9,5399		
0,40	28,605	28,605	0,31	51,059	51,209	0,73	11,843	11,933	0,94
	-			21,689			11,840		
	28,516			51,359			12,024		

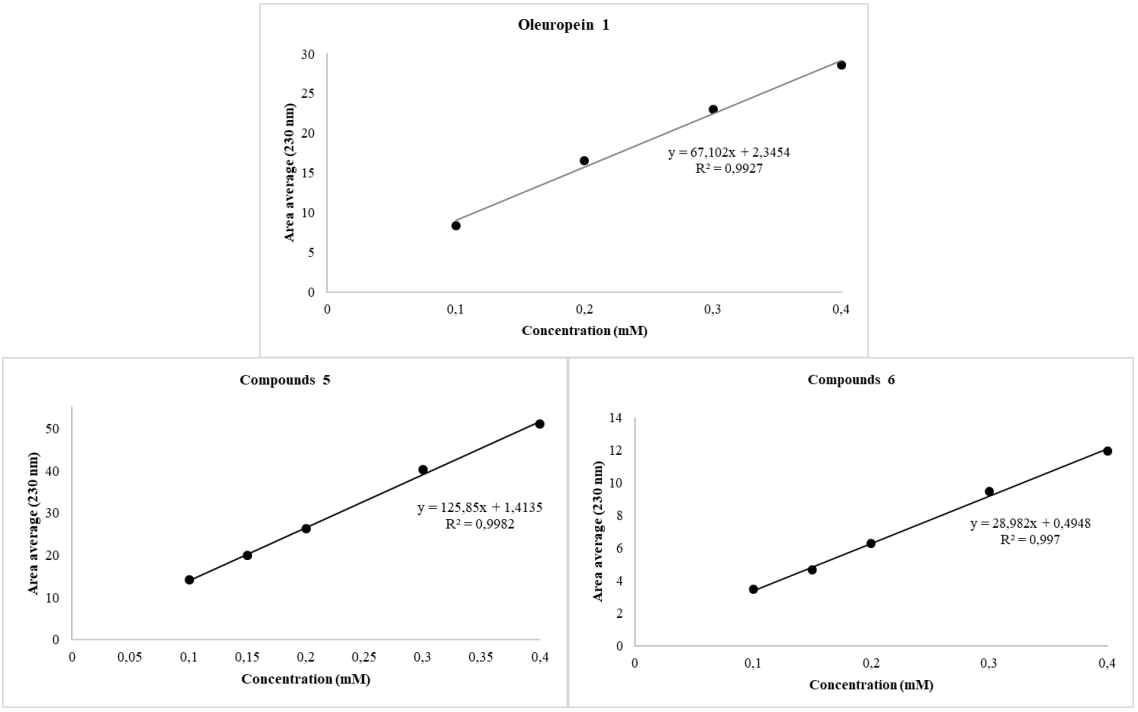

Figure 7.27. Calibration curves of oleuropein 1, compounds 5 and 6, at 230 nm.

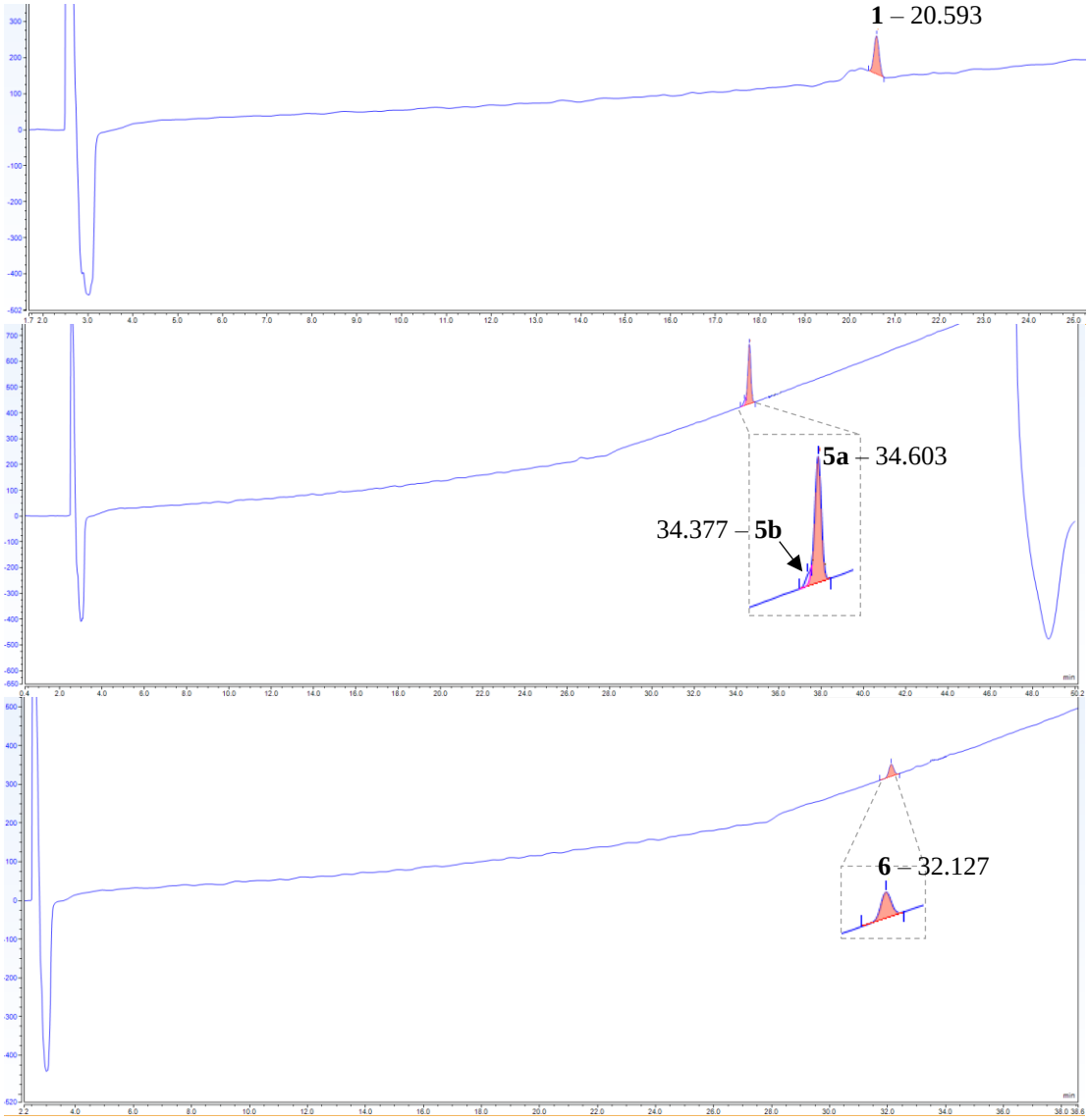

Figure 7.28. Chromatograms of oleuropein 1, compounds 5 and 6.

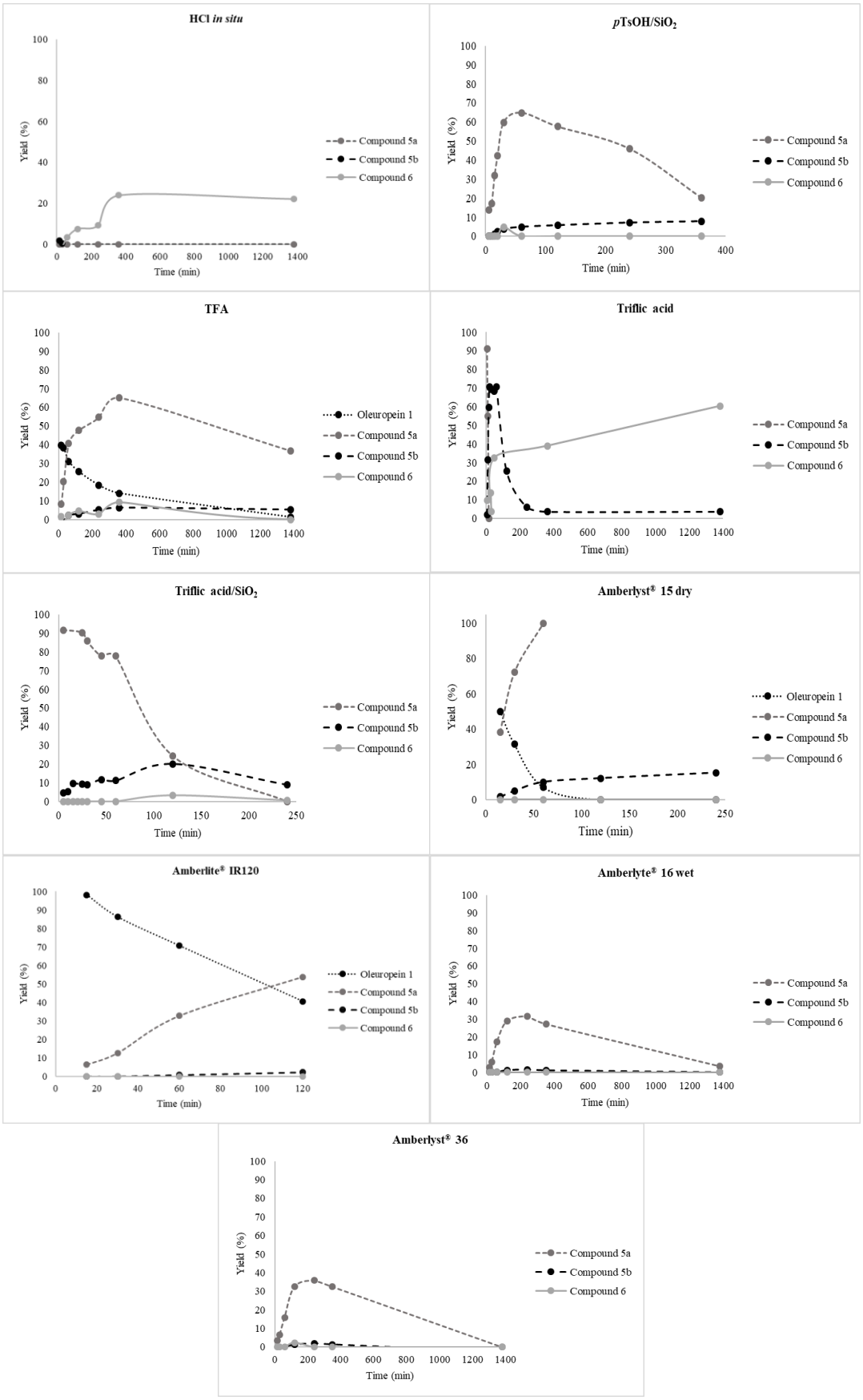

Figure7.29. Examples of methanolysis reaction profiles for different acids and acidic resins, at 70 ºC.

Table 7.2. Main results obtained from the screening of acids experiments, after 6 hours.

Entry	Acid Promoter	Conversion (%)	5a (%)	5b (%)	6 (%)
1	HCl *in situ*	100	0	0	24
2	*p*TsOH.H_2O	100	0	18	57
3	*p*TsOH.H_2O/SiO_2	100	20	8	0
4	Triflic acid	100	0	4	39
5	Triflic acid/ SiO_2[a]	100	0	9	0
6	TFA	85	65	6	9
7	Amberlyst® 15 dry[3]	100	84	15	0
8	Amberlyst® 16 wet	100	27	1	0
9	Amberlyst® 36 wet	100	33	1	0
10	Amberlite® IRC86	0	0	0	0
11	Amberlite® IR120[4]	40	54	2	0

2 mmol of acid promoter (1M) and 20 mg of oleuropein in 2 mL of dry CH_3OH, 70 ˚C, argon atmosphere.

At 1h and 2h the retention times did not correspond to the correct ones, because the run conditions were not exactly the same as for the standard chromatographic conditions (ex. %TFA, temperature).

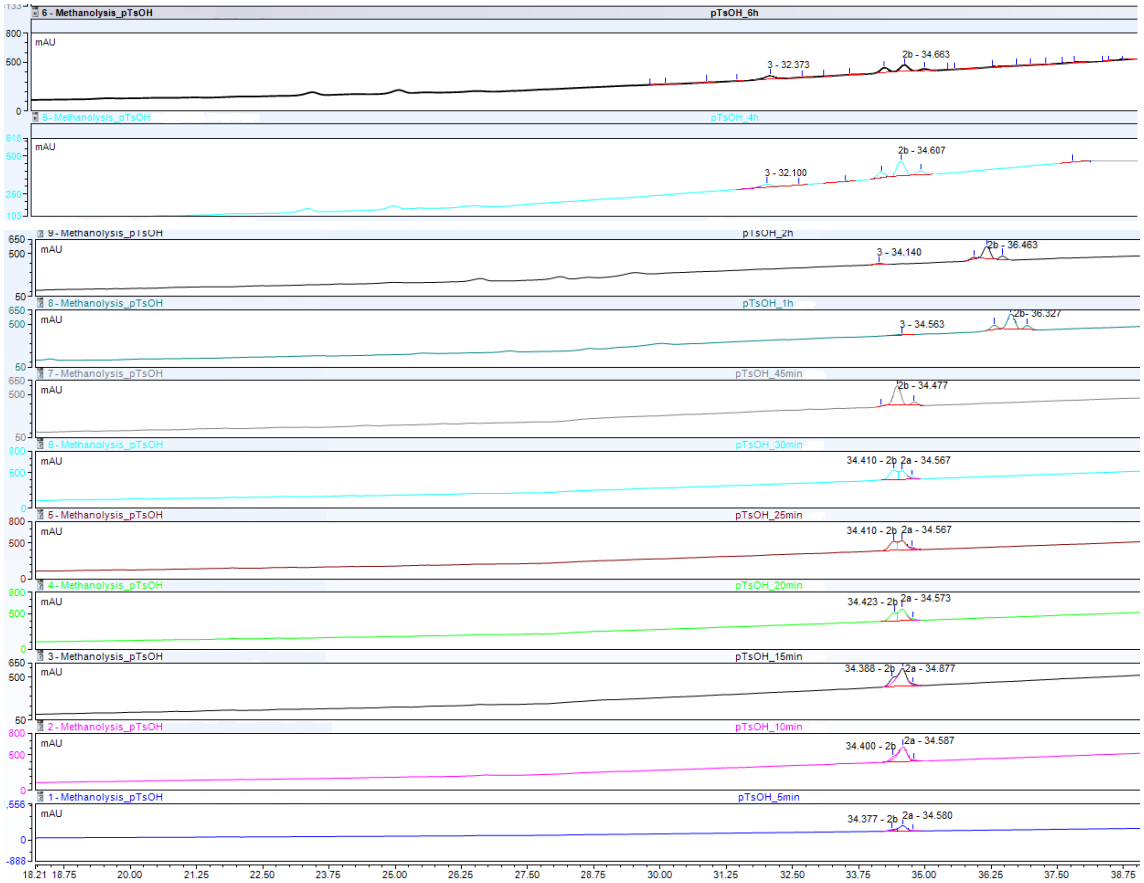

Figure 7.30. Chromatograms of the methanolysis reaction of oleuropein 1, using *p*TsOH.H_2O; 2 represents compound 5 and 3 represents compound 6.

[3] Results at 4 hours.
[4] Results at 2 hours.

Table 7.3. Results from temperature effect experiments, after 2 hours.

Entry	Temperature (˚C)	5a (%)	5b (%)	6 (%)
1	60	0	17	39
2	70	0	5	56
3	80	0	5	≈100

Table 7.4.Yields from methanolysis reaction of crude mixture.

Time (min)	5a (%)	5b (%)	6 (%)
15	10,76	7,959	0
30	1,303	10,27	0
60	0	10,73	4,006
120 (2h)	0	7,299	17,00
240 (4h)	0	3,770	21,04
1380 (23h)	0	0	≈100

In chromatograms corresponding to 2h, 4h and 23h was visible that the retention times of compounds **5b** and **6** did not correspond to the correct ones, because the run conditions were not exactly the same as for the standard chromatographic conditions (ex. %TFA, temperature). The first chromatogram up is relative to the amount of oleuropein in the crude.

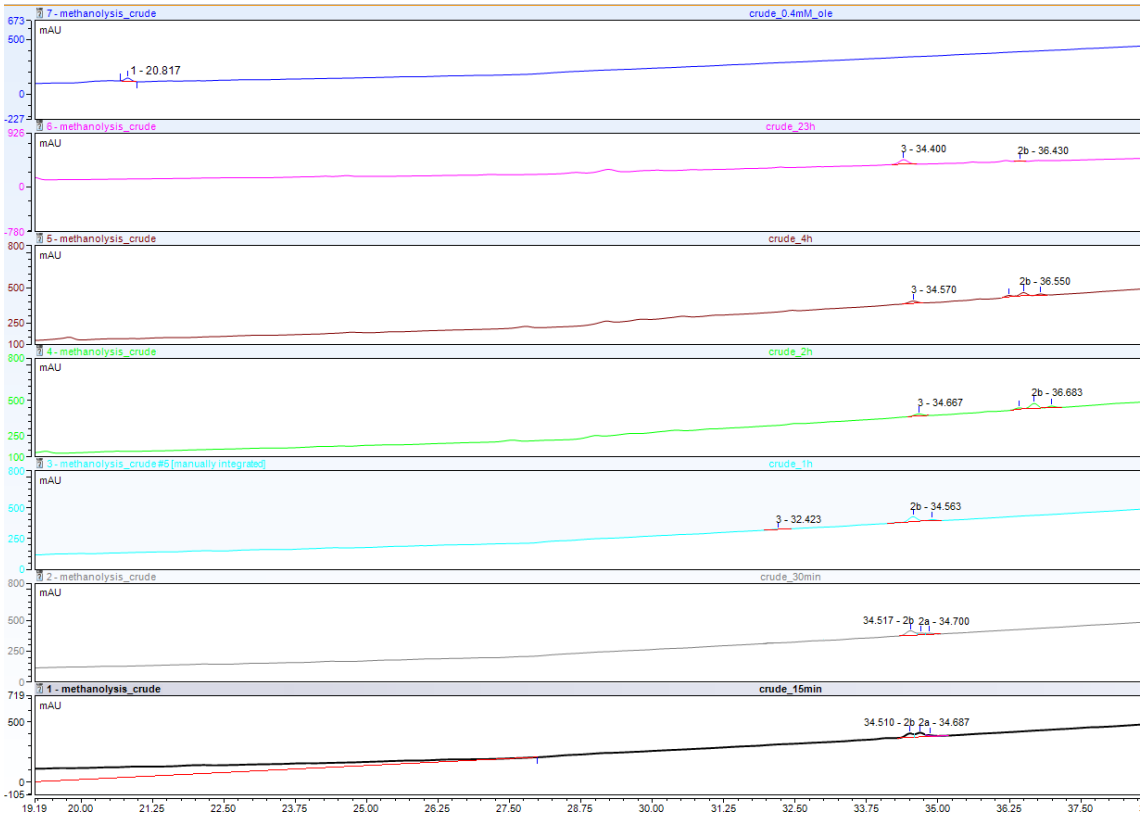

Figure 7.31. Chromatograms of the methanolysis reaction with crude, using *p*TsOH.H_2O, at 70 ºC; 2 represents compound 5 and 3 represents compound 6.

7.7. Appendix VII – Continuous flow experiments

Syringe diameter = 5 mm

Injected Volume = 1000 µL

Table 7.5. Weights for flow calculation.

Residence Time (min)	1	5	10
Reactor (g)		61.0233	
Reactor + Resin (g)	61.3476	61.3386	61.3230
Amount of resin (g)	0.3243	0.3153	0.2997
Reactor + Resin + CH_3OH* (g)	61,5956	61,6770	61,6170
Amount of methanol (g/mL)	0.5480/0.314	0.3384/0.4280	0.294/0.372

* Methanol density = 0,791 g/mL

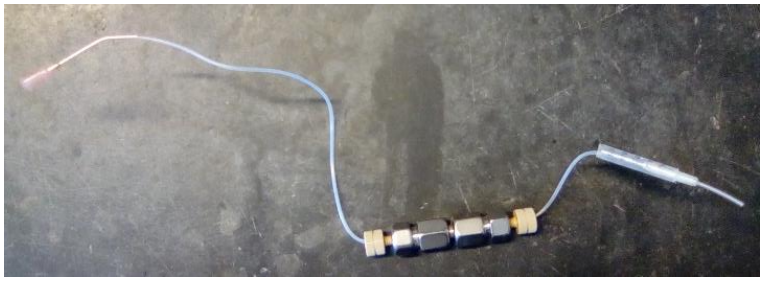

Figure 7.32. Reactor for continuous flow experiments.

Figure 7.33. Continuous flow system.

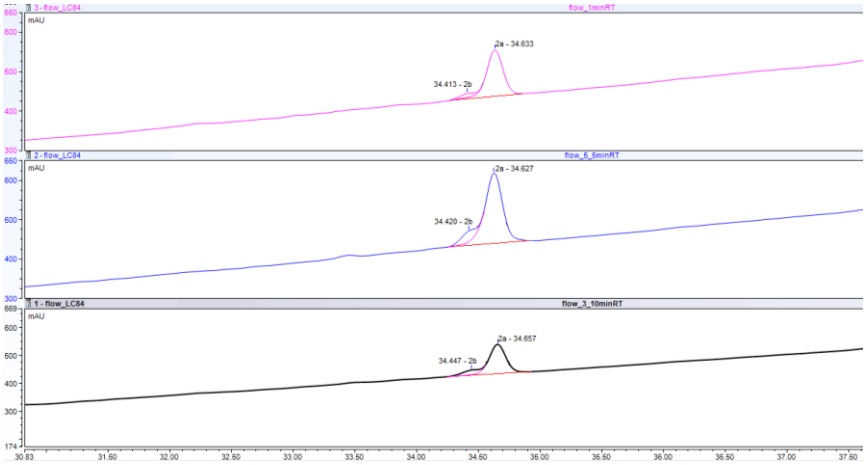

Figure 7.34. Chromatograms from continuous flow experiences, of 1 min, 5 min and 10 min of residence time.

Table 7.6. Data for flow calculation in resin robustness evaluation.

Residence Time (min)	**5**
Reactor (g)	61.0233
Reactor + Resin (g)	61.3645
Amount of resin (g)	0.3412
Reactor + Resin + CH_3OH* (g)	61.6258
Amount of methanol (g/mL)	0.2613/0.330
Flow (µL/min)	66

* Methanol density = 0,791 g/mL

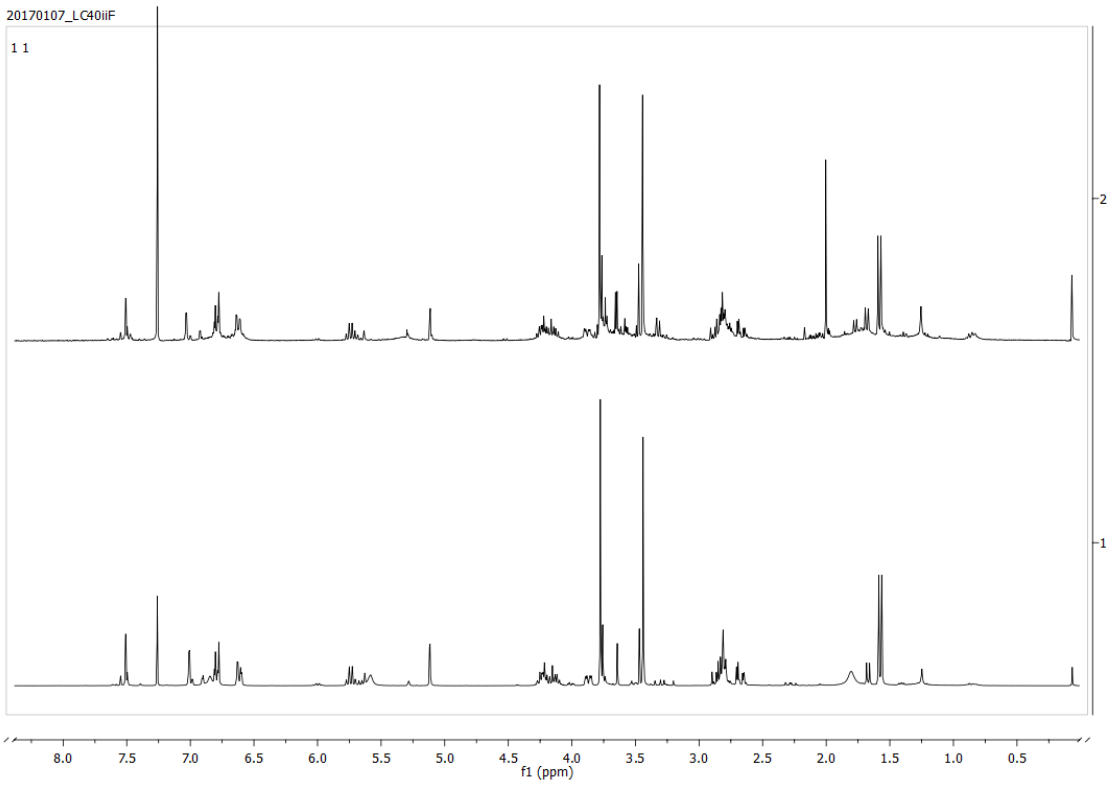

Figure 7.35. ^{1}H NMR spectra of 5a crude sample from flow (up) and previous isolated 5 (down).

7.8. Appendix VIII – Computational Calculations

Cartesian Coordinates

Trans

SCF energy: -957.525267464 Hartree
Free energy: -957.271632 Hartree

C	-0.444335000	1.429543000	-0.838479000
O	0.689860000	1.453159000	0.042198000
C	0.981201000	0.408343000	0.863357000
C	0.309582000	-0.931697000	0.608476000
O	1.820470000	0.563121000	1.720193000
C	1.074708000	-1.757128000	-0.483572000
C	2.469131000	-2.164402000	-0.045558000
C	2.482163000	-3.387286000	0.839293000
O	1.789150000	-4.516103000	0.192480000
C	0.715714000	-4.232496000	-0.551908000
C	0.288664000	-2.992169000	-0.880980000
C	-0.906521000	-2.798430000	-1.710363000
C	3.608552000	-1.536467000	-0.358337000
O	-1.302765000	-1.707386000	-2.096893000
H	1.904694000	-3.210837000	1.762657000
O	-1.551686000	-3.952205000	-2.018824000
C	-2.715999000	-3.804050000	-2.843698000
H	-0.468067000	0.545858000	-1.480665000
H	0.321489000	-1.475414000	1.556306000
H	1.151866000	-1.127324000	-1.374389000
H	0.207080000	-5.130286000	-0.887289000
H	4.525903000	-1.961061000	0.042223000
H	-2.455773000	-3.349736000	-3.803556000
H	-3.098883000	-4.814663000	-2.990553000
H	-3.463974000	-3.179295000	-2.347986000
C	3.782043000	-0.290772000	-1.175385000
H	4.471897000	-0.472083000	-2.010223000
H	2.847352000	0.103360000	-1.581551000
H	4.228678000	0.499114000	-0.558290000
H	-0.729601000	-0.822033000	0.290575000
O	3.757276000	-3.809523000	1.131263000
C	3.839710000	-4.787487000	2.164213000
H	3.359059000	-4.427895000	3.085143000
H	3.375483000	-5.730787000	1.856775000
H	4.903344000	-4.946972000	2.351072000
H	-1.377314000	1.486176000	-0.265816000
H	-0.349905000	2.327969000	-1.451089000

Cis

SCF energy: -957.527022155 Hartree
Free energy: -957.273004 Hartree

C	-2.315889000	0.816624000	-0.050630000
O	-1.654973000	0.848304000	1.223338000
C	-1.046329000	-0.253040000	1.746682000
C	-0.768285000	-1.439161000	0.836564000
O	-0.681787000	-0.209990000	2.898948000
C	0.588817000	-1.249647000	0.070431000
C	1.795687000	-1.314618000	0.987198000

C	2.311695000	-2.701989000	1.262919000
O	2.574340000	-3.429304000	0.026350000
C	1.709700000	-3.229877000	-0.984332000
C	0.754911000	-2.276534000	-1.035619000
C	-0.098301000	-2.141758000	-2.224900000
C	2.432243000	-0.269895000	1.531227000
O	-0.908562000	-1.240991000	-2.389344000
O	1.384175000	-3.410119000	2.026243000
C	1.843853000	-4.674555000	2.494828000
O	0.091721000	-3.118518000	-3.147995000
C	-0.706455000	-3.006354000	-4.334782000
H	-1.674723000	0.447380000	-0.854263000
H	-0.696510000	-2.323983000	1.468801000
H	0.559138000	-0.266555000	-0.410922000
H	3.293318000	-2.687551000	1.751887000
H	1.880016000	-3.924546000	-1.799475000
H	3.298346000	-0.487022000	2.158596000
H	2.783914000	-4.566711000	3.055269000
H	1.998022000	-5.379098000	1.669731000
H	1.068821000	-5.055063000	3.162805000
H	-0.497998000	-2.067503000	-4.855034000
H	-0.425721000	-3.857991000	-4.955567000
H	-1.771147000	-3.045778000	-4.089248000
C	2.088723000	1.185775000	1.425515000
H	2.959522000	1.765356000	1.092578000
H	1.257831000	1.387023000	0.745412000
H	1.799967000	1.570773000	2.411340000
H	-1.561181000	-1.586149000	0.100371000
H	-3.223062000	0.203004000	0.000048000
H	-2.600855000	1.851360000	-0.250914000